# GEOLOGIC HAZARDS MAPPING: IDENTIFYING SINKHOLES AND KARST SUSCEPTIBLE AREAS IN WORTH, CERRO GORDO, MITCHELL, AND FLOYD COUNTIES

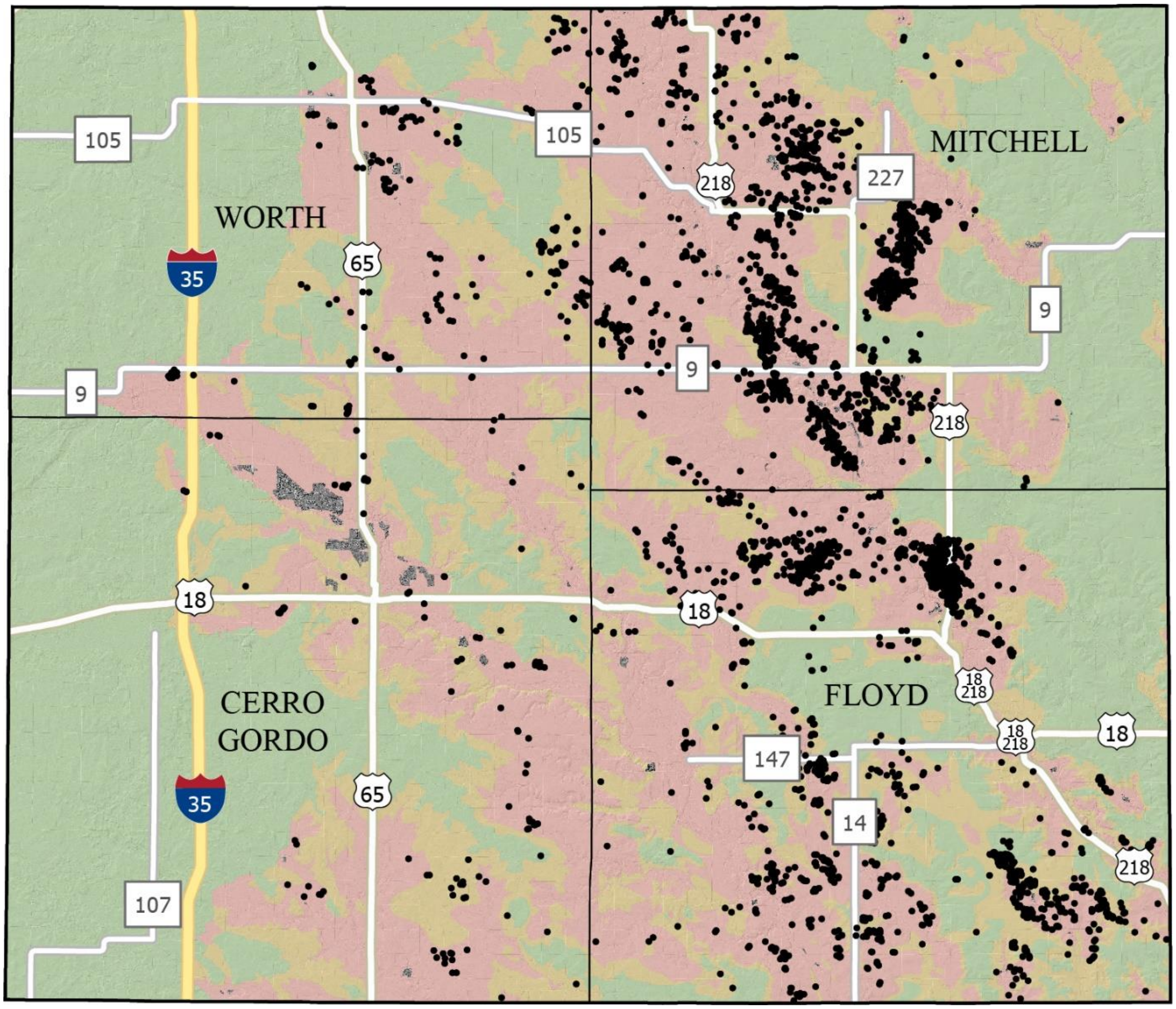


Iowa Geological Survey Technical Information Series 59

Iowa Geological Survey
Keith Schilling, State Geologist
March 2021

# GEOLOGIC HAZARDS MAPPING: IDENTIFYING SINKHOLES AND KARST SUSCEPTIBLE AREAS IN WORTH, CERRO GORDO, MITCHELL, AND FLOYD COUNTIES

**March, 2021**

Prepared by:
Stephanie Tassier-Surine (Principal Investigator), Geologist, IGS
Phil Kerr, Geologist, IGS
Ryan Clark, Geologist, IGS
Calvin Wolter, GIS Analyst, IDNR
Jason Vogelgesang, Hydrogeologist, IGS
Allison Kusick, IGS Student Intern, UI-EES

**Iowa Geological Survey**
IIHR-Hydroscience & Engineering
University of Iowa
Iowa City, Iowa 52242
Telephone: 319-335-1575

Sponsored by the Iowa Department of Transportation (Project HR-3018)
Iowa Geological Survey Technical Information Series 59

**Disclaimer**

*The contents of this report reflect the views of the authors, who are responsible for the facts and the accuracy of the information presented herein. The opinions, findings, and conclusions expressed in this publication are those of the authors and not necessarily those of the sponsors.*

*The sponsors assume no liability for the contents or use of the information contained in this document. This report does not constitute a standard, specification, or regulation. The sponsors do not endorse products or manufacturers. Trademarks or manufacturers' names appear in this report only because they are considered essential to the objectives of the document.*

**Statement of Non-Discrimination**

*Federal and state laws prohibit employment and/or public accommodation discrimination on the basis of age, color, creed, disability, gender identity, national origin, pregnancy, race, religion, sex, sexual orientation or veteran's status. If you believe you have been discriminated against, please contact the Iowa Civil Rights Commission at 800-457-4416 or Iowa Department of Transportation's affirmative action officer. If you need accommodations because of a disability to access the Iowa Department of Transportation's services, contact the agency's affirmative action officer at 800-262-0003.*

# TECHNICAL REPORT DOCUMENTATION PAGE

<table>
<tr><td>1. Report No.<br>HR-3018</td><td>2. Government Accession No.</td><td>3. Recipient's Catalog No.</td></tr>
<tr><td colspan="2" rowspan="2">4. Title and Subtitle<br>Geologic hazards mapping: Identifying sinkholes and karst susceptible areas in Worth, Cerro Gordo, Mitchell, and Floyd counties</td><td>5. Report Date<br>March 31, 2021</td></tr>
<tr><td>6. Performing Organization Code</td></tr>
<tr><td colspan="2">7. Author(s)<br>Stephanie Tassier-Surine (IGS), ORCID:0000-0003-4577-0837<br>Phil Kerr (IGS), ORCID:0000-0002-3498-0014<br>Ryan Clark (IGS), ORCID:0000-0002-4355-5351<br>Calvin Wolter (IDNR), ORCID:0000-0002-2979-5789<br>Jason Vogelgesang (IGS), ORCID:0000-0002-9179-0890<br>Allison Kusick (IGS student intern), ORCID:0000-0002-5968-9338</td><td>8. Performing Organization Report No.<br>Iowa Geological Survey Technical Information Series 59 (TIS-59)</td></tr>
<tr><td colspan="2" rowspan="2">9. Performing Organization Name and Address<br>Iowa Geological Survey<br>The University of Iowa<br>300 Trowbridge Hall<br>Iowa City, IA 52242</td><td>10. Work Unit No.</td></tr>
<tr><td>11. Contract or Grant No.<br>Project Number HR-3018</td></tr>
<tr><td colspan="2" rowspan="2">12. Sponsoring Agency Name and Address<br>Iowa Department of Transportation<br>800 Lincoln Way<br>Ames, IA 50010</td><td>13. Type of Report and Period Covered<br>Final Report (May 1, 2019 to March 31, 2021)</td></tr>
<tr><td>14. Sponsoring Agency Code<br>If available, enter the office code or acronym if a sponsoring agency (such as FHWA or NHTSA) is named in field #12. For FHWA office codes, see https://fhwaapps.fhwa.dot.gov/foisp/hqphone.do]</td></tr>
<tr><td colspan="3">15. Supplementary Notes<br>Conducted in cooperation with the U.S. Department of Transportation, Federal Highway Administration.</td></tr>
</table>

**16. Abstract**

The Iowa Geological Survey (IGS) updated the sinkhole coverage and karst susceptibility map for a four-county area in north-central Iowa including Worth, Cerro Gordo, Mitchell, and Floyd counties (Figure 1). Results more than doubled the number of mapped sinkholes and significantly refined the karst susceptibility map for the region. This work was enhanced due to recent surficial and bedrock geologic mapping completed by the IGS as part of the United States Geological Survey (USGS) STATEMAP program. These recent geologic maps improved upon the Bedrock Geologic Map of Iowa (Witzke et al., 2010) and provided the basis for determining areas with bedrock that typically form karst features and sinkholes. The surficial geologic maps allowed IGS geologists to consider the characteristics of surficial geologic materials when identifying areas with high karst potential, whereas previous karst assessments had only considered the thickness of surficial materials.

The IGS evaluated the location and accuracy of data points in the IGS GeoSam database. A series of horizontal to vertical spectral ratio (HVSR) passive seismic points were also collected to check the depth to bedrock in areas of limited data. The 25 foot contour bedrock elevation map produced by previous mapping efforts was adjusted as necessary, but did not warrant a complete remap of the bedrock topography. During the evaluation of the sinkhole data, it was noted that the identified sinkholes took on numerous surficial expressions. The IGS utilized electrical resistivity (ER) methods to investigate the subsurface character of several sinkholes with different land uses and surficial material cover. As part of the study, the newly produced sinkhole coverage was used to validate the karst susceptibility map.

| 17. Key Words | 18. Distribution Statement |
|---|---|
| Iowa, sinkholes, karst, surficial geology, bedrock geology, Worth County, Cerro Gordo County, Mitchell County, Floyd County | No restrictions. |

| 19. Security Classif. (of this report) | 20. Security Classif. (of this page) | 21. No. of Pages | 22. Price |
|---|---|---|---|
| Unclassified | Unclassified | 74 | |

Form DOT F 1700.7 (8-72) Reproduction of completed page authorized

**TABLE OF CONTENTS**

## LIST OF FIGURES

## LIST OF TABLES

## LIST OF APPENDICES

## ABSTRACT

The Iowa Geological Survey (IGS) updated the sinkhole coverage and karst susceptibility map for a four-county area in north-central Iowa including Worth, Cerro Gordo, Mitchell, and Floyd counties (Figure 1). Results more than doubled the number of mapped sinkholes and significantly refined the karst susceptibility map for the region. This work was enhanced due to recent surficial and bedrock geologic mapping completed by the IGS as part of the United States Geological Survey (USGS) STATEMAP program. These recent geologic maps improved upon the Bedrock Geologic Map of Iowa (Witzke et al., 2010) and provided the basis for determining areas with bedrock that typically form karst features and sinkholes. The surficial geologic maps allowed IGS geologists to consider the characteristics of surficial geologic materials when identifying areas with high karst potential, whereas previous karst assessments had only considered the thickness of surficial materials.

The IGS evaluated the location and accuracy of data points in the IGS GeoSam database. A series of horizontal to vertical spectral ratio (HVSR) passive seismic points were also collected to check the depth to bedrock in areas of limited data. The 25 foot contour bedrock elevation map produced by previous mapping efforts was adjusted as necessary, but did not warrant a complete remap of the bedrock topography. During the evaluation of the sinkhole data, it was noted that the identified sinkholes took on numerous surficial expressions. The IGS utilized electrical resistivity (ER) methods to investigate the subsurface character of several sinkholes with different land uses and surficial material cover. As part of the study, the newly produced sinkhole coverage was used to validate the karst susceptibility map.

## INTRODUCTION

Sinkholes are a prevalent problem in certain geologic terrains that can result in large and costly impacts to infrastructure (Weary and Doctor, 2014). The USGS estimates an average annual cost of at least 300 million dollars related to sinkhole damage over the last 15 years (https://www.usgs.gov/faqs/how-much-does-sinkhole-damage-cost-each-year-united-states?qt-news_science_products=3#qt-news_science_products). Sinkholes may take on a variety of shapes and sizes, but are generally related to certain rock types or specific geologic formations. The thickness of Quaternary cover is also a significant factor. Achieving a better understanding of this relationship has the potential to inform design engineers and mitigate infrastructure failure.

Iowa's varied geologic settings and history have resulted in a range of potential hazards to public safety and infrastructure. As such, the Iowa Geological Survey (IGS) undertook a study to identify sinkholes and update the karst susceptibility map in north-central Iowa including Worth, Cerro Gordo, Mitchell, and

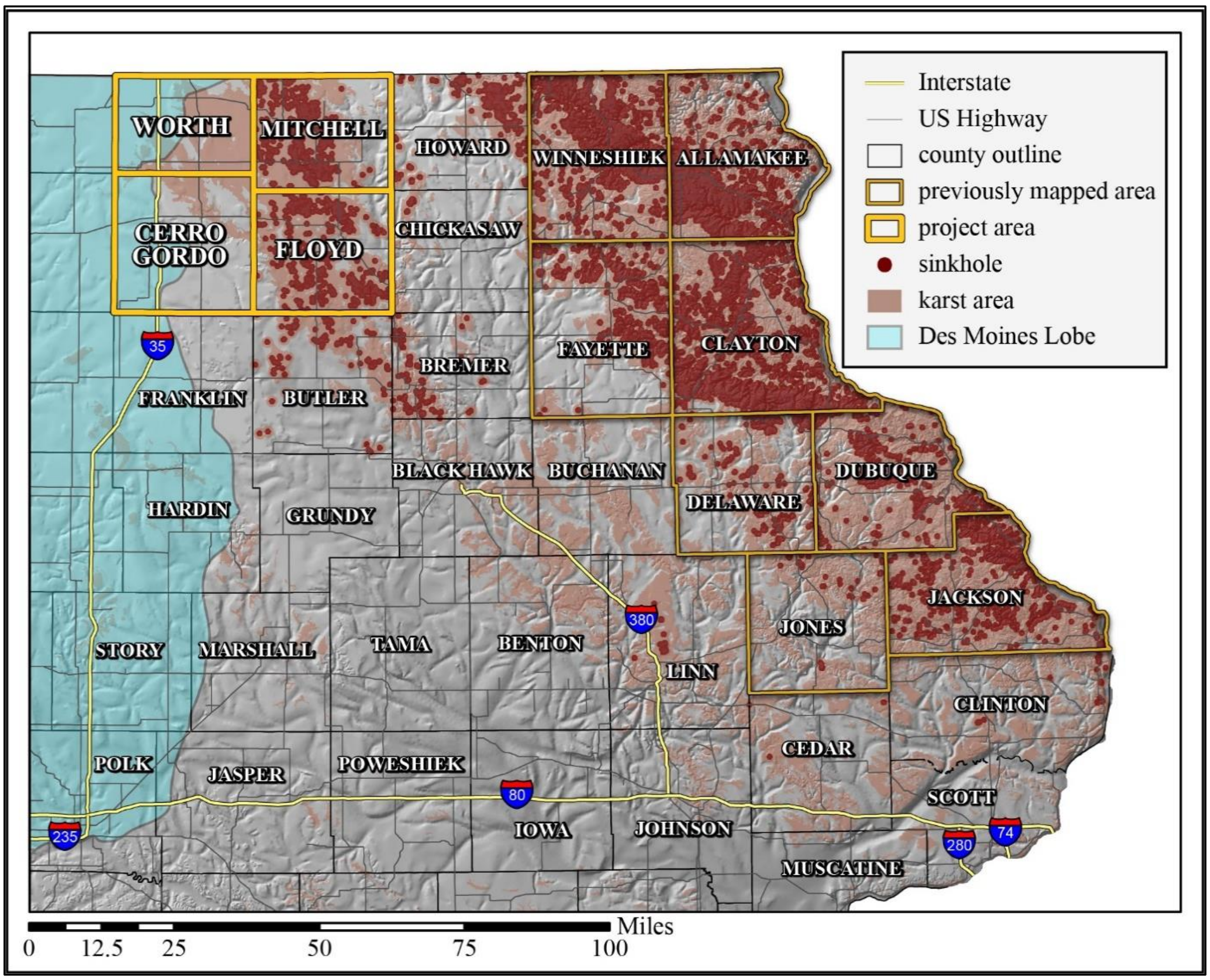


*Figure 1: Map of northeast Iowa showing the existing sinkholes (red) and karst areas (pink). The previously mapped eight county area is outlined in yellow and the current four county project area is outlined in bold yellow. The Des Moines Lobe is shown in blue.*

Floyd counties. The natural dissolution of near-surface carbonate bedrock (limestone and dolomite) can lead to surface subsidence and the formation of sinkholes, caves, and disappearing streams, collectively known as karst. Damage to roadways, retaining walls, and other infrastructure in Iowa has occurred from sinkhole collapse. The IGS receives numerous information requests each year related to sinkholes and subsidence and has completed several geophysical investigations in recent years (Vogelgesang et al., 2020; Vogelgesang and Clark, 2012). Identifying karst prone areas and mapping sinkholes will assist the Iowa Department of Transportation (IDOT), county hazard mitigation planning, and infrastructure design.

Current hazard maps and GIS coverages are incomplete or out of date. The original sinkhole data for Iowa was based on the Natural Resource Conservation Service (NRCS) county soil surveys. These data have proven to vastly underrepresent the number of sinkholes in Iowa. The availability of LiDAR (Light Detection and Ranging), updated geologic maps, and bedrock topography coverages, combined with historic aerial photos and other datasets allowed for substantial improvements to the existing sinkhole dataset.

This research project consisted of three primary objectives:

- **Sinkhole Identification**- this effort was designed to identify sinkholes and depressions in the project area by utilizing all available resources and more recent data sets.
- **Karst Susceptibility Mapping**- even if a sinkhole is not readily visible, a region may still be prone to karst development. This map is intended to categorize zones within the project area that are likely to form karst features even if sinkholes are not identified. Delineations were determined by utilizing the IGS's data and knowledge of the regional geologic units and depth to bedrock.
- **Field Assessment of Mapped Sinkholes**- the IGS utilized geophysical methods to evaluate the subsurface character of several sinkholes to better understand their expression.

## PREVIOUS WORK

The first comprehensive sinkhole mapping project by the IGS was completed in 1982 (Hallberg and Hoyer). As part of that effort, sinkholes were mapped in a 22 county area in northeast Iowa. A total of 12,700 sinkholes were identified based on soil surveys, IGS color infrared aerial photography, and published and unpublished reports containing field identification. Comparison with bedrock geologic maps showed that the highest concentrations of sinkholes occurred in three areas: the Silurian rocks in southern Clayton and eastern Fayette counties; Ordovician Galena Group rocks in southwestern Allamakee County and portions of Clayton and Winneshiek counties; and Middle Devonian rocks adjacent to the Cedar River in Mitchell, Floyd, Chickasaw, and Bremer counties. Lithology, erosional relief, and thickness of Quaternary materials were identified as primary factors in the distribution of sinkholes in these areas.

The availability of LiDAR initiated a project by the Iowa Department of Natural Resources (IDNR) that mapped an eight county area in northeast Iowa (Figure 1) nearly ten years ago. This mapping identified 33,729 sinkholes, but was never completed for the remainder of the state. This effort provided a large improvement on the total number of sinkholes identified and helped contribute to the NE Iowa Watershed and Karst Map (Hruby et al., 2010) that is used by state regulators to determine whether to permit confined animal feeding operations (CAFOs) in the region. However, the remainder of the state still relies primarily on county soil survey data which may be more than 30 years old, predating LiDAR, and varies from county to county. These sinkhole and karst potential shapefiles are available on the Iowa GEODATA website (https://geodata.iowa.gov/). The surficial and bedrock geology of the Upper Iowa River Watershed was mapped in 2011 which included mapping sinkholes and springs (Wolter et al., 2011).

From 2010 until 2018, the IGS mapped the surficial and bedrock geology of a four county area (Worth, Cerro Gordo, Mitchell, and Floyd) in north-central Iowa as part of the USGS STATEMAP program (Quade et al., 2012; Liu et al., 2012, 2015, 2018; Tassier-Surine et al., 2015, 2016; Clark et al., 2016; Kerr et al., 2018). This area includes several transportation corridors (portions of state highways 9, 27, and 14; US highways 18, 65, and 218; and Interstate 35) and population centers (Clear Lake, Mason City, and Charles City) and is known to have a large number of sinkholes that could impact existing roadways and infrastructure. Additionally, the bedrock topography (aka the elevation of the bedrock surface) was mapped at a 25 foot contour interval for these counties, improving upon the previous statewide bedrock topography which used a 50 foot contour interval. Depth to bedrock data is further improved for this area as hundreds of GeoSam data points were more accurately located during these recent mapping efforts. The combination of new data sources provided the opportunity for the development of a much more comprehensive sinkhole and karst potential map. For the current project, the four county area was surveyed by the same methods utilized by the IDNR within the eight county area in 2010. This procedure, coupled with more accurate bedrock subdivisions and surficial material characterization created during recent STATEMAP mapping and the revised 25 foot bedrock topography coverage, allowed for improved identification and characterization of sinkholes and karst prone areas.

## GEOLOGIC SETTING

The surficial geology of the region has a complex history. The four county area straddles two landform regions, the Des Moines Lobe (DML) and the Iowan Surface (Figures 2 and 3). The DML consists of glacial materials deposited during the most recent glacial advance (Dows Formation). Due to the thickness of these deposits, it was not investigated as having potential for sinkholes. East of the DML lies the Iowan Surface, which consists of a series of glacial till units and outwash associated with the younger DML glacier advance. As many as seven glacial advances occurred during the Pre-Illinoian Episode between 0.5 and 2.6 million years ago (Wolf Creek and Alburnett formations). In portions of all four counties, the Pre-Illinoian materials are overlain by the younger Mid-Wisconsin Sheldon Creek Formation. These materials cover most of Worth and Cerro Gordo counties and the western two thirds of Mitchell and Floyd counties. During the formation of the Iowan Surface, this area underwent erosion and colluvial processes related to a period of intense cold and periglacial conditions. Superimposed on top of these

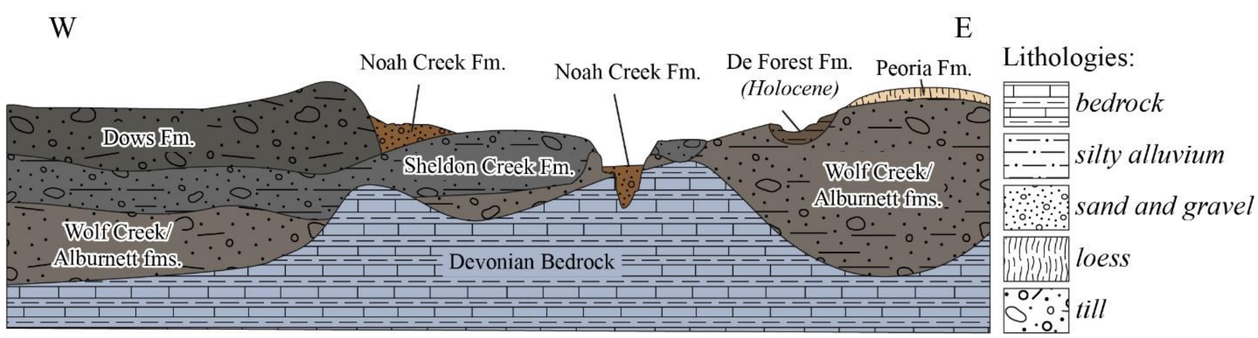


*Figure 2: Generalized cross-section showing the Quaternary stratigraphic units in the project area. The cross-section extends west to east from the DML landform region onto the Iowan Surface.*

glacial till deposits are a series of intermittent sand and gravel bodies associated with these erosional events. Also of importance for this project are the outwash deposits (Noah Creek Formation sand and gravel) related to the later advance of the DML glacier during the late Wisconsin. As a result, significant sand and gravel bodies, outwash terraces, and fan deposits are present, primarily in Worth County. These materials would not inhibit water movement, regardless of thickness, which could lead to karst and sinkhole formation in the underlying bedrock.

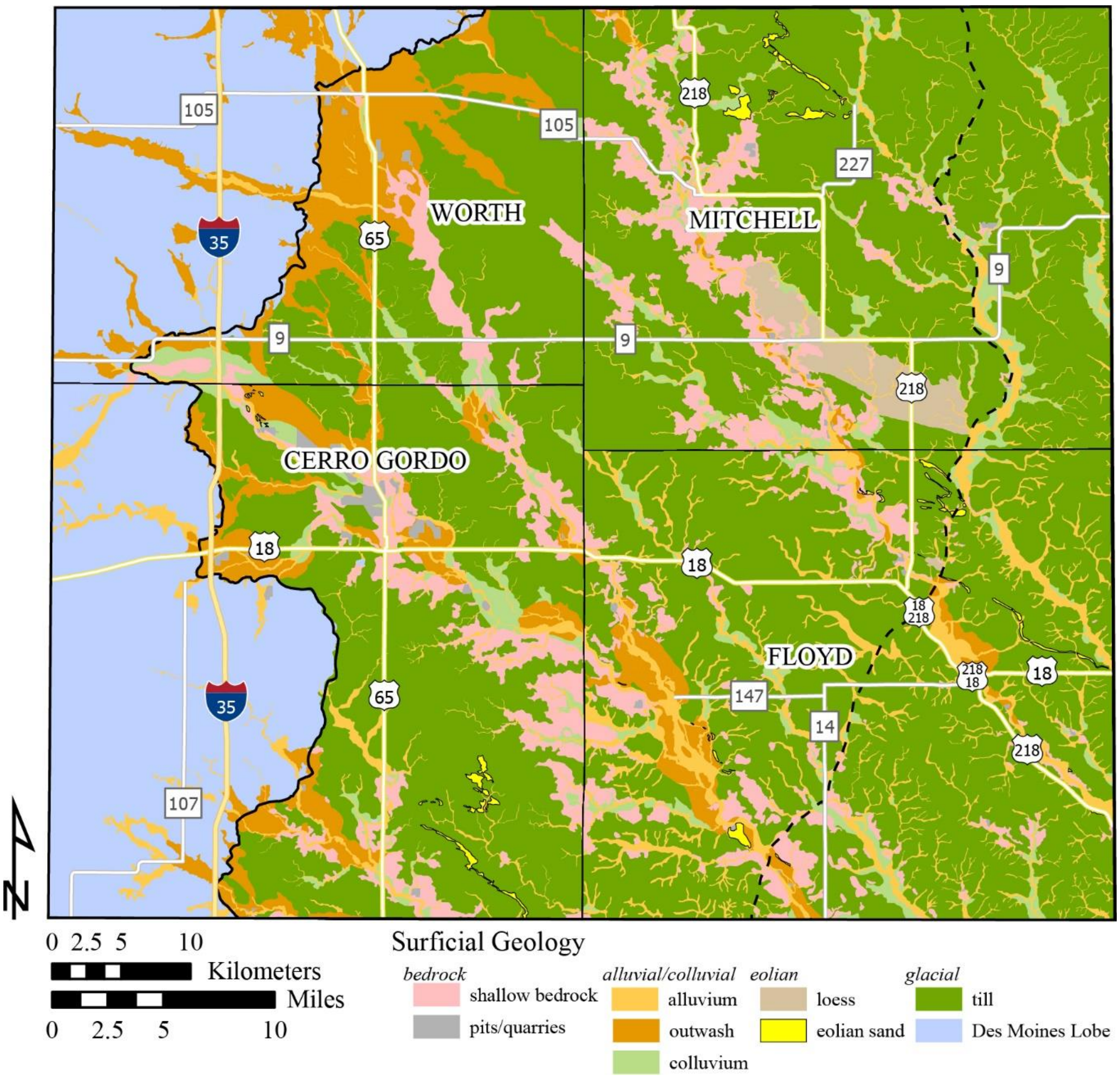


*Figure 3: The surficial geologic map of the project area grouped in to basic lithologies. The solid black line represents the boundary of the Des Moines Lobe. The dashed line represents the boundary between the Sheldon Creek Formation to the west and the Pre-Illinoian Wolf Creek/Alburnett formations to the east.*

Paleogeographically, the four-county project area lies within the Devonian Iowa Basin, a region of thickened shelf carbonate and shale that was deposited from the Late Eifelian through early Frasnian stage (Witzke et al., 1988). The Devonian strata in the project area are (in ascending order) the Little Cedar, Coralville, Lithograph City, Shell Rock, and Lime Creek formations (Figures 4 and 5). Wapsipinicon Group strata occur at the bedrock surface only in a deep channel along the eastern edge of the project area and likely have no impact on karst susceptibility. Unfossiliferous, lithographic to sub-lithographic limestones occur in several formations; most notably the Idlewild Member of the Lithograph City Formation and the Owen Member of the Lime Creek Formation. Originating from pure lime mudstones in shallow marine environments, these highly soluble rocks can occur with thin interbedded shales that have little to no ability to inhibit karst development. Dolomitic lithologies are also prevalent throughout the Cedar Valley Group. The only notable shale units within the project area belong to the Lime Creek Formation, in particular the Juniper Hill Member. The Cerro Gordo Member exhibits wide lithologic variability, both laterally and vertically, including shale, limestone, and dolomitic limestone.

Erosional outliers of Cretaceous age strata overlying Devonian rocks occur within the project area and typically consists of sandstone, shale/mudstone, and conglomerate. Many of the sandstone and conglomeratic units are cemented with iron. Cretaceous outliers are not considered to be susceptible to karst, unless they are thin enough to allow karst features in underlying Devonian carbonate units to propagate to the surface.

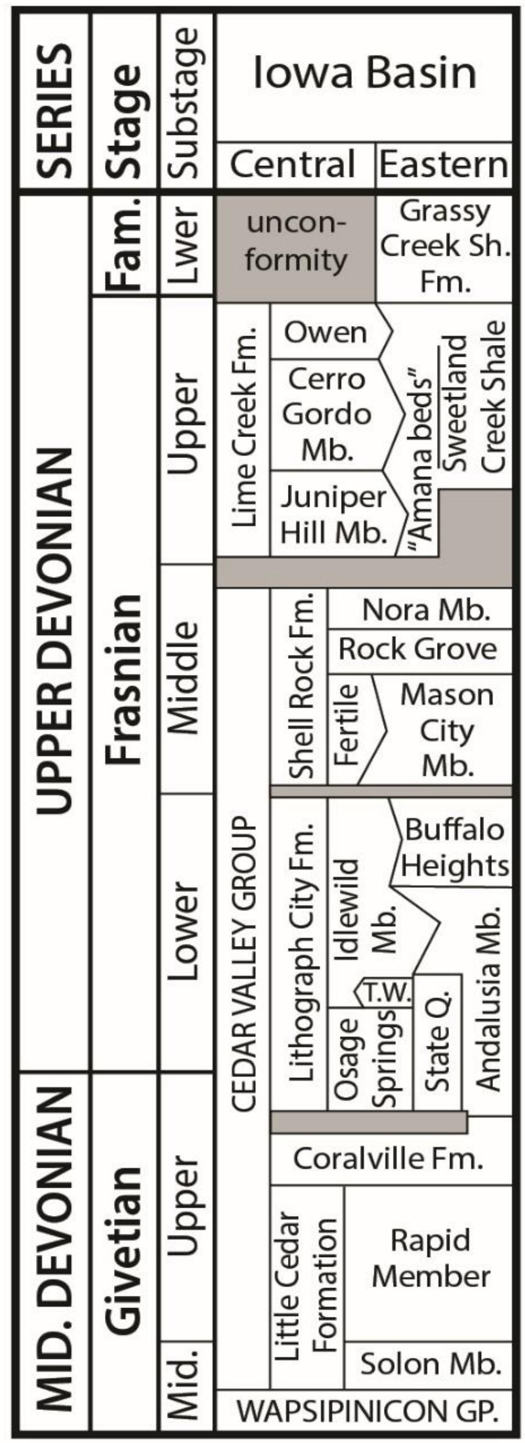


*Figure 4: Lithostratigraphic correlation chart of Middle and Upper Devonian strata of the Iowa Basin. Modified from Day et al., 2008.*

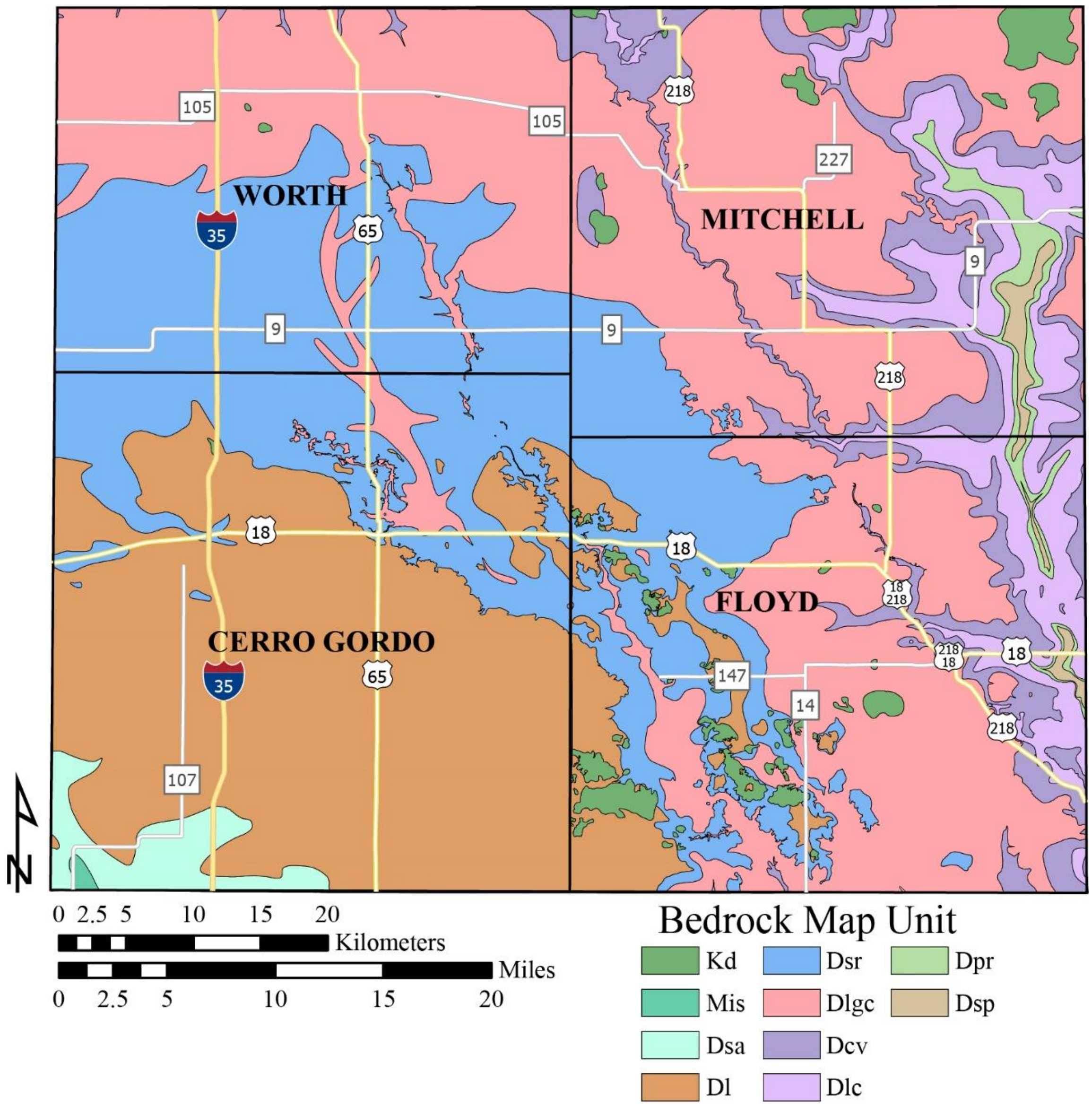


*Figure 5: The 1:100,000 scale bedrock geologic map of Worth, Cerro Gordo, Mitchell, and Floyd counties.*

## METHODOLOGY

The research plan was divided into three primary objectives: 1) Sinkhole Identification, 2) Karst Susceptibility Mapping, and 3) Field Assessment. Each objective consisted of a series of phases that built upon each other. As necessary based on the acquired data, each phase was revisited when new data evaluation suggested that an update was warranted.

### Sinkhole Identification

Phase 1 of sinkhole identification consisted of a desktop ArcGIS exercise to identify depressions (Figure 6). Data sets included the NRCS SSURGO spot symbols, LiDAR digital elevation models (DEM), LiDAR Hillshade, LiDAR fill difference, nine sets of aerial images (1930s, 1950s, 1960s, 1970s, 1980s, 1990s,

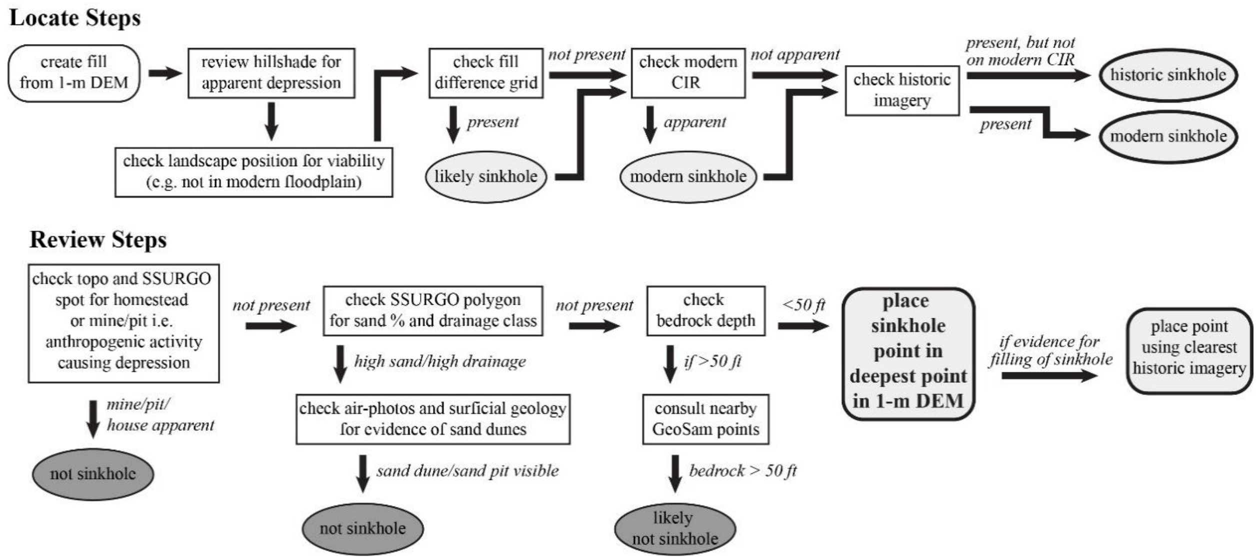


*Figure 6: Flow chart showing the decision making process for sinkhole identification.*

2002, 2010, and 2018), USGS 1:24,000 topographic maps, and continuous vegetation coverages. The LiDAR fill difference file was generated using the fill tool and subtracted from the DEM in ArcMap (Figure 7). The fill tool calculates the relative difference of elevation values between cells to create a raster that removes non-contributing areas to the watershed, i.e., it fills in topographic depressions. The difference between this raster and the original DEM is then calculated and used to visually locate sinks. During Phase 1, all depressions were included regardless of the possible interpretation for their formation. Data points were only removed if the fill difference value was determined to be erroneous, e.g., clearly caused by road ditches or a pit/quarry. Data fields were appended to the sinkhole shapefile to indicate which of the categories was present for each data point.

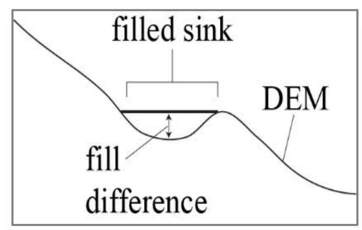


*Figure 7: An illustration of the sink fill tool. The fill difference represents the value between the created raster without sinks and the original DEM.*

Phase 2 of sinkhole identification included verifying the data set generated during Phase 1 and was completed with a geologic interpretation in mind (Figure 8). Both phases were a sequential process as outlined in Figures 6 and 8. The initial identification was based on the DEM and hillshade files which would identify a modern depression. Historic aerial imagery was then checked to identify historic sinkholes, those that may have filled in naturally or by human activities and are not currently visible. During this check, anthropogenic depressions were also identified. These would include homestead features such as basements, dug pits or mines, as well as infrastructure features such as culverts or drainage ditches. If one or more of these sources indicated a sinkhole, the surficial geology of the site was considered. The surficial geologic unit was assessed using the IGS 1:100,000 scale surficial geologic maps and then compared to the NRCS SSURGO data. The sand percent and drainage class of the soil series were evaluated from the NRCS county soil survey maps (Buckner and Highland, 1976; DeWitt, 1981; Voy, 1975, 1995). For example, several locations in the mapping area include eolian sand bodies that are mapped either by the county soil surveys or IGS county surficial maps (Quade et al., 2012; Tassier-Surine et al., 2015, 2016; Kerr et al., 2018). In these locations, depressions may have formed in the intra-dune areas and are not related to karst formation or sinkholes. Depressions were also identified in valley settings where outwash sand and gravel are mapped. Questions arose as to whether these depressions were related to sand deposition and erosion or were related to the underlying bedrock. The mapped bedrock geologic unit and depth to bedrock were also considered in this stage. If the depth to bedrock was greater than 50 feet and/or not a karst prone unit, other possibilities for the depression were evaluated. If the location indicated a carbonate bedrock unit and a reasonable depth (<100 ft) to bedrock, it was categorized as a sinkhole.

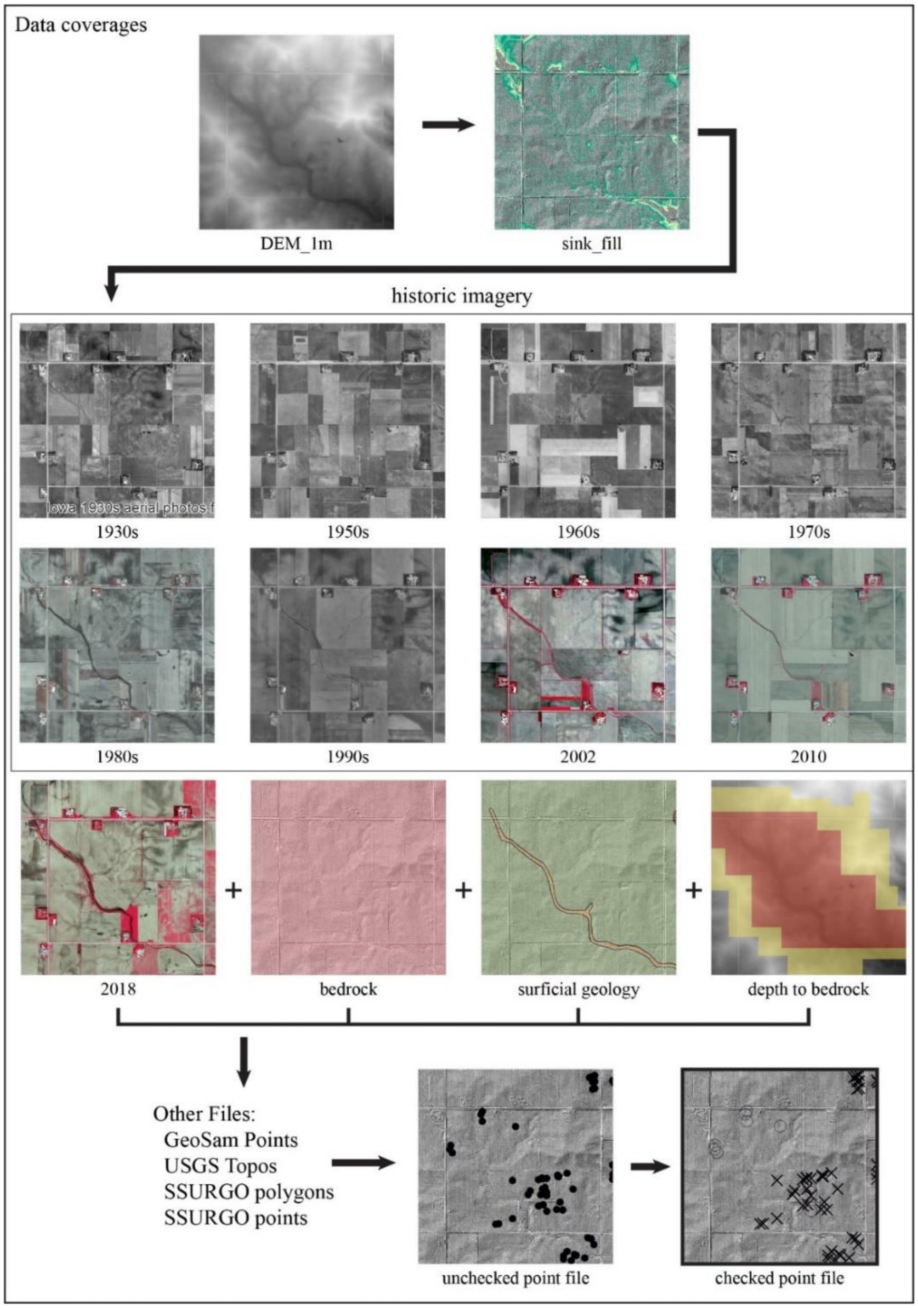


*Figure 8: Data sources used for Phase 2 sinkhole identification.*

## Well Locations

The IGS GeoSam database of well drilling records is the primary source for subsurface geologic data in Iowa. Previous mapping work has shown that establishing the accuracy of the well point locations is critical to the quality of mapping. Based on the early results from Phase 1 of the sinkhole identification objective, it was decided to reevaluate the well locations in the IGS GeoSam database for the project area. The GeoSam points in Mitchell and Floyd counties were already vetted during the recent STATEMAP projects and were not reexamined. Well records in Worth and Cerro Gordo counties were evaluated for locational accuracy and corrected as needed. Points that had an associated striplog or quality driller's log were given priority. The well points were matched to their plotted location using historic plat books, county assessors' information, notes on the driller's logs, and if necessary, contacting landowners.

## Geology

Upland surficial mapping units consisting of glacial till or till derived sediments (erosion surface sediments) are either Pre-Illinoian till (Qwa2, Qwa3) or Sheldon Creek Formation deposits (Qsc2). These materials do not readily transmit water and were not considered prone to forming karst unless they were less than 25 feet thick over carbonate bedrock. Thin alluvial (Qal) or organic sediments (Qo) located on the uplands were grouped with the till due to their fine-grained nature and being typically less than ten feet to a less permeable unit. While the colluvial units (Qnw2) contain some coarse materials, they are not considered karst susceptible and usually overlie less permeable till. Mapping units that consist of a significant thickness of sand and gravel (Qalit, Qali-ht, Qoch, Qof, and all Qnw units) or sand and gravel directly on top of bedrock (Qnw3, Qalb, Qbr) were included in the high karst susceptible category if the depth to bedrock was less than 50 feet. Eolian units (Qps1, Qe) are found in both the valley and upland and may consist of either loess (silt-sized) or fine sand materials transported by wind. In areas where these deposits are relatively thick (>10 feet) they often occur as dune features. In these settings, intra-dune depressions are often present, but do not indicate a sinkhole. Eolian units are assigned to the valley or upland designation based on their landscape position. Particular care was taken when reviewing driller's logs that indicated clay overlying shale bedrock because the Devonian Lime Creek Formation, the only unit containing thick (>10') shale in the area, was not thought to extend in into Worth County. As such, the 'shale' in the logs was assumed to be Pre-Illinoian till when determining the depth to bedrock. Drilling efforts during the Worth County mapping projects confirmed this to be the case. Surficial geologic mapping units were grouped based on their landscape position (Figure 9) in order to better characterize them with regard to karst susceptibility.

Bedrock units likely to promote karst forming materials include the Devonian Little Cedar (Dlc), Coralville (Dcv), Lithograph City (Dlgc), Shell Rock (Dsr), and Lime Creek (Dl) formations (Figure 5). Based on the distribution of sinkholes in Cerro Gordo and Floyd counties, further evaluation of the Lime Creek Formation was conducted as it is contains both shale and carbonate intervals which were not differentiated as separate mapping units on the county scale bedrock geologic maps. The Lime Creek Formation consists of three distinct members (in ascending order): the Juniper Hill, Cerro Gordo, and Owen. The basal unit, the Juniper Hill Member, is primarily a shale and is not considered to be karst prone. The Cerro Gordo Member is a mix of carbonate (limestone and dolomite) and interbedded shale, with facies variation occurring both horizontally and vertically. The upper unit, the Owen Member, is a sub-lithographic limestone that is susceptible to forming karst. In order to account for the lithologic

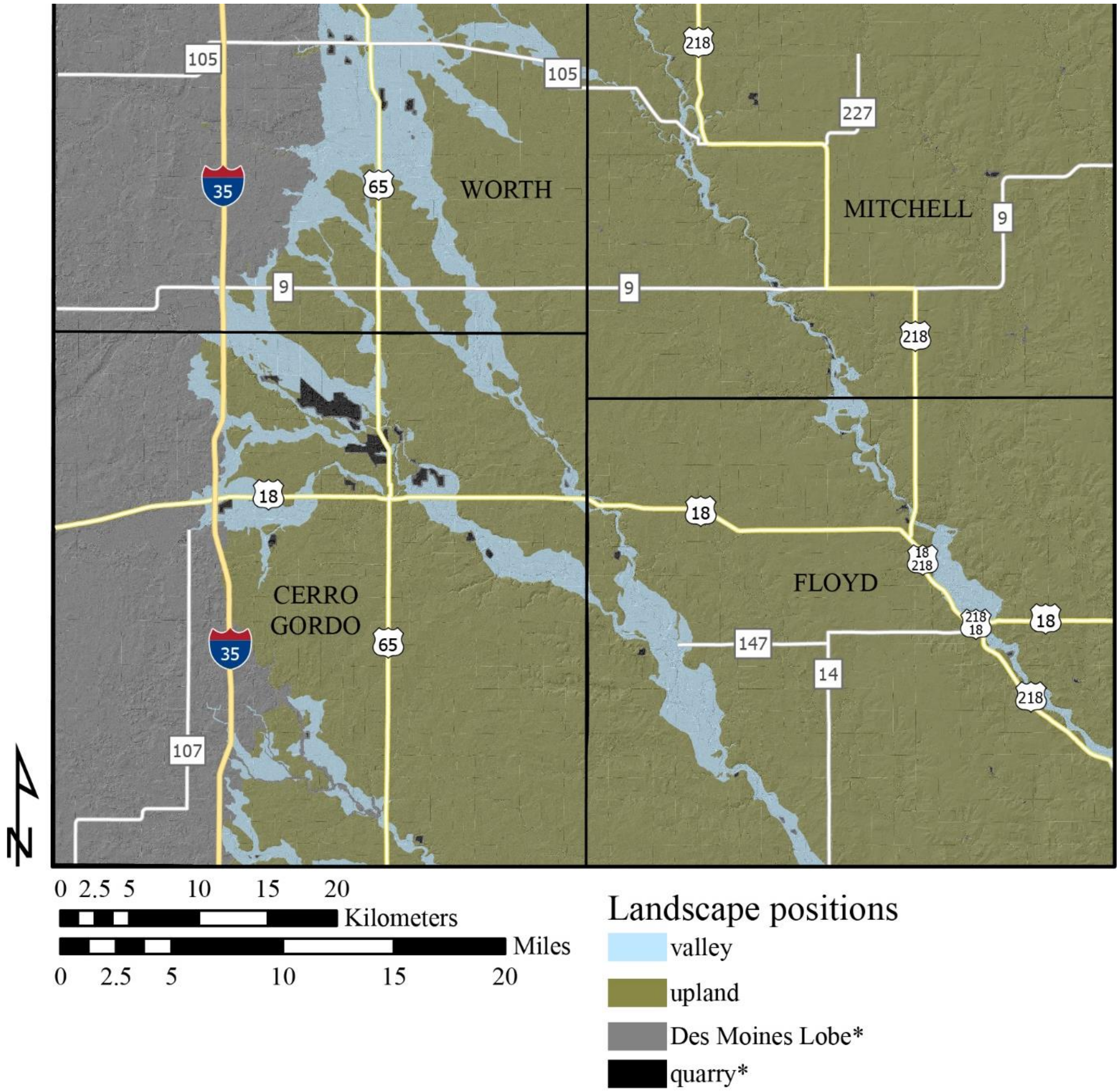


*Figure 9: Map of the landscape position of the area. Derived from the 1:100,000 scale surficial geologic maps of Worth, Mitchell, Cerro Gordo, and Floyd counties. The Des Moines Lobe and quarry locations were not considered in this project.*

differences, the IGS subdivided the Lime Creek Formation based on its members (see the results section). Two hundred wells containing the Lime Creek Formation were checked for accuracy and the top bedrock unit was denoted. The purpose of mapping the members of the Lime Creek Formation was to help correlate depressions with a more refined understanding of the underlying bedrock lithologies.

## Geophysics

## Electrical Resistivity (ER)

ER geophysical investigations were conducted to help characterize sinkholes and depressions identified during Phase 2 of the sinkhole identification objective. Karst related voids, such as sinkholes, filled with soil or other surficial materials can be anomalously conductive when compared to surrounding competent bedrock, which is generally resistive. ER geophysical surveys were completed at three sites:

the private property of Dennis Rachut west of the town of Osage, Mitchell County Conservation Board (CCB) property south of the town of Mitchell, and the Falk Quarry property south of the town of Northwood. The Rachut property is a farmed site with sinkholes and depressions and a mapped depth to bedrock of less than 25 feet, but with subdued topography and no bedrock outcrop nearby. The Mitchell CCB property has sinkholes with good surface expression and bedrock exposures close to the site. The Falk property has shallow bedrock and identified sinkholes, but differs from the other two sites in that the surficial materials are sandy as opposed to till or till-derived sediments. The IGS chose these sites to give a variety of sinkhole types to compare in the ER evaluation. Several ER lines were conducted at each property. Two lines were completed at the Rachut property, each crossing a different sinkhole/depression. The first was readily visible on various sources in Phase 1 and the second was less obvious. At the Mitchell CCB property two lines were run crossing sinkholes and an additional line was run perpendicular between two sinkholes to evaluate potential connectivity that is not apparent on the surface as a depression. Three lines were run at the Falk site, two crossing the same sinkhole perpendicular to each other, and a third crossing a different sinkhole.

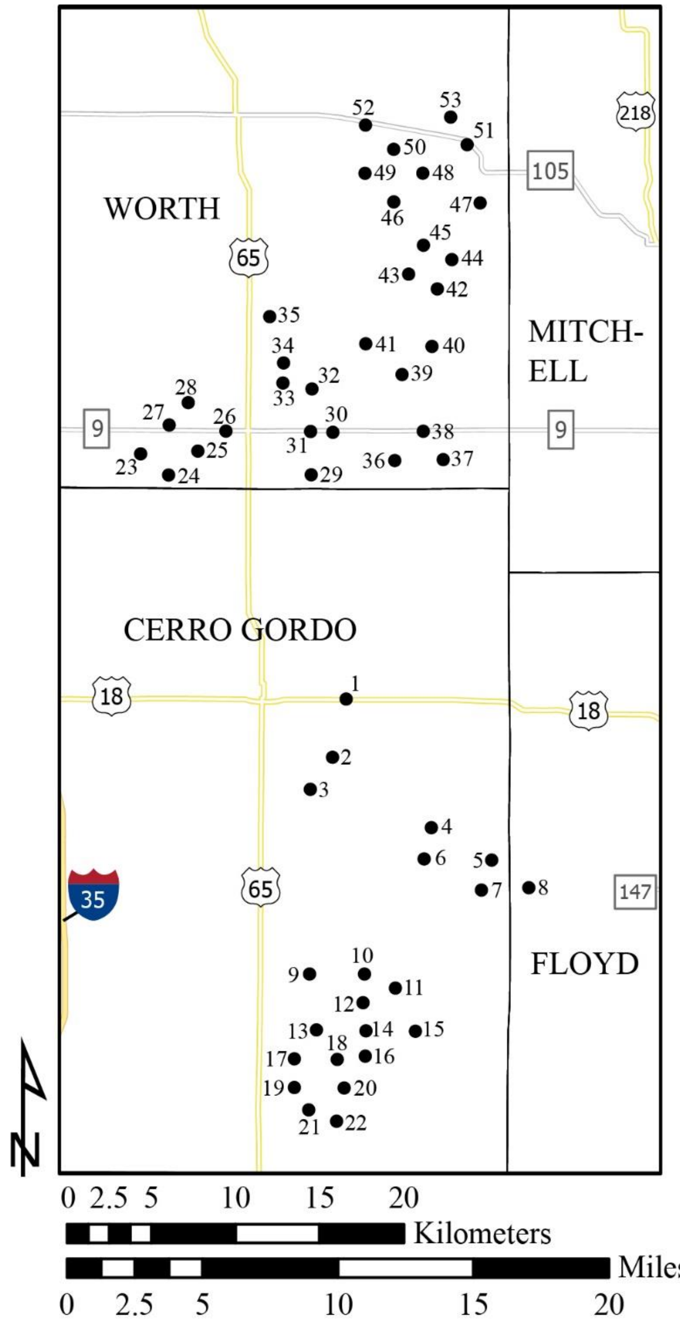


*Figure 10: Locations of passive seismic collection sites.*

An Advanced Geosciences, Inc. (AGI) SuperSting R8 electrical resistivity meter was used for this investigation. An electrode spacing of 10 feet (3.0 meters) was utilized on every line except the south line at the Falk site, to ensure high-resolution data were collected and adequate depths were imaged. An electrode spacing of 10 feet (4.0 meters) was used along the south line at the Falk site. A Juniper Systems Geode precision GPS was used to identify starting, ending, and additional locations along each ER line. Field data were collected using a dipole-dipole array and processed using AGI EarthImager 2D software. Transects of sufficient length were run to obtain electrical resistivity data to depths ranging from 26 to 183 feet below the ground surface at each site.

## Passive Seismic

Horizontal to vertical spectral ratio (HVSR) passive seismic was used to aid in identifying the depth to bedrock in areas with little control from well records in the IGS GeoSam data set. Two areas of interest were targeted, one in southeastern Worth County and another in eastern Cerro Gordo County (Figure 10). During Phase 1, depressions were detected in these areas, and in some cases the depth to bedrock was mapped as greater than 50 feet, but the existing bedrock elevation contours were drawn with little control. Thus, the IGS conducted passive seismic surveys at strategic locations to confirm bedrock depths. HVSR passive seismic uses ambient (background) seismic noise to collect data related to the velocity of seismic waves through geologic materials. The data were processed using the Grilla software package wherein seismic velocity variations are calculated as unit contacts (less consolidated surficial materials on top of bedrock).

Data were collected at a series of calibration points to determine the average characteristic velocity for each surficial material (e.g., glacial till or alluvium). Boring records with a known depth to bedrock in the IGS's GeoSam database (strip logs or driller's logs) were used as calibration points. The resonance frequency was then determined from the passive seismic data at each 'unknown' station and used to calculate the bedrock depth for these sites.

Calculations are made according to the following equation which relates the shear wave velocity (Vs) of a particular unit to the resonance frequency (fo) of the site multiplied by four times the thickness of the layer (Z), in this case depth to bedrock, in meters:

$$Vs=fo(4Z)$$

The top left image in Figure 11 shows the horizontal to vertical spectral ratio. The first primary peak delimits the resonance frequency for the site. A high frequency indicates a shallow depth to bedrock and

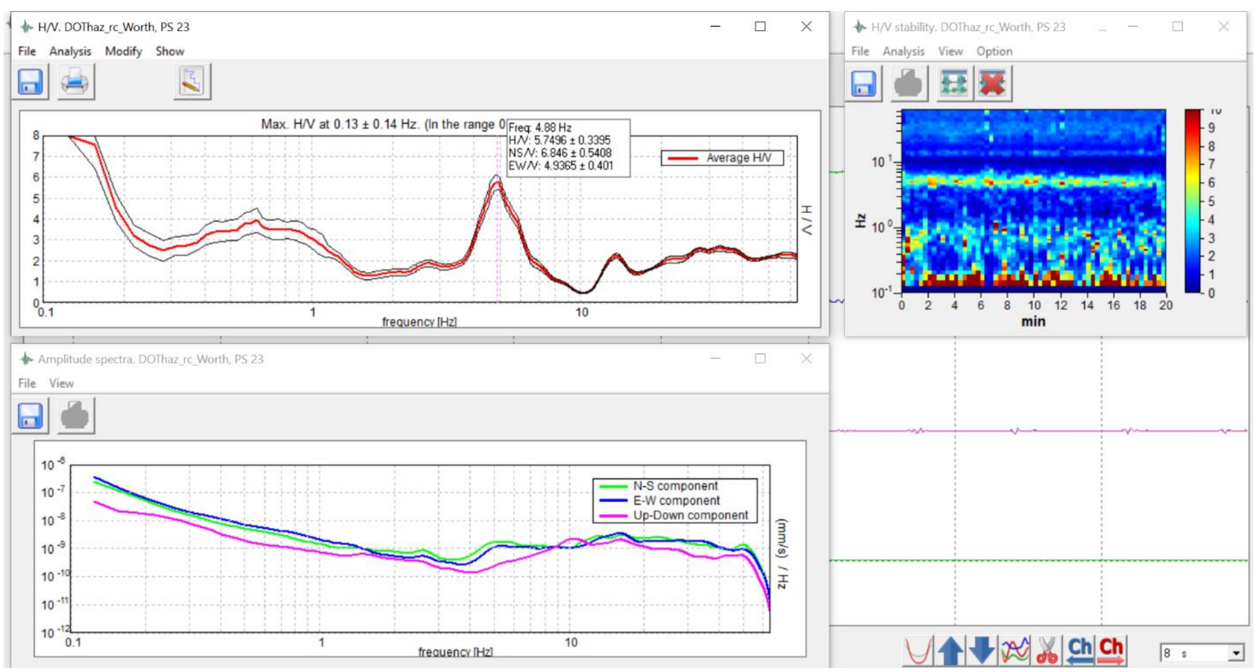


*Figure 11: An example of a passive seismic data collection point in Worth County.*

a low frequency indicates a deeper bedrock depth. The bottom left image shows the single component spectra for the horizontal north-south (NS) and east-west (EW) components, and the vertical ambient seismic noise. In a 'good' reading, the resonance frequency graph will have a single high amplitude peak with the single line spectra (on the diagram directly below) showing a separation, or 'eye', between the vertical and horizontal (NS and EW) spectra. The graphic in the top right shows the horizontal to vertical ratio throughout the length of the 20 minute data collection time period.

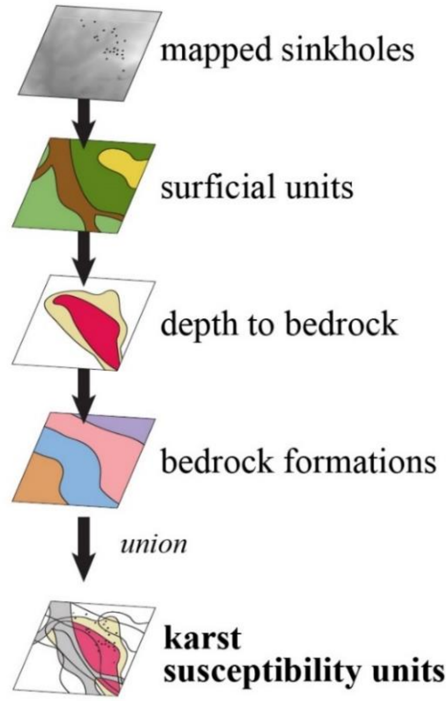


*Figure 13: Flow chart depicting the process by which multiple data sets were compiled to generate the karst susceptibility coverage.*

## Karst Susceptibility Mapping

In order to generate a karst susceptibility map, we selected data sets that would be useful to evaluate the potential for karst development. Applicable datasets included sinkhole points, surficial and bedrock geologic units, depth to bedrock/bedrock topography, and LiDAR. Production of the karst susceptibility coverage consisted of merging the pertinent data sets into a single shapefile in ArcMap using the *union* tool. This function computes a geometric union of the inputs and generates polygons based on overlaps between data sets (Figure 12). The results were then combined and new polygons were created based the overlapping boundaries and combinations of features. This created a seamless map of the four-county study area where each polygon contains attributes or values from the layers used. This resultant data set allows for each polygon to be given a karst susceptibility designation based on the combination of characteristics outlined below (Figure 13, Table 1).

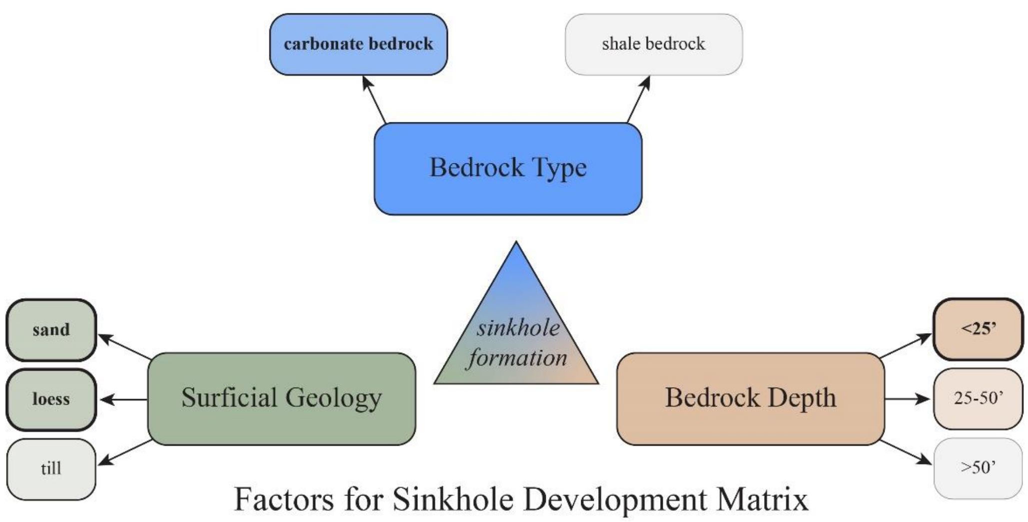


*Figure 12: A theoretical model for factors of karst formation at a given site. Variable boxes that are bold and have a greater hue are thought to lead to increased karst development.*

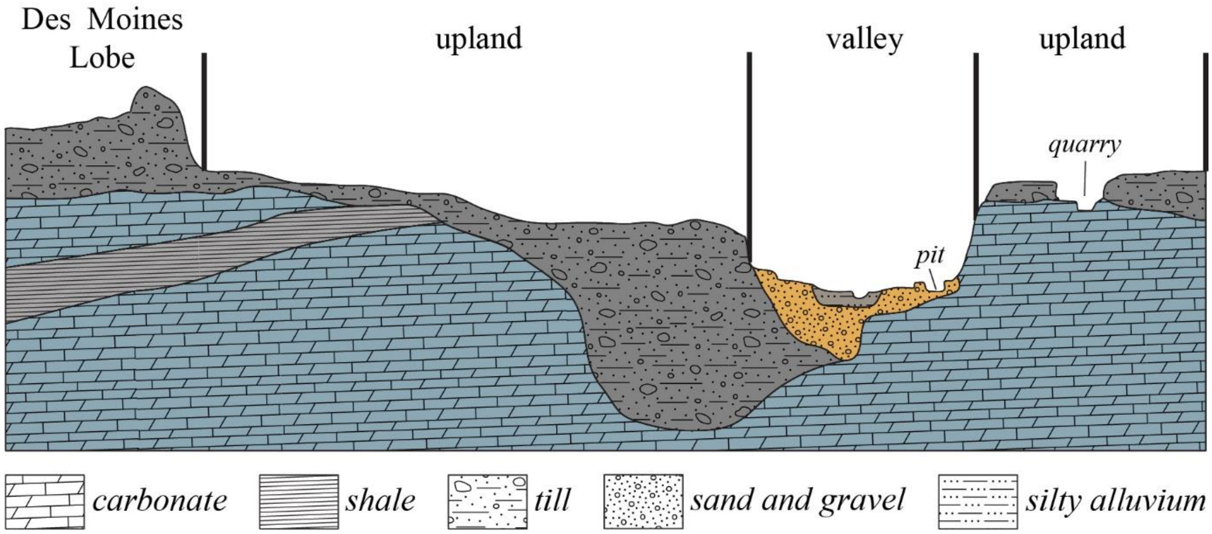


*Figure 14: A generalized cross-section showing the relationships between landscape position, surficial materials, and bedrock geology used to construct the karst susceptibility classifications.*

The surficial geologic sediments were divided into three major landform categories that related to the surficial geologic units (Figure 14): DML, upland, and outwash-valley units. These distinctions convey the difference in the surficial material properties. The DML region comprises the western quarter of the project area. This area was recently glaciated during the Late Wisconsin, resulting in thick deposits of clay-rich DML till. This relatively young landscape region is riddled with closed depressions that are not related to karst features. Therefore, our efforts were focused on the landscape to the east. The upland landscape generally consists of clay-rich glacial tills and units that have till between them and the bedrock surface. The valley units included those that are in any major river valley (Cedar, Shell Rock, Winnebago, etc.) that contained glacial outwash (primarily sand and gravel) from the Des Moines Lobe to the west. These materials are loosely consolidated and thus would more readily erode and fall into sinkholes. River valleys that did not drain the Des Moines Lobe, such as the Little Cedar and Wapsipinicon rivers, contain relatively thin deposits of coarse sand and gravel with fine grained alluvium and are consequently grouped into the upland category.

Karst susceptibility was categorized into three classifications: high, moderate, and low (Table 1, Figure 15). The designations are based on the most significant factor for karst formation for each individual mapped polygon. When considering bedrock geology, a combination of bedrock type (carbonate or shale) and depth to bedrock are the primary factors for karst formation. For upland areas underlain by carbonate, depth to bedrock is the most significant factor. Upland areas of less than 25 feet to carbonate bedrock were given a high risk classification regardless of surficial geology. The 25-50 feet depth to bedrock range over carbonate was given a moderate classification. Shale was only found underlying the upland areas. Since shale is generally not susceptible to karst, the classifications are low risk, save for the less than 25 feet category. This zone was given a moderate risk category due to the potential for localized erosion of the shale near the edges of the mapped shale units. This may expose carbonate bedrock where karst may develop. This localized effect was observed during an investigation of sinkholes near Mason City (Vogelgesang et al., 2020), demonstrating that the scale of this project may not identify every sinkhole or karst prone area existing at a site specific scale. Areas within the 'valley' designation are a combination of multiple surficial geologic mapping units, such as fine-grained alluvium and coarser grained outwash mapped in the major river valleys. These surficial units are hydraulically conductive allowing for both rapid development of karst and mobilization of unconsolidated alluvial sediments into underlying karst networks. As such, we grouped these units into two karst susceptibility designations. Areas of less than 50 feet to bedrock are classified as high risk, while areas of greater than 50 feet are classified as moderate risk. The entire DML region is considered low risk for karst susceptibility due to the young landscape and thick till deposits.

An evaluation of the karst susceptibility designations was conducted by cross-referencing the mapped sinkholes with the newly created karst susceptibility polygons. Using the spatial join function in ArcGIS, the total number of sinkholes was calculated for each polygon. The total number of mapped sinkholes was then divided by the area of each polygon to calculate the density of sinkholes per square kilometer. This produced a value of karst density for each polygon. The karst density value, combined with the underlying bedrock formation, depth to bedrock value, and surficial geologic material was used to check our karst susceptibility classifications for each designation. The scale of the karst susceptibility map is equivalent to the scale of the surficial and bedrock geologic maps (1:100,000).

*Table 1: Karst susceptibility classifications.*

| landscape position | depth to bedrock | bedrock lithology | karst susceptibility |
|---|---|---|---|
| valley | <25' | carbonate | high |
| valley | 25-50' | carbonate | high |
| valley | >50' | carbonate | moderate |
| upland | <25' | carbonate | high |
| upland | 25-50' | carbonate | moderate |
| upland | >50' | carbonate | low |
| upland | <25' | shale | moderate |
| upland | 25-50' | shale | low |
| upland | >50' | shale | low |
| Des Moines Lobe | N/A | N/A | low |
| pit/quarry | N/A | N/A | N/A |

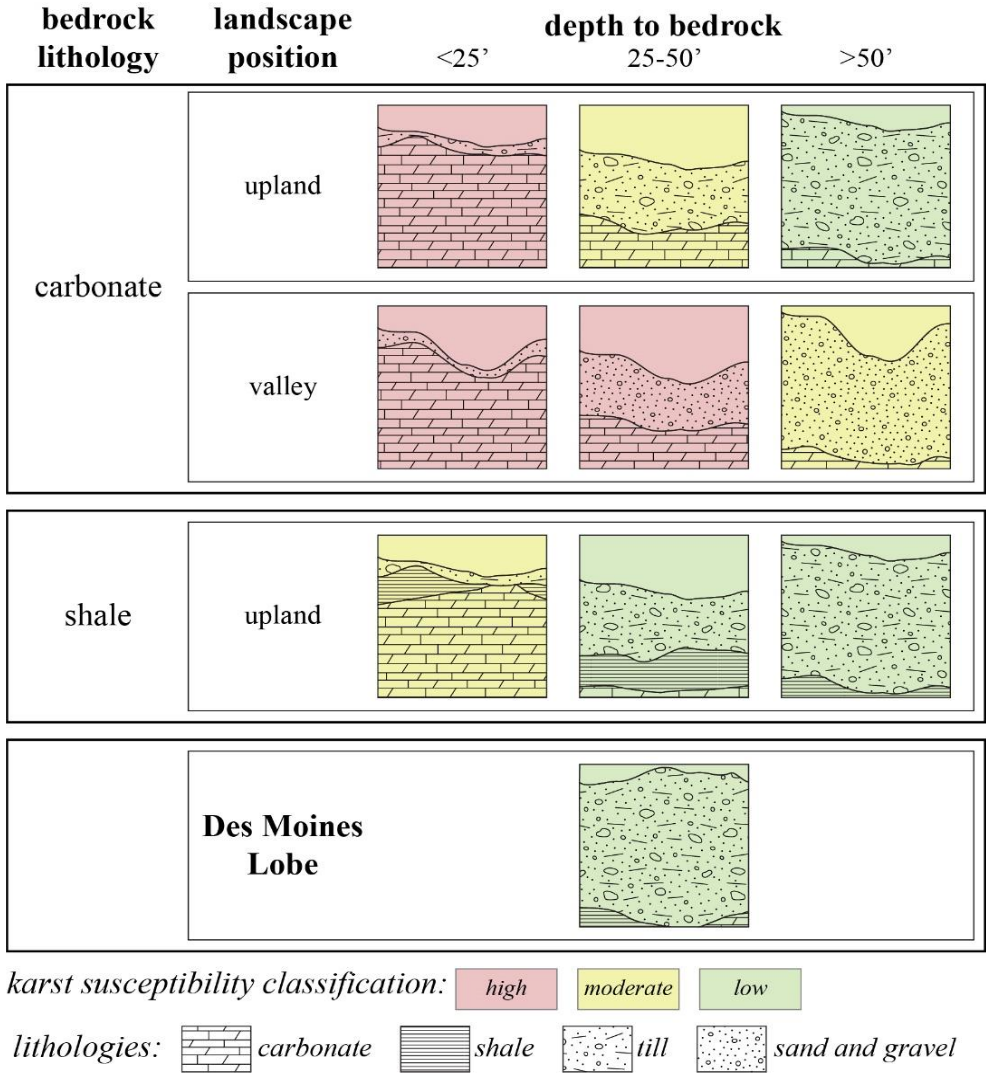


*Figure 15: A visual representation of factors for karst susceptibility. The Des Moines Lobe is not susceptible to karst and was not part of this investigation.*

# RESULTS

## Sinkhole Identification

The Phase 1 assessment identified 5,401 depressions in the four-county project area. LiDAR DEM and fill differences were the data sets that most commonly identified a depression. By tabulating the number of occurrences based on individual data sets, it gives an increased degree of confidence in those points that appeared in multiple sources and decreases the odds of a data point being subjectively selected.

The previous sinkhole data set contained 2,425 points. This file was derived from the NRCS SSURGO spot symbol data, which is often inconsistent from county to county. For example, far fewer sinkholes were

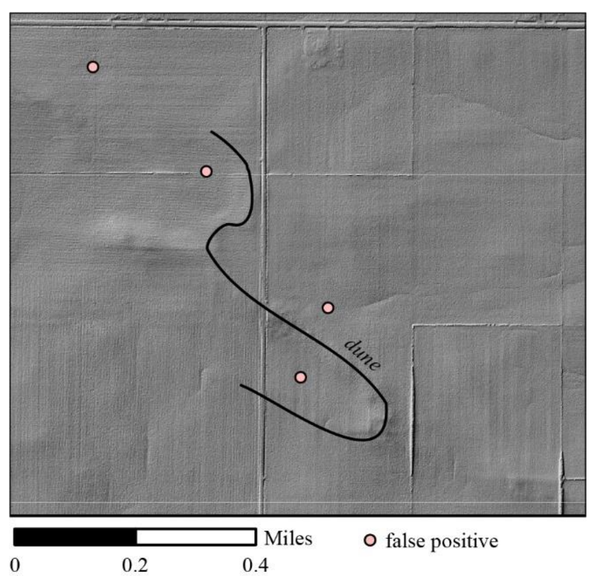


*Figure 16: An example of false positives from the fill difference coverage. Depression formed in parabolic dunes rather than sinkholes.*

mapped as spot symbols in Worth and Cerro Gordo counties when compared with Mitchell and Floyd. This is likely caused by the differences in mapping styles among individual soil mappers as the regional geology does not change significantly at the county line. It should also be noted that soil mappers often do not map heavily developed areas, creating a natural gap in coverage within city boundaries thus requiring detailed review of pre-development aerial imagery.

The new coverage contains 4,175 depressions that could be confidentially called sinkholes. This is 1,750 more than the previous coverage. Depressions not thought to be sinkholes were removed by the processes outlined in the methodology section (Figure 6). By carefully examining each depression from the initial data set, the team was able to eliminate over 1,100 points from consideration across the project area. Of these, 112 were considered 'anthropogenic' depressions, likely resulting from agricultural or urban development activities. Over 800 points were removed because they were identified as depressions related to surficial geologic features rather than from sinkhole formation. Oxbow lakes, old meander scars, parabolic dunes, and incipient gullies were the main false positives in this category. Figure 16 shows an example of depressions mapped in area with parabolic dunes in Cerro Gordo County.

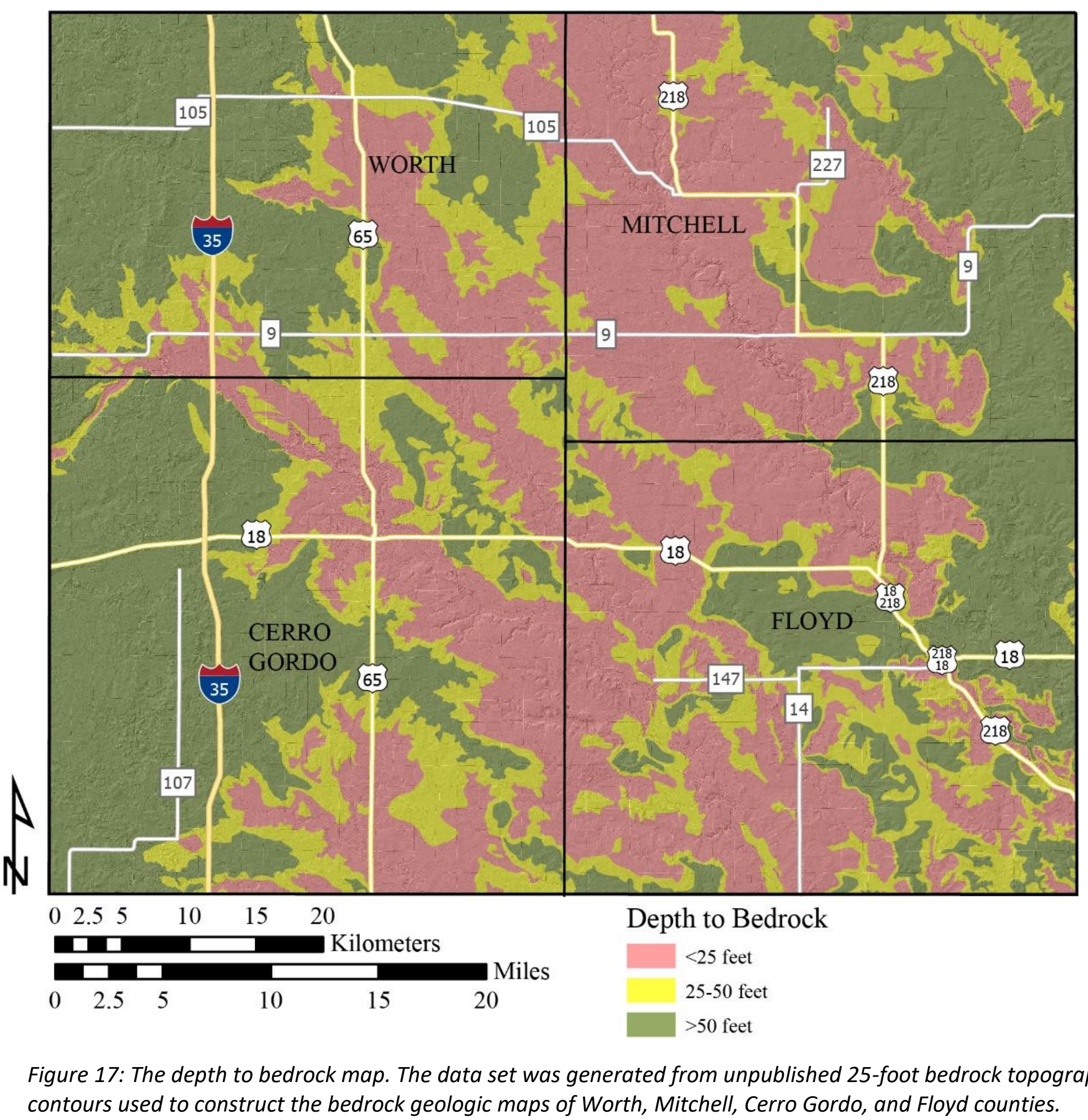


*Figure 17: The depth to bedrock map. The data set was generated from unpublished 25-foot bedrock topography contours used to construct the bedrock geologic maps of Worth, Mitchell, Cerro Gordo, and Floyd counties.*

## Bedrock Topography

### Passive Seismic

Passive seismic methods were employed in areas where subsurface data was limited. There were two primary focus areas, one in southeastern Worth County and a second in eastern Cerro Gordo County (Figure 10). A total of 53 data points were collected. Data was collected at 31 sites in Worth County (7 calibration and 25 unknowns), 21 sites in Cerro Gordo County (4 calibration and 17 unknowns), and one unknown site in western Floyd County. Due to the similarity of surficial geologic materials in the area, all ten calibration sites were designated as either till or alluvium to obtain the average seismic velocity for each lithologic designation. Seven of the calibration sites consisted of till and were averaged to yield a seismic velocity of 276 meters per second (m/s). Two alluvial sites gave an average seismic velocity of 141 m/s. These averages are similar to values calculated in other parts of the state for till over bedrock and alluvium over bedrock respectively. Two calibration sites were not used because one was too shallow to bedrock to give an accurate result and the other was taken near a boring that did not reach bedrock. The passive seismic data table and profiles are located in Appendix A.

### Well Locations

In Worth County, 644 GeoSam well points were reviewed. Of those, 184 were drilled after the statewide bedrock geologic map was completed in 2010. A total of 389 were found to be accurately located and 87 needed to be moved. Of the 150 points checked in Cerro Gordo County, 90 were correct and 50 were moved, while 10 could not be confirmed. Mitchell and Floyd counties were mapped more recently and the points in those counties had already been reviewed and validated.

Based on the relocation of wells in Worth and Cerro Gordo counties, the incorporation of data from wells drilled since the geologic mapping was completed, and the results of the passive seismic data; it was determined that the bedrock topography map for those areas did not need updating. This data was then subtracted from the surface DEM to create the depth to bedrock coverage (Figure 17).

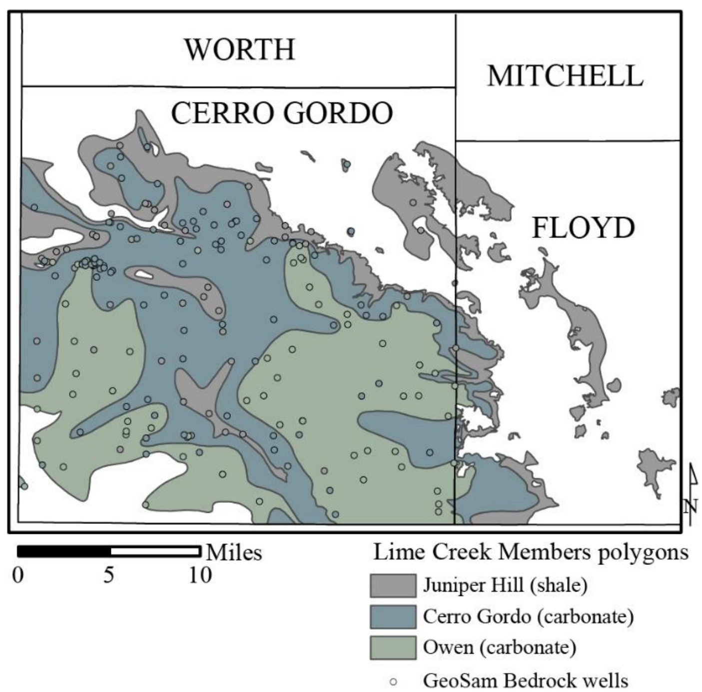


*Figure 18: Map showing the delineation of the members of the Devonian Lime Creek Formation. Circles indicate wells with lithologic descriptions used for member identification.*

### Subdivision of the Lime Creek Formation

To evaluate the role of shale in karst susceptibility, the members of the Lime Creek Formation were delineated into its three members: Owen, Cerro Gordo, and Juniper Hill. Well locations were validated as part of checking the bedrock topography. With the accurately located data, staff reviewed 235 well records that were within the area mapped as the Lime Creek Formation (Figure 18). Two hundred and fifteen of these encountered bedrock. The strip logs were reviewed and the Lime Creek Formation was redrawn with each member as a distinct mapping unit.

Surficial geologic units for till or till-derived sediments were not typically found to host sinkholes unless the depth to bedrock was less than 50 feet. Alluvial sediments, particularly those related to DML outwash, were considered karst susceptible if the underlying bedrock geologic unit was carbonate, regardless of the depth to bedrock. However, there are no mapped occurrences of shale within these river valleys, so the association is not part of the susceptibility categories.

In areas that were mapped as greater than 50 feet to bedrock but showed a large number of depressions, further evaluation of the geology revealed that eolian sand deposits had created depressions as intra-dune blowouts.

## Electrical Resistivity (ER)

The IGS completed ER assessments at three locations in the project area. Results and associated information from the ER geophysical surveys are located in Appendix B. ER was focused on evaluating the subsurface characteristics of selected sinkholes and the surrounding terrain. The IGS targeted sinkholes in a variety of settings, but all three sites were in areas where the depth to bedrock was less than 25 feet. The Rachut site represents an area that has been cultivated, and the sinkholes have been repeatedly filled in, and where there is glacial till over carbonate bedrock. The Falk site represents an area that has also been cultivated and sinkholes filled in, but where the overlying sediment package is mostly fine to coarse grained glacial outwash. The Mitchell CCB site represents an area that has not been recently cultivated. The area immediately surrounding the sinkholes is a restored prairie environment, and the sinkholes have been left alone for a long period of time.

ER survey results show how the subsurface responds to electrical charge. In general, ER results correspond well to geologic materials in the subsurface. Results can also be indicative of subsurface moisture, porosity, dissolved electrolytes, temperature of pore water, etc., and can be influenced by anthropogenic disturbances (fill material, culverts, drains, buried utilities, etc.). For these reasons, interpretation of ER data must be made alongside available site information, such as drilling data, utility maps, and other pertinent data sets. Results from each of the three sites will be discussed below. For all sites, the ER line is shown in black and the mapped sinkholes are shown as white circles. Surface profiles are corrected for elevation on all ER cross-sections. Individual nodes are designated as black dots on the surface profile. The interpreted bedrock surface is shown as a dashed line. More resistive units are red and more conductive areas appear blue. Also note that the resistivity scale is not normalized between graphics.

## Rachut Property

The Rachut property is situated in an area where the depth to bedrock is generally less than 25 feet with glacial till and/or reworked colluvial sediments over sub-lithographic limestone of the Lithograph City Formation. Two ER lines were run (Figure 19), one on the northeast side of the property (Rachut A-A' line) and one on the southwest portion of the property (Rachut B-B' line).

At the Rachut A-A' line, the orientation was north-south crossing a prominent mapped sinkhole (Figures 19 and 20). This sinkhole has been farmed around for many years and has vegetation and trees growing in it. The sinkhole dips several feet below the surrounding surface. The ER data shows a conductive zone directly below the surface depression and is interpreted to be the subsurface expression of the sinkhole.

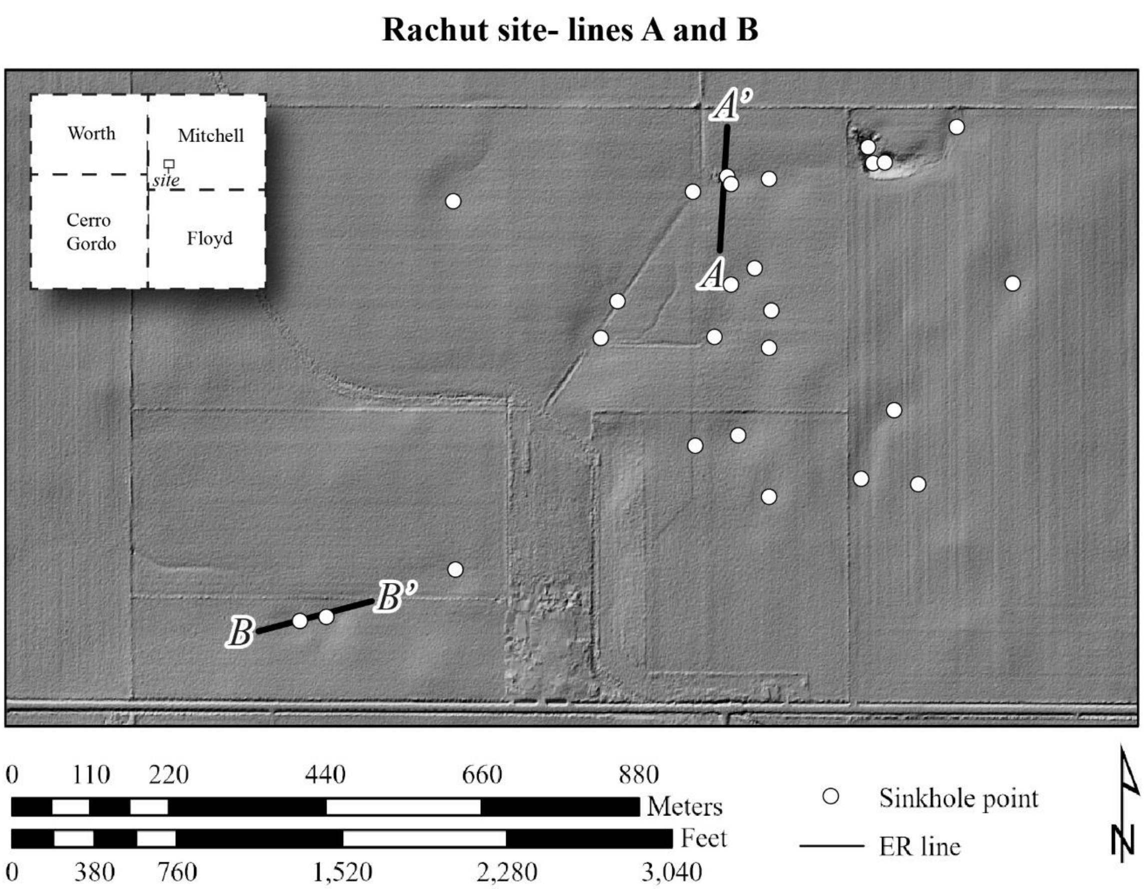


*Figure 19: Site map of the Rachut Property.*

*Figure 20: A photograph of the sinkhole from the A-A' line on the Rachut Property. Note the vegetation difference from the row-crop agriculture.*

Additionally, two other conductive zones are noted, one on each side, and may represent the formation of depressions in the bedrock surface and/or sinkholes that do not have surface expression. The bedrock surface is estimated to be 15 to 20 feet below the surface and corresponds well with the IGS's bedrock elevation map in that area.

The depression at the Rachut B-B' line does not have a strong surface expression. A small area of lower resistivity was detected below the mapped sinkhole as well as two additional areas on the edge of where the line was run. It could not be determined for certain if these were bedrock features or edge artifacts of the data. The estimated depth to bedrock is similar at this site, approximately 15 to 20 feet below the surface. It should also be noted that the density of sinkholes is much greater to the east of the Rachut property. There are no mapped sinkholes immediately to the west. This, combined with the ER results, could indicate that we are reaching the edge of the karst region.

*Figure 21: A photo showing a sinkhole near the Rachut site. This sinkhole is represented by a cluster of 3 points in the NE corner of Figure 19.*

## Mitchell County Conservation Board (CCB) Site

The Mitchell CCB site is similar to the Rachut property in that the depth to bedrock is less than 25 feet and the sinkholes are well-developed, but differs in that the sinkholes at this site appear to possibly have a subsurface connection as a possible 'sinkhole complex'. This site is underlain by sub-lithographic limestone of the Lithograph City Formation, which is exposed to the east of the site along the bluff line of the Cedar River. Three ER lines were run at this site (Figure 22). The most prominent sinkhole at the site was too large to image, so the second largest was chosen.

The Mitchell C-C' line was run north-south through a well-developed sinkhole. The surface topography dropped nearly 15 feet and the sinkhole was filled with what appeared to be blocks of *in-situ* limestone

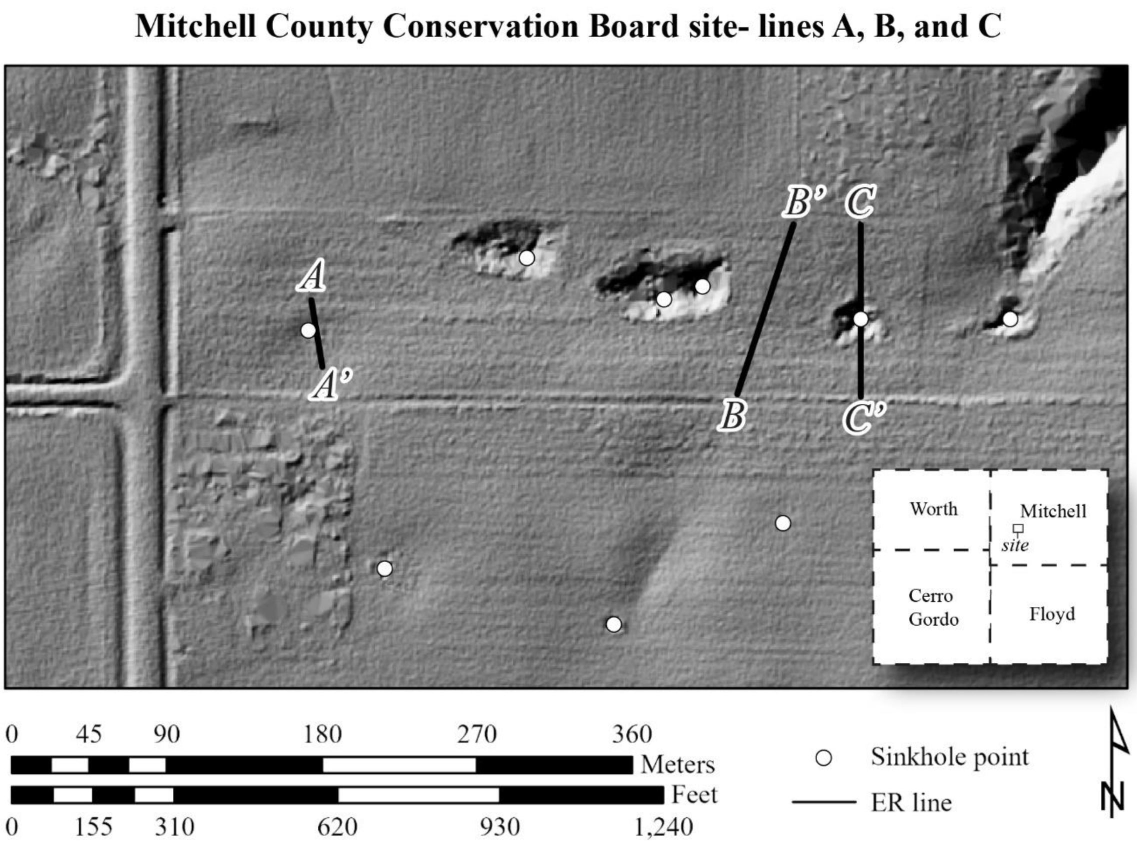


*Figure 22: Site map of the Mitchell County Conservation Board location.*

bedrock along with trees and vegetation. Human fill material (metal and other debris) was also noted at the site. The IGS does not know the history of this site; however, based on historical aerial photography the site may have been cultivated in the past. The data from this line are more difficult to interpret than the others due to extreme high and low resistivity values observed in the region of the sinkhole's surface expression. This 'noise' may be due to either very shallow bedrock or human infilling of the sinkholes.

To test the idea that the major sinkholes at the Mitchell CCB site could be connected, the Mitchell B-B' line was run between the two most prominent sinkholes on the site, perpendicular to the west-east trending axis of the sinkhole complex. An area of resistant material occurs at around 10 feet below the surface and is interpreted to be competent bedrock. An area of low resistivity is located just below this and extends to a depth of up to 35 feet. The IGS interprets this area to be either a fractured zone in the bedrock or a possible infilled void network. Either way, it provides good evidence of subsurface connectivity between sinkholes.

The Mitchell A-A' line was run north-south over a smaller and less prominent depression on the west edge of the property. The data are somewhat inconclusive, likely due to the short line length compared with lines run at other sites. An area of low resistivity is present at the site of the depression and extends to the south. This could be indicative of fractured rock, however, a longer line would have been necessary to further characterize this feature.

## Falk Property

Three lines were run at the Falk property (Figure 23). All three were run across apparent sinkholes. The primary difference at this site is that the surficial deposits consist primarily of sand and gravel (outwash) materials. There are numerous places within the project area where depressions are noted in areas of sand and gravel. The IGS wanted to investigate whether or not the features were related to the sand deposition and subsequent erosion or if they were related to underlying bedrock features. Also of note is that the three sinkholes mapped at the Falk A-A' line collapsed in 2015 and were captured by a 2016-2018 color infrared aerial photograph. These and other sinkholes have been repeatedly filled in by the

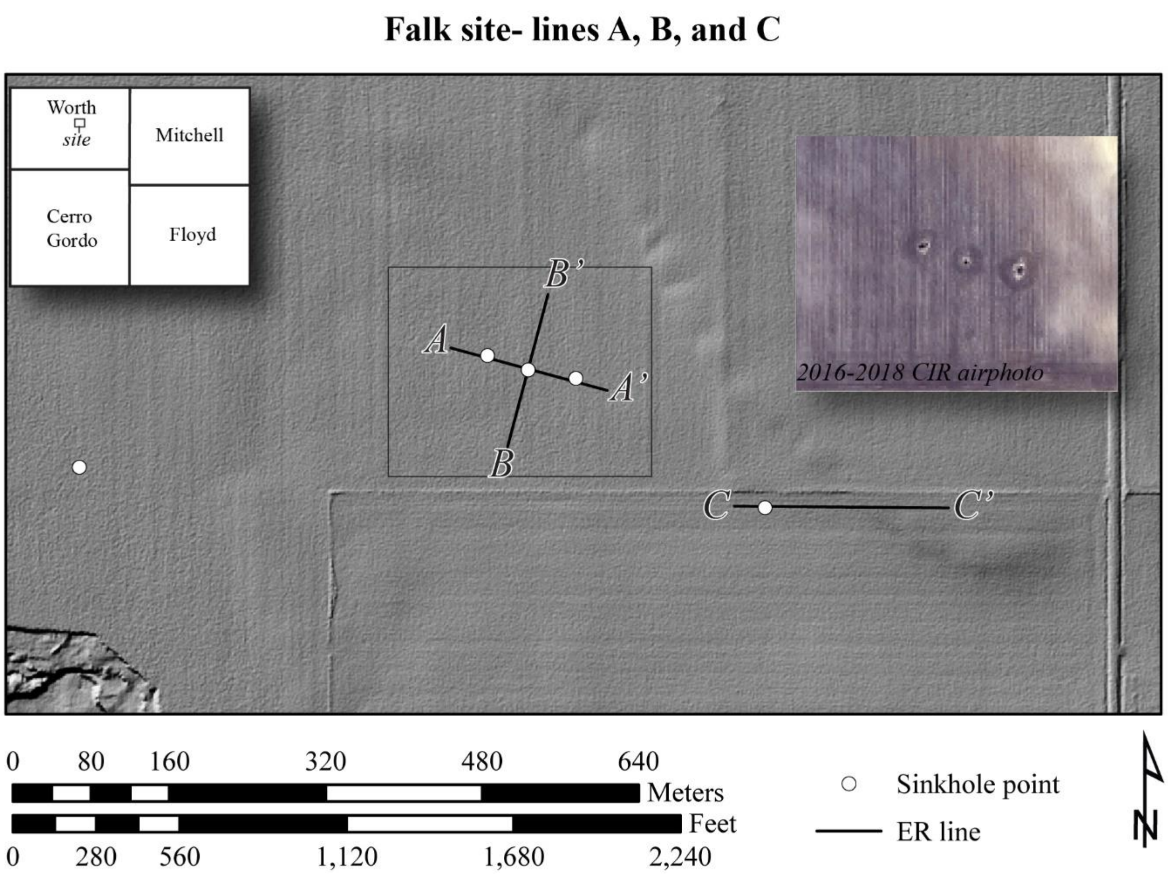


*Figure 23: Site map of the Falk site. Inset image is a color infrared aerial photograph from 2016-2018 showing the sinkholes along the A-A' line.*

landowner (personal communication). According to the bedrock geologic map, this area is underlain by dolomitic limestone of the Shell Rock Formation.

The Falk A-A’ line transects the three mapped sinkholes. Each of these is apparent on the ER data corresponding to zones of lower resistivity. The bedrock surface is estimated to be around 10 to 15 feet below ground and matches the IGS depth to bedrock map for this area. The Falk B-B’ line was run perpendicular to the Falk A-A’ line and crosses the center sinkhole. This feature is prominent in the ER data and confirms its presence. No other irregularities are identified on the bedrock surface. The bedrock at this line location is also estimated to be within 10 to 15 feet of the surface.

The Falk C-C’ line runs east-west across a less prominent sinkhole. The line was shifted to the east to evaluate the transition onto a prominent sand and gravel outwash terrace. The area corresponding to the mapped sinkhole does show a lower resistivity zone, but the complexity of the surficial geology makes interpreting the other ER data difficult. The IGS believes that drilling would be necessary to fully interpret these data.

## Karst Susceptibility Mapping

The karst susceptibility map represents the relative risk for karst-prone bedrock to form sinkholes (Figure 24). The union of the bedrock and surficial maps with the depth to bedrock file resulted in almost 8,500 unique polygons for the four-county area. As described in the methodology section, a karst

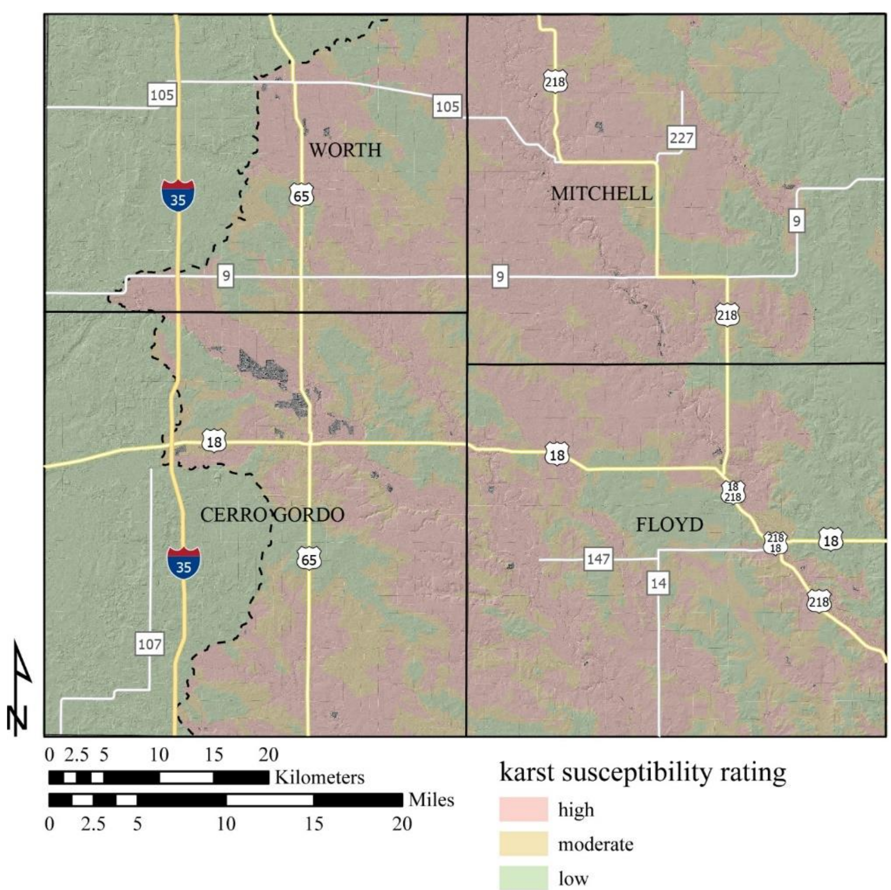


*Figure 24: The karst susceptibility map of the project area. Pits and quarries are not included in the analysis and appear gray. The Des Moines Lobe boundary is shown as a dashed line.*

susceptibility rating was assigned based on the relationship between the surficial and bedrock geology and the depth to bedrock. For clarity, the area of the Des Moines Lobe will not be included in our calculations unless noted.

Based on our classifications, 46% of Worth, Cerro Gordo, Floyd, and Mitchell counties are in the high risk classification, 26% in the moderate, and 28% of the area is in the low category. In general, upland areas with less than 25’ of Quaternary cover over Devonian carbonate adjacent to major rivers are zones with high risk for sinkhole development.

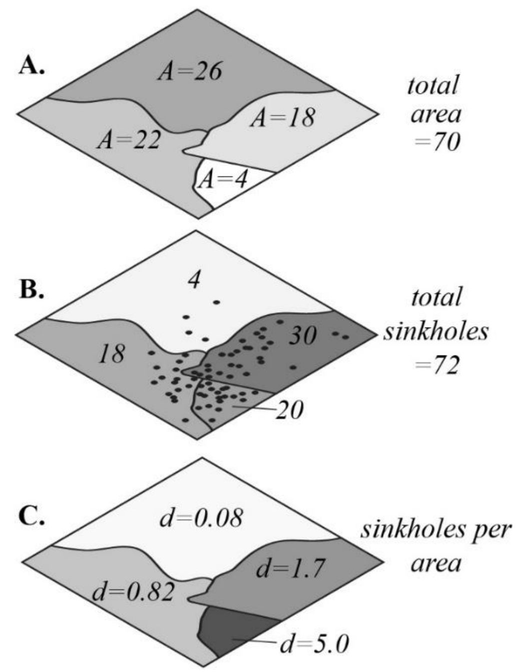


*Figure 25: A demonstration of density to standardize the relationship between polygons and sinkholes.*

## Statistical Analysis

Part of the rationale behind mapping the four-county area was that this region is one of the most intensely studied areas by the IGS in recent decades. The confidence and familiarity with the data sets has allowed analysis of the relationship between sinkhole formation and the local geology. As such, the mapped sinkholes were used to test the karst susceptibility map’s classifications and to investigate relationships between mapping units. Sinkholes mapped in the project area are assumed to be accurately placed and represent true karst features. In order to test its significance, different data sets were normalized using the density of sinkholes per $km^2$. By doing so, it can be determined if there are geologic settings that promote karst formation. With an equal distribution of 4,175 sinkholes across the four-county area (3,972 $km^2$), the average density would be 1.05 sinkholes/$km^2$. Actual results were compared against that value. Densities that fall greatly above or below were considered significant. Figure 25 shows a simplified example of the normalization process. Map A shows the area of each polygon, while Map B shows the number of sinkholes in each polygon. Map C shows the density. Note that the highest count is not necessarily the densest.

### *Depth to Bedrock*

To test the validity of using depth to bedrock as a criterion, we summed the areas of each of the depth to bedrock classifications (<25, 25-50, and >50 feet) across all bedrock and surficial categories (Figures 26 and 27). Sinkholes that fell within the >50 feet interval were not automatically discounted in the review process, so the two data sets were independently generated. The total sum of all sinkholes per category were then divided by the area. The result is that the category of <25 feet has a density of 1.93 sinkholes/$km^2$, or nearly double the average density for the study area. Almost 85% of mapped sinkholes fall within this zone while it only occupies 46% of the study area. The 25-50 feet category, which is 28% of the study area, has a value of 0.51 sinkholes/$km^2$, which is about half the average density. Only 13% of mapped sinkholes are found in this interval. Lastly, the >50 feet interval has a density of 0.03 sinkholes/$km^2$. This is a fraction of the average sinkhole density even though the area covers 53% of the study area. These results confirm that the depth to bedrock classifications of <25, 25-50, and >50 feet are appropriate when assessing karst susceptibility.

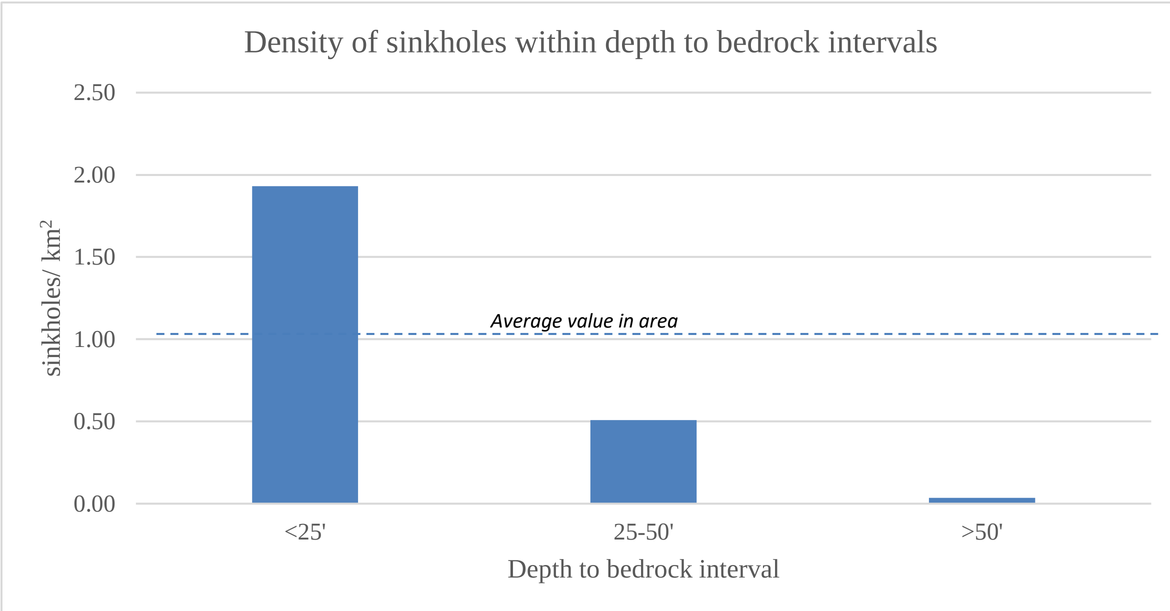


*Figure 26: Graph showing sinkhole density plotted against the karst susceptibility depth to bedrock intervals.*

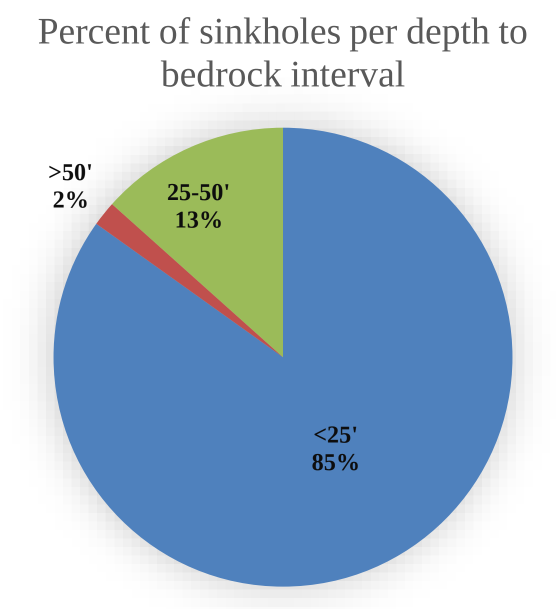


*Figure 27: A pie chart showing the percentages of sinkholes per depth to bedrock interval.*

### *Surficial Geology*

To test the significance of the surficial geology, we evaluated the two designations, upland and valley, in a similar fashion to the depth to bedrock classifications (Figure 28). The upland category accounts for 88% of the study area and has a density of 1.15 sinkholes/km$^2$. Over 96% of the sinkholes fall within this zone, leaving only 4% of sinkholes in the valleys. The valley designation has a density of 0.37 sinkholes/km$^2$ and 12% of the area. While there is a distinction between the two zones, it should be noted that the character of the valley sediments would mask the expression of sinkholes due to the loose nature of the materials present. Additionally, the relative difference in elevation of the water table between the two zones may play a role in karst and sinkhole expression.

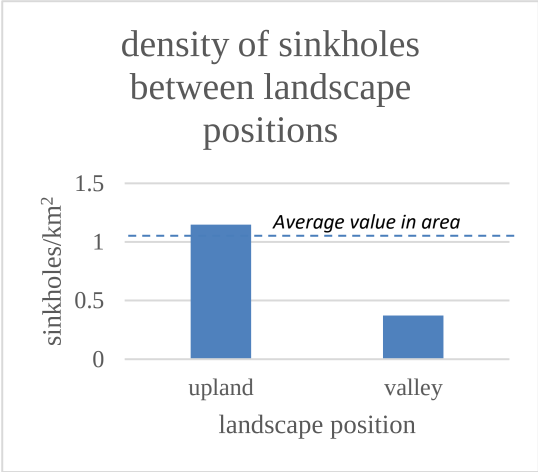


*Figure 28: Graph showing sinkhole density plotted against the landscape position designation.*

### *Bedrock Lithology*

A comparison of sinkhole density and bedrock geology shows a clear relationship between the unit at the bedrock surface and the density of karst in an area. The density of sinkholes was calculated for each bedrock formation on the 1:100,000 scale county maps across each depth to bedrock classification. Formations that are dominated by carbonate and occur within the <25 feet depth to bedrock classification showed above average sinkhole density (Figure 29). Tellingly, the Lime Creek Formation (Dl), which contains substantial shale intervals, has significantly lower sinkhole density than the regional average in the <25 feet to bedrock classification. The highest density zone is where the Lithograph City Formation (Dlgc) is less than 25 feet from the surface. The lithology of this unit consists of sub-lithographic (microcrystalline) limestone above dolomite. The properties of sub-lithographic limestone are thought to play a significant role in the generation (and preservation) of sinkholes. Table 2 shows each bedrock map unit and depth to bedrock classification. By using the mapped sinkholes as a test for validity in karst susceptibility, compelling relationships were identified that should be investigated in the future. Although the interplay between surficial and bedrock geology is important, the bedrock lithology in areas with a depth to bedrock less than 25 feet appears to be the primary factor for karst development and sinkhole formation.

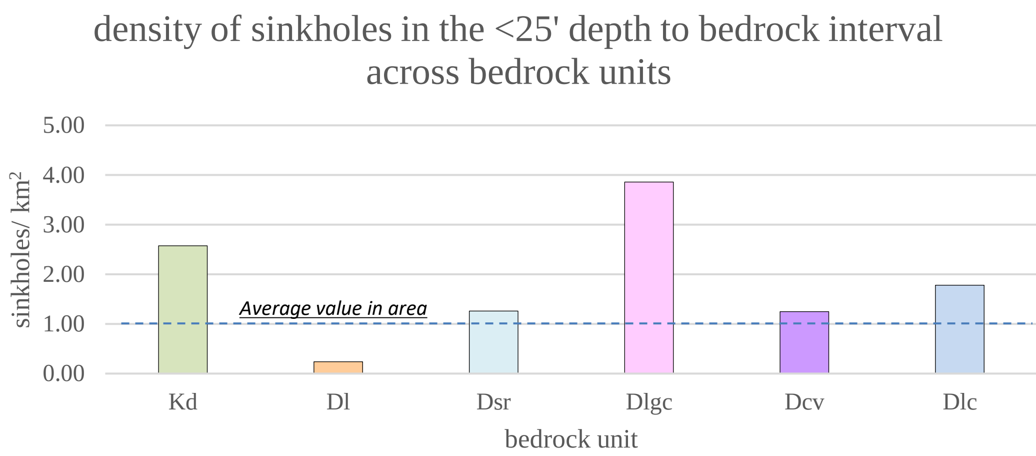


*Figure 29: Graph showing sinkhole density plotted for bedrock units within the <25 feet depth to bedrock classification. Note that Kd represents Cretaceous outliers comprised of sandstone and shale and likely reflects the values of the underlying Devonian units.*

| Bedrock unit/depth to bedrock | *sinkhole count* | *Area(km)* | Sinkhole density |
|---|---|---|---|
| **Kd*** | ***120*** | ***92.40*** | **1.30** |
| <25' | *119* | *46.23* | 2.57 |
| 25-50' | *1* | *24.24* | 0.04 |
| >50' | *0* | *21.93* | 0.00 |
| **Dl**** | ***105*** | ***663.59*** | **0.16** |
| <25' | *82* | *343.59* | 0.24 |
| 25-50' | *22* | *197.39* | 0.11 |
| >50' | *1* | *122.61* | 0.01 |
| **Dsr** | ***537*** | ***697.10*** | **0.77** |
| <25' | *468* | *371.51* | 1.26 |
| 25-50' | *66* | *217.36* | 0.30 |
| >50' | *3* | *108.22* | 0.03 |
| **Dlgc** | ***3080*** | ***1418.49*** | **2.17** |
| <25' | *2672* | *692.49* | 3.86 |
| 25-50' | *365* | *384.47* | 0.95 |
| >50' | *43* | *341.54* | 0.13 |
| **Dcv** | ***140*** | ***295.28*** | **0.47** |
| <25' | *99* | *79.34* | 1.25 |
| 25-50' | *27* | *43.32* | 0.62 |
| >50' | *14* | *172.62* | 0.08 |
| **Dlc** | ***14*** | ***256.07*** | **0.05** |
| <25' | *7* | *3.93* | 1.78 |
| 25-50' | *1* | *8.05* | 0.12 |
| >50' | *6* | *244.09* | 0.02 |

*Table 2: Sinkhole density values by depth to bedrock classification for each bedrock unit. Bolded numbers represent the totals for each mapping unit. *Kd values likely represent the underlying bedrock. **Dl values represent both carbonate and shale lithologies within the formation.*

## CONCLUSIONS

The IGS more than doubled the number of mapped sinkholes in Worth, Cerro Gordo, Mitchell, and Floyd counties and made substantial improvements to the karst susceptibility map for the same area. These updates were possible due to both an increase in the amount of data available and the quality of the data. Key data for sinkhole identification was the availability of LiDAR as well as geologic data in the IGS GeoSam database. Recent IGS surficial and bedrock mapping provided a much improved understanding of the lithologic character and distribution of geologic units. The 25 foot contour interval bedrock topography map was also of greater value than the 50 foot contour interval from the statewide map. The IGS was able to establish relationships between these data sets and the identified sinkholes to create an updated karst susceptibility map.

The results of this study identified two primary factors that affect the formation of sinkholes: the depth to the bedrock surface and bedrock lithology (carbonate or shale). The majority of sinkholes occur in areas where the bedrock surface is less than 25 feet below the land surface. This illustrates the need for a more detailed bedrock elevation map for karst prone areas of the state to capture this relationship. The bedrock geologic map units dominated by carbonate lithologies correlated very closely with the areas that formed sinkholes. Subdividing the Lime Creek Formation into its three members further refined the karst susceptibility map by delineating the Juniper Hill Member, a shale unit. An understanding of the surficial geologic mapping units was also helpful in determining if depressions were in fact sinkholes. A series of eolian dune features in Worth and Cerro Gordo counties were determined to be the cause of many depressions that were identified in the Phase 1 assessment that were not actually sinkholes. Conversely, it was determined that outwash sand and gravel units may require extra scrutiny. Outwash deposits allow for rapid groundwater infiltration that may expedite karst development while masking the surface expression of sinkholes due to sand collapse.

Geophysical survey methods utilized during the project assisted with determining the depth to bedrock and evaluating the subsurface character of sinkholes. Passive seismic data was used to confirm bedrock depth in areas of limited subsurface data. ER results were effective in evaluating the subsurface expression of sinkholes in a variety of geologic settings, including those occurring as sinkhole ‘complexes’. ER also confirmed that the depressions visible in valley settings with outwash as the surface material, did in fact form due to underlying bedrock karst.

## FUTURE WORK

Based on the current study, the IGS feels this methodology could be applied throughout the state at various scales and/or levels of detail. A Phase 1 sinkhole assessment could be completed for the remaining counties known to have karst potential or are of interest to the IDOT based on existing or planned roadways as a risk prevention measure. The karst susceptibility methods could also be applied across the state as a first cut to identify areas for a more detailed Phase 2 study. Additionally, the State of Iowa is currently acquiring new higher resolution LiDAR for the entire state. It has been just over 10 years since the original sinkhole identification project was completed for the eight county area in northeast Iowa. The current study demonstrates that the LiDAR DEM fill difference data sets identified the greatest number of depressions and therefore are the most comprehensive data set. An evaluation comparing the 2010 data set with new LiDAR could yield significant information into the development of karst and how often sinkholes open, close, and redevelop. Comparing the 10 year data from each would likely be most indicative of change for a given area. Additionally, this process may be executed with little or no field work, depending on the level of accuracy desired for a given project area.

For future site-specific investigations, the use of ER has proven to be a reliable method for characterizing karst features and terrains. The best example from this study was from the Mitchell CCB site where the data collected between two well-developed sinkholes showed a highly conductive zone (possibly fractured bedrock or a void network) below a resistant layer (interpreted to be the bedrock top). ER methods are relatively quick and non-destructive. However, areas with complex geology may require drilling to more fully interpret the results.

## PRODUCTS AND TECHNOLOGY TRANSFER

In addition to this report, the IGS will transfer the sinkhole data and karst susceptibility map coverage to the IDOT as ArcGIS shapefiles and .kmz files. The sinkhole data set includes the location, fields for each data source used (yes/no), an evaluation of whether each feature was determined to be a sinkhole or depression of non-karst origin, and the surficial and bedrock geologic unit mapped for each location. The sinkhole data will be incorporated into the IDNR sinkhole coverage that is available on the statewide GeoData website (https://geodata.iowa.gov/) and will also be used to update the karst map in the Animal Feeding Operations (AFO) Siting Atlas for the state (https://programs.iowadnr.gov/maps/afo/). The IGS will also provide a shapefile and .kmz of the updated Lime Creek Formation subdivisions on the bedrock geologic map as well as the 25 foot contour interval bedrock elevation map and Quaternary thickness map for the four-county project area. This report will be available as Technical Information Series 59 on the IGS publications page (https://www.iihr.uiowa.edu/igs/publications/search). Presentations of this data will be made at relevant local, regional, and national conferences and meetings, and at the request of the IDOT.

## ACKNOWLEDGEMENTS

The Technical Advisory Committee (TAC) provided direction and valuable discussion throughout the duration of the project. The TAC consisted of the following members:

Adriana Schnoebelen, Project Champion, IDOT, Office of Construction and Materials- Geology Section
Brian Gossman, IDOT, Office of Construction and Materials- Geology Section
M. Robert Dawson, IDOT, Office of Construction and Materials- Geology Section
Adrianne Knight, IDOT, Office of Design- Soils Section
Michelle Barger, IDOT, Office of Design- Soils Section
Mary Kay Solberg, IDOT, Office of Location and Environment
Ryan Clark, Iowa Geological Survey
Calvin Wolter, Iowa Department of Natural Resources

Landowners allowing access to their properties for ER surveys included Dennis Rachut, the Mitchell County Conservation Board, L.R. Falk Construction Co., and Wayne Trenhaile. Trent Lambert (IDNR) assisted with making landowner contacts. Vanessa Goetz (IDOT) provided administrative support and guidance with the IDOT funding process.

## REFERENCES


Buckner, R.L., and Highland, J.D., 1976, Soil survey of Worth County, Iowa: U.S. Department of Agriculture, Soil Conservation Service, 130p.

Clark, R., Liu, H., Kerr, P., Tassier-Surine, S., Rowden, R., and Streeter, M., 2016, Bedrock geologic map of Mitchell County, Iowa: Iowa Geological Survey, Open File Map OFM-16-1, 1:100,000 scale map sheet.

Day, J.E., Witzke, B.J., and Bunker, B.J., 2008, Overview of Middle and Upper Devonian Cedar Valley Group and Lime Creek Formation carbonate platform facies, faunas, and event stratigraphy of northern Iowa, *in* Groves, J.R., Walters, J.C., and Day, J.E., (eds.) Carbonate platform facies and faunas of the Middle and Upper Devonian Cedar Valley Group and Lime Creek Formation, northern Iowa: Iowa Geological and Water Survey, Guidebook Series No. 28, p. 15-41.

DeWitt, Thomas A., 1981, Soil Survey of Cerro Gordo County, Iowa: U.S. Department of Agriculture, Soil Conservation Service, 214 p., 84 map sheets.

Hallberg, G.R. and Hoyer, B.E., 1982, Sinkholes, hydrogeology, and groundwater quality in northeast Iowa: Iowa Geological Survey, Open File Report 82-3, 120p.

Hruby, C.E., Wolter, C.F., McKay, R.M., and Bounk, M.J., 2010, NE Iowa Watershed and Karst Map, Iowa Geological and Water Survey, Open File Map OFM-10-7, 1:264,810 scale map sheet.

Kerr, P., Tassier-Surine, S., Streeter, M., Liu, H., and Clark, R., 2018, Surficial Geologic Map of Floyd County, Iowa: Iowa Geological Survey, Open File Map OFM-18-2, 1:100,000 scale map sheet.

Liu, H., McKay, R., Rowden, R., Quade, D., Tassier-Surine, S., and Giglierano, J., 2012, Bedrock Geology of Worth County, Iowa, scale 1:100,000: Iowa Geological and Water Survey, Open File Map OFM-12-1.

Liu, H., Clark, R., Fields, C., McKay, R., Rowden, R., Tassier-Surine, S., Kerr, P., and Streeter, M., 2015, Bedrock geology of Cerro Gordo County, Iowa: Iowa Geological Survey, Open File Map OFM-15-1, 1:100,000 scale map sheet.

Liu, H., Kerr, P., Clark, R., and Tassier-Surine, S., 2018, Bedrock Geologic Map of Floyd County, Iowa: Iowa Geological Survey, Open File Map OFM-18-1, 1:100,000 scale map sheet.

Quade, D., Tassier-Surine, S., Liu, H., McKay, R.M., and Giglierano, J.D., 2012, Surficial Geology of Worth County, Iowa, scale 1:100,000: Iowa Geological and Water Survey, Open File Map OFM-12-2.

Tassier-Surine, S., Quade, D., Kerr, P., Streeter, M., Liu, H., Clark, R., Fields, C., McKay, R., and Rowden, R., 2015, Surficial geology of Cerro Gordo County, Iowa: Iowa Geological Survey, Open File Map OFM-15-2, 1:100,000 scale map sheet.

Tassier-Surine, S., Kerr, P., Clark, R., Streeter, M., and Liu, H., 2016, Surficial geologic map of Mitchell County, Iowa: Iowa Geological Survey, Open File Map OFM-16-2, 1:100,000 scale map sheet.

Vogelgesang, J., Kerr P., Clark, R., and Streeter, M., 2020, Geophysical investigation and geologic evaluation along US 18, near Mason City, Iowa: Iowa Geological Survey, prepared for the Iowa Department of Transportation, Soils Section, 44p.

Vogelgesang, J.A. and Clark, R.J., 2012. Geological and Geophysical Field Investigation, Deer Creek Lake, Plymouth County, Iowa: Iowa Geological Survey, Miscellaneous Publication, MP-42, 21 p.

Voy, K.D. and Highland, J.D., 1975, Soil Survey of Mitchell County, Iowa: U.S. Dept. of Agriculture, Soil Conservation Service, 125 p. with 70 map sheets.

Voy, K.D., 1995, Soil Survey of Floyd County, Iowa: U.S. Department of Agriculture, Soil Conservation Service, 260 p. plus 63 map sheets.

Weary, D.J. and Doctor, D.H., 2014, Karst in the United States: A digital map compilation and database: US Geological Survey Open File Report 2014-1156, 23p.

Witzke, B.J., Bunker, B.J., and Rogers, F.S., 1988, Eifelian through lower Frasnian stratigraphy and deposition in the Iowa area, central midcontinent, U.S.A., *in* McMillan, N.J., Embry, A.F, and Glass, D.J. (eds.) Devonian of the World, Canadian Soc. of Petroleum Geologists, Memoir 14, vol. I, p. 221-250.

Witzke, B.J., Anderson, R.R., and Pope, J.P., 2010, Bedrock geologic map of Iowa, 1:500,000: Iowa Geological Survey, Open File Map OFM-2010-01.

Wolter, C.F., McKay, R.M., Liu, H., Bounk, M.J., and Libra, R.D., 2011, Geologic mapping for water quality projects in the Upper Iowa River Watershed: Iowa Geological and Water Survey, Technical Information Series TIS-54, 38p.

# APPENDIX A

## Passive Seismic Data Table and Profiles

**Passive Seismic Data Table:** Locational and calculation values for the 53 passive seismic data points. Calibration points are highlighted. The frequency values were determined from the profiles shown on the following pages. For the calibration points, the velocity was calculated and used to calculate the depth for the 'unknown' points. The 'Depth Difference' was determined by subtracting the calculated value from the depth to bedrock raster. Negative values indicate a result deeper than the raster value.

| Name | Lat. | Long. | County | Calibration Point | Geology | Freq. | Calculated Velocity | Calculated Depth | Depth Diff. (ft) |
|---|---|---|---|---|---|---|---|---|---|
| PS-1 | 43.1483 | -93.1366 | CG | | Qsc2 | 7.16 | | 31.6 | 15.4 |
| PS-2 | 43.1191 | -93.1463 | CG | | Qalb | 3.75 | | 30.8 | -25.8 |
| PS-3 | 43.1025 | -93.1619 | CG | | Qsc2 | 1.67 | | 135.5 | -100.5 |
| PS-4 | 43.0831 | -93.0779 | CG | | br | 21.41 | | 10.6 | -10.6 |
| PS-5 | 43.067 | -93.036 | CG | W33452 | br | 19.69 | 96 | | |
| PS-6 | 43.0632 | -93.0826 | CG | | Qsc2 | 11.41 | | 19.8 | 0.2 |
| PS-7 | 43.0524 | -93.043 | CG | | br | 3.75 | | 21.9 | 20.1 |
| PS-8 | 43.0526 | -93.0103 | Floyd | | Qsc2 | 4.63 | | 48.9 | 8.1 |
| PS-9 | 43.0089 | -93.1613 | CG | | Qsc2 | 4.75 | | 47.6 | -2.6 |
| PS-10 | 43.0089 | -93.1254 | CG | W61413 | Qsc2 | 3.66 | 244 | | |
| PS-11 | 43.0016 | -93.1027 | CG | | Qsc2 | 4.16 | | 54.4 | -9.4 |
| PS-12 | 42.9944 | -93.1223 | CG | | Qsc2 | 4.13 | | 54.8 | -51.8 |
| PS-13 | 42.9801 | -93.1525 | CG | | Qsc2 | 7.09 | | 31.9 | -19.9 |
| PS-14 | 42.9798 | -93.123 | CG | | Qe | 5.09 | | 44.5 | -31.5 |
| PS-15 | 42.9798 | -93.0936 | CG | | Qsc2 | 4.22 | | 53.6 | -39.6 |
| PS-16 | 42.967 | -93.1235 | CG | W29010 | Qsc2 | 6.47 | 237 | | |
| PS-17 | 42.9656 | -93.1725 | CG | | Qsc2 | 5.31 | | 42.6 | 8.4 |
| PS-18 | 42.965 | -93.1428 | CG | | Qsc2 | 6.88 | | 32.9 | -1.9 |
| PS-19 | 42.9512 | -93.1767 | CG | W61432 | Qal | 10.26 | 238 | | |
| PS-20 | 42.9508 | -93.1381 | CG | | Qsc2 | 5.00 | | 45.3 | -33.3 |
| PS-21 | 42.9367 | -93.1629 | CG | | Qsc2 | 11.93 | | 19.0 | 51.0 |
| PS-22 | 42.9339 | -93.1433 | CG | | Qsc2 | 8.98 | | 25.2 | 35.8 |
| PS-23 | 43.2727 | -93.2804 | Worth | W24643 | Qnw2 | 4.88 | 297 | | |
| PS-24 | 43.262 | -93.2609 | Worth | | Qnw2 | 7.00 | | 16.5 | -9.5 |
| PS-25 | 43.2742 | -93.2406 | Worth | | Qsc2 | 6.00 | | 19.3 | -10.3 |
| PS-26 | 43.2844 | -93.2211 | Worth | | Qsc2 | 4.06 | | 55.7 | -34.7 |
| PS-27 | 43.2874 | -93.2606 | Worth | | Qsc2 | 7.00 | | 32.3 | -27.3 |
| PS-28 | 43.2988 | -93.2474 | Worth | | Qsc2 | 3.73 | | 60.7 | -38.7 |
| PS-29 | 43.2623 | -93.1617 | Worth | W53998 | Qsc2 | 23.08 | 141 | | |
| PS-30 | 43.2839 | -93.1467 | Worth | W74715 | Qsc2 | 2.93 | 372 | | |
| PS-31 | 43.2843 | -93.1622 | Worth | | Qsc2 | 5.17 | | 43.8 | -43.8 |
| PS-32 | 43.3059 | -93.1613 | Worth | W65082 | Qsc2 | 8.26 | 506 | | |
| PS-33 | 43.3089 | -93.1815 | Worth | W71756 | Qsc2 | 5.13 | 313 | | |
| PS-34 | 43.3191 | -93.1811 | Worth | | Qsc2 | 5.39 | | 42.0 | -10.0 |

| | | | | | | | | | |
|---|---|---|---|---|---|---|---|---|---|
| PS-35 | 43.3426 | -93.1908 | Worth | | Qsc2 | 6.59 | | 34.3 | 11.7 |
| PS-36 | 43.2696 | -93.1036 | Worth | | Qsc2 | 25.95 | | 8.7 | 41.3 |
| PS-37 | 43.2701 | -93.0699 | Worth | | Qsc2 | 6.25 | | 36.2 | 22.8 |
| PS-38 | 43.2845 | -93.0838 | Worth | | Qsc2 | 6.84 | | 33.1 | 1.9 |
| PS-39 | 43.3133 | -93.0986 | Worth | | Qsc2 | 29.90 | | 7.6 | 32.4 |
| PS-40 | 43.3276 | -93.0778 | Worth | | Qsc2 | 5.59 | | 40.5 | -30.5 |
| PS-41 | 43.3289 | -93.1239 | Worth | W29557 | Qsc2 | 3.60 | 266 | | |
| PS-42 | 43.3568 | -93.0741 | Worth | | Qsc2 | 4.78 | | 47.3 | -7.3 |
| PS-43 | 43.3643 | -93.0941 | Worth | | Qsc2 | 5.28 | | 42.9 | -13.9 |
| PS-44 | 43.3717 | -93.064 | Worth | | Qsc2 | 7.84 | | 28.9 | 23.1 |
| PS-45 | 43.379 | -93.0838 | Worth | | Qsc2 | 4.52 | | 50.1 | -13.1 |
| PS-46 | 43.401 | -93.1045 | Worth | | Qsc2 | 3.52 | | 64.3 | -9.3 |
| PS-47 | 43.4005 | -93.0443 | Worth | | Qsc2 | 5.88 | | 38.5 | 18.5 |
| PS-48 | 43.4156 | -93.0843 | Worth | | Qsc2 | 4.22 | | 53.6 | 12.4 |
| PS-49 | 43.4155 | -93.1246 | Worth | | Qsc2 | 3.20 | | 70.7 | -1.7 |
| PS-50 | 43.4277 | -93.1046 | Worth | | Qsc2 | 3.94 | | 57.4 | -17.4 |
| PS-51 | 43.4301 | -93.0534 | Worth | | Qnw | 9.03 | | 12.8 | 43.2 |
| PS-52 | 43.44 | -93.1243 | Worth | | Qsc2 | 4.19 | | 54.0 | 14.0 |
| PS-53 | 43.4441 | -93.0649 | Worth | W75291 | Qnw | 8.13 | 137 | | |

Cerro Gordo and Floyd counties: PS1-PS22

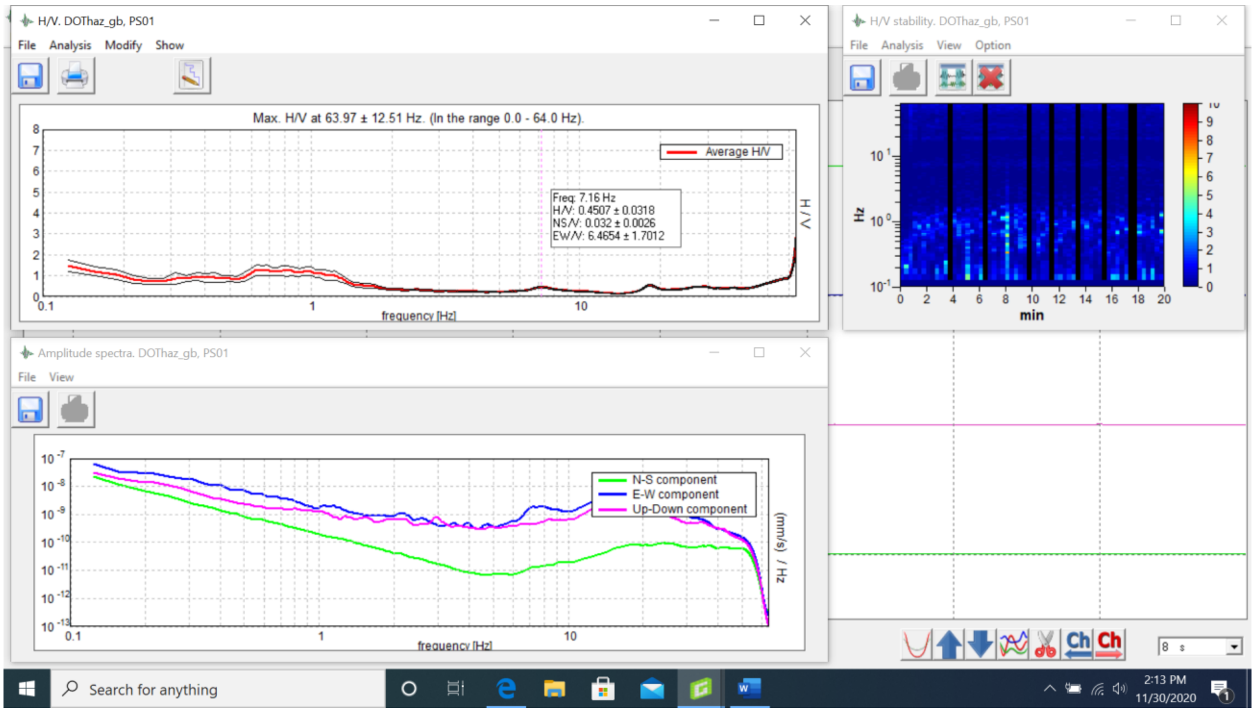


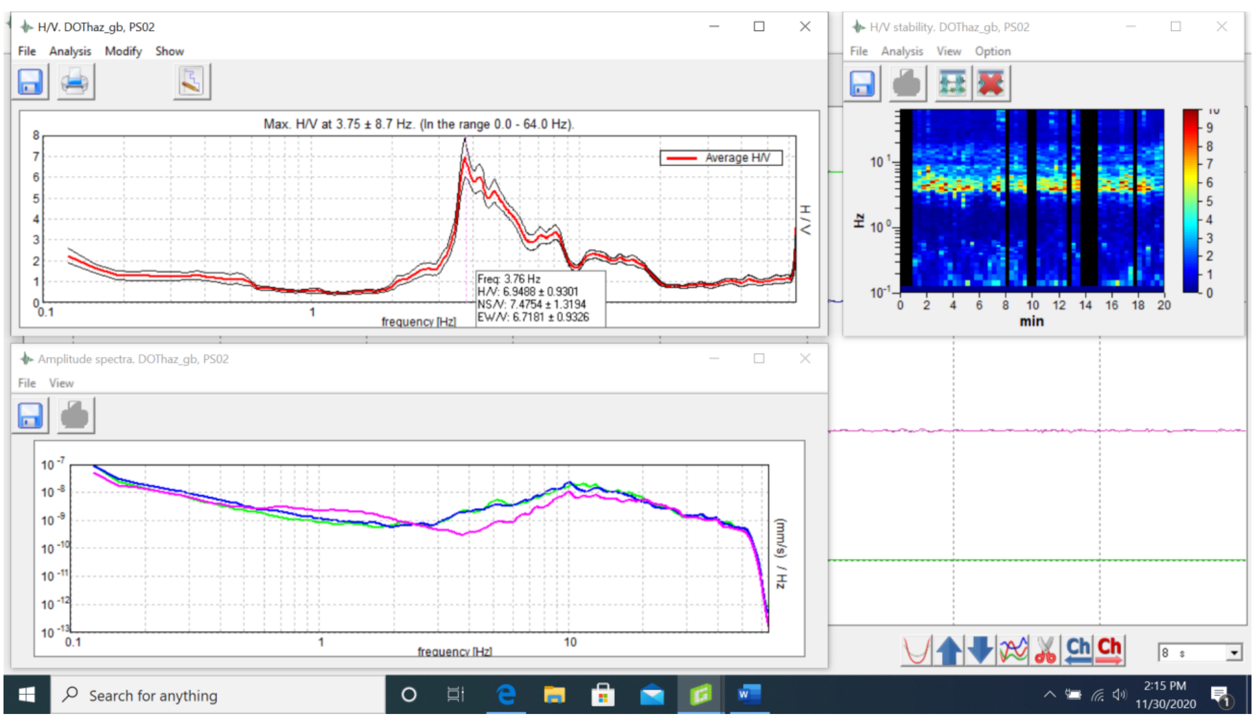

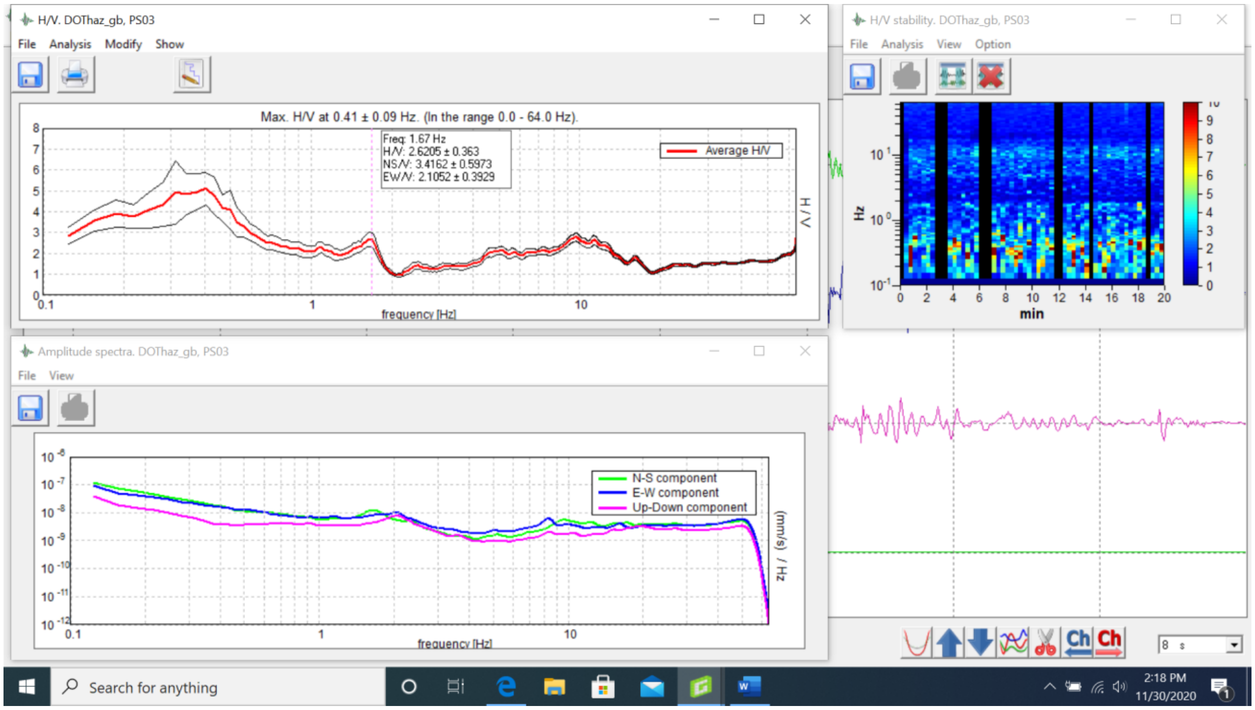
H/V. DOThaz_gb, PS03
File Analysis Modify Show
Max. H/V at 0.41 ± 0.09 Hz. (In the range 0.0 - 64.0 Hz).
Freq: 1.67 Hz
H/V: 2.6205 ± 0.363
NS/V: 3.4162 ± 0.5973
EW/V: 2.1052 ± 0.3929
Average H/V
frequency [Hz]
H/V stability. DOThaz_gb, PS03
File Analysis View Option
Hz
min
Amplitude spectra. DOThaz_gb, PS03
File View
N-S component
E-W component
Up-Down component
frequency [Hz]
(mm/s) / Hz
Search for anything
2:18 PM
11/30/2020

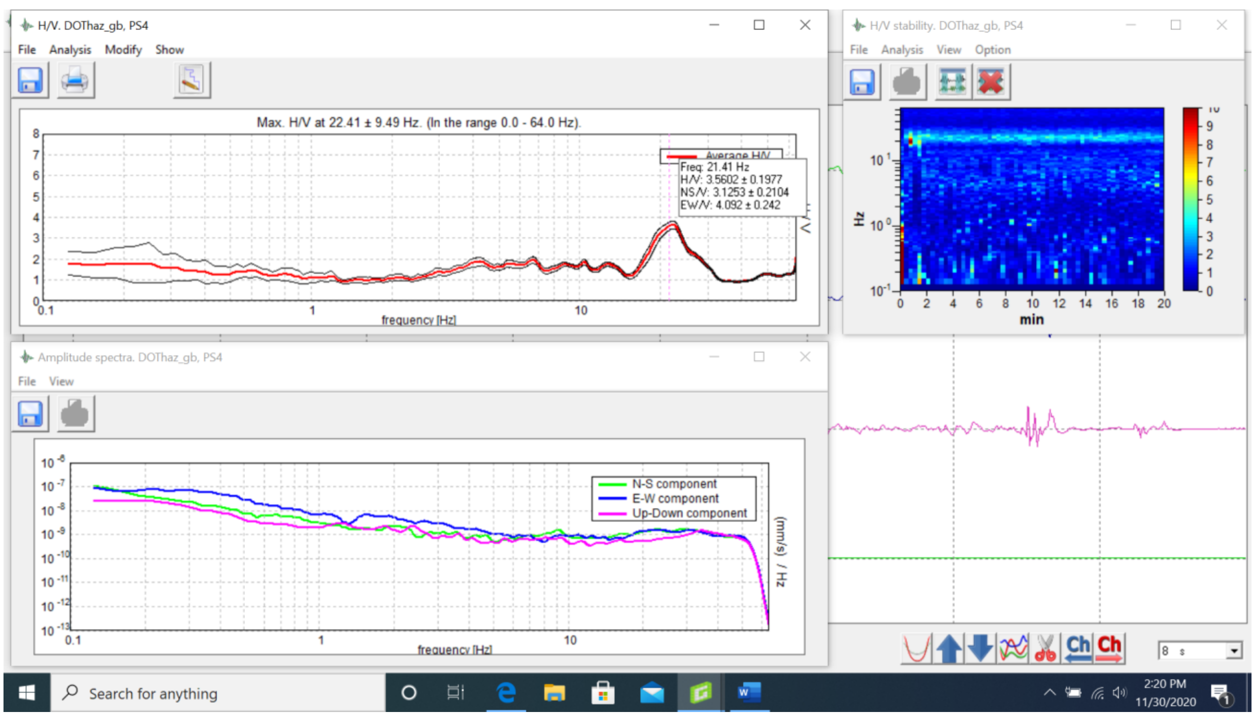
H/V. DOThaz_gb, PS4
File Analysis Modify Show
Max. H/V at 22.41 ± 9.49 Hz. (In the range 0.0 - 64.0 Hz).
Average H/V
Freq: 21.41 Hz
H/V: 3.5602 ± 0.1977
NS/V: 3.1253 ± 0.2104
EW/V: 4.092 ± 0.242
frequency [Hz]
H/V stability. DOThaz_gb, PS4
File Analysis View Option
Hz
min
Amplitude spectra. DOThaz_gb, PS4
File View
N-S component
E-W component
Up-Down component
frequency [Hz]
(mm/s) / Hz
Search for anything
2:20 PM
11/30/2020

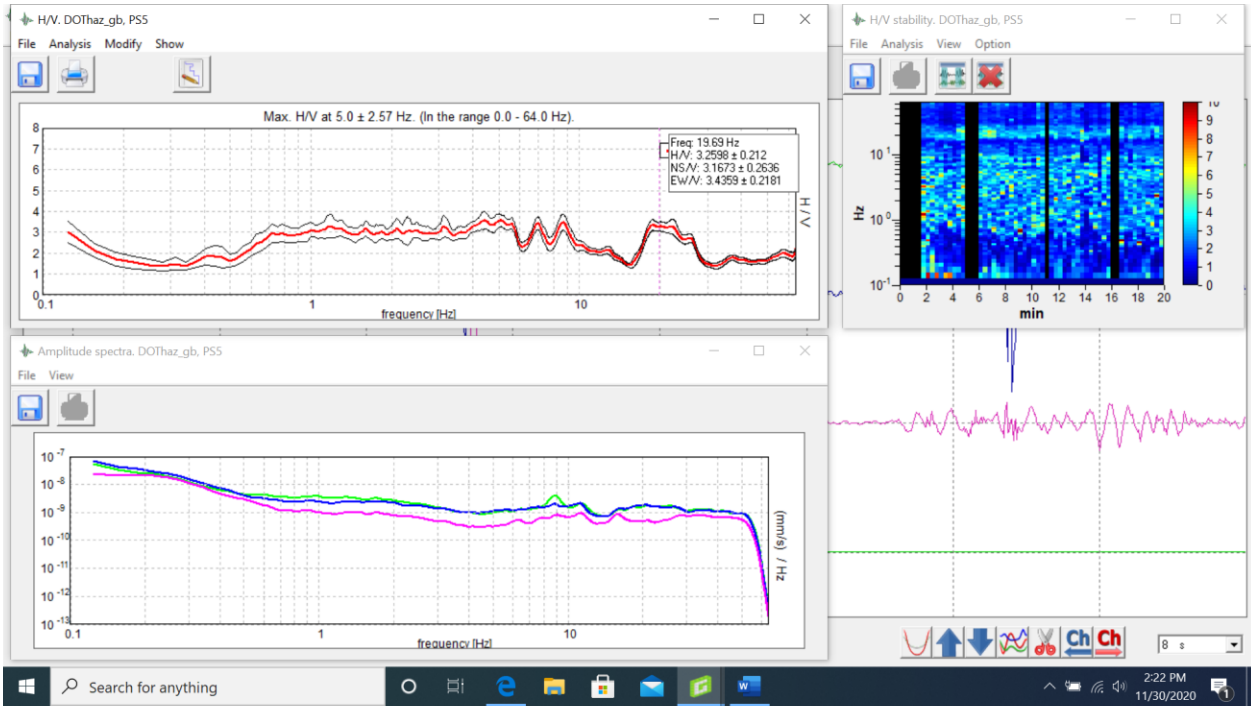
H/V. DOThaz_gb, PS5
Max. H/V at 5.0 ± 2.57 Hz. (In the range 0.0 - 64.0 Hz).
Freq: 19.69 Hz
H/V: 3.2598 ± 0.212
NS/V: 3.1673 ± 0.2636
EW/V: 3.4359 ± 0.2181
frequency [Hz]
H / V
H/V stability. DOThaz_gb, PS5
Hz
min
Amplitude spectra. DOThaz_gb, PS5
frequency [Hz]
(mm/s) / Hz
Search for anything
2:22 PM
11/30/2020

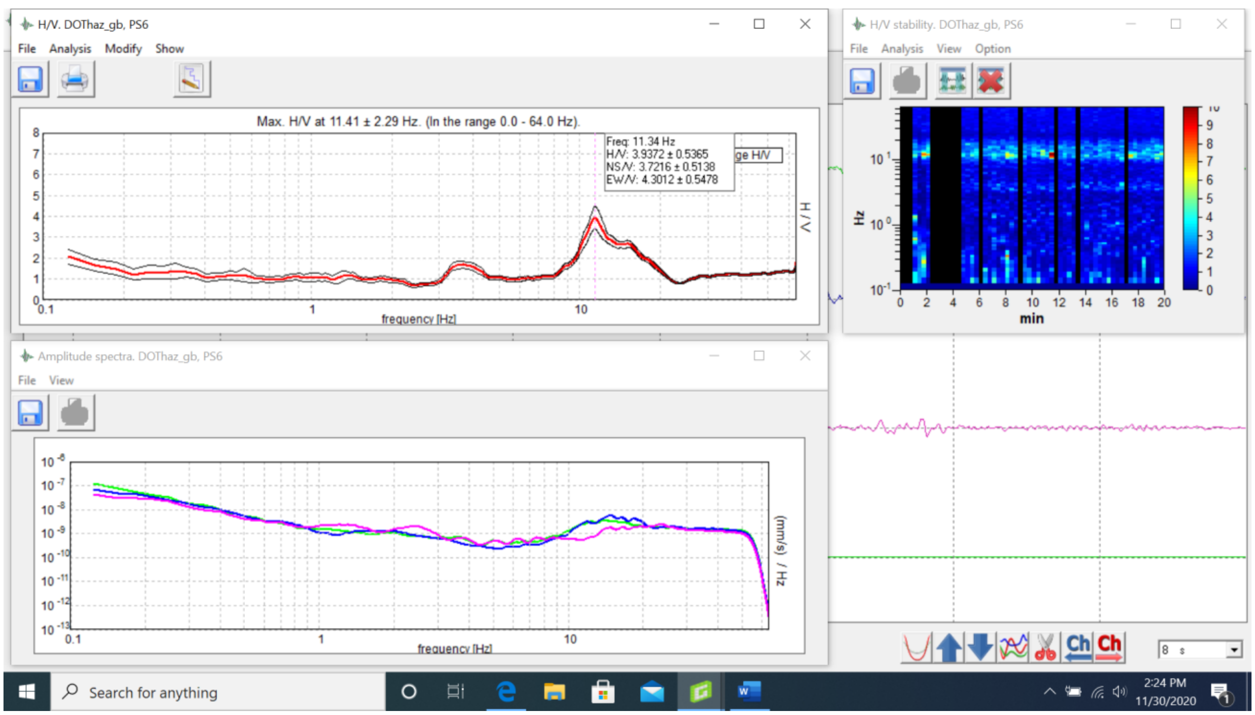
H/V. DOThaz_gb, PS6
Max. H/V at 11.41 ± 2.29 Hz. (In the range 0.0 - 64.0 Hz).
Freq: 11.34 Hz
H/V: 3.9372 ± 0.5365
NS/V: 3.7216 ± 0.5138
EW/V: 4.3012 ± 0.5478
frequency [Hz]
H / V
H/V stability. DOThaz_gb, PS6
Hz
min
Amplitude spectra. DOThaz_gb, PS6
frequency [Hz]
(mm/s) / Hz
Search for anything
2:24 PM
11/30/2020

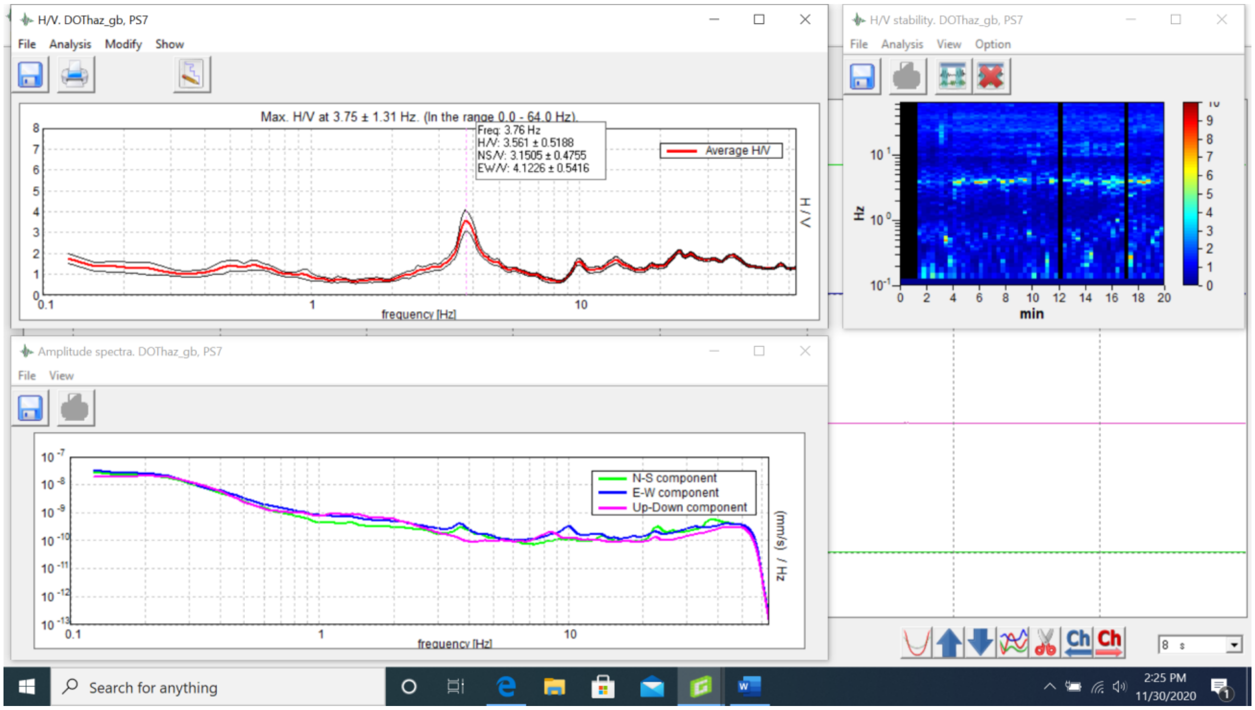
H/V. DOThaz_gb, PS7
File Analysis Modify Show
Max. H/V at 3.75 ± 1.31 Hz. (In the range 0.0 - 64.0 Hz).
Freq: 3.76 Hz
H/V: 3.561 ± 0.5188
NS/V: 3.1505 ± 0.4755
EW/V: 4.1226 ± 0.5416
Average H/V
frequency [Hz]
H/V stability. DOThaz_gb, PS7
File Analysis View Option
Hz
min
Amplitude spectra. DOThaz_gb, PS7
File View
N-S component
E-W component
Up-Down component
(mm/s) / Hz
frequency [Hz]
Search for anything
2:25 PM
11/30/2020

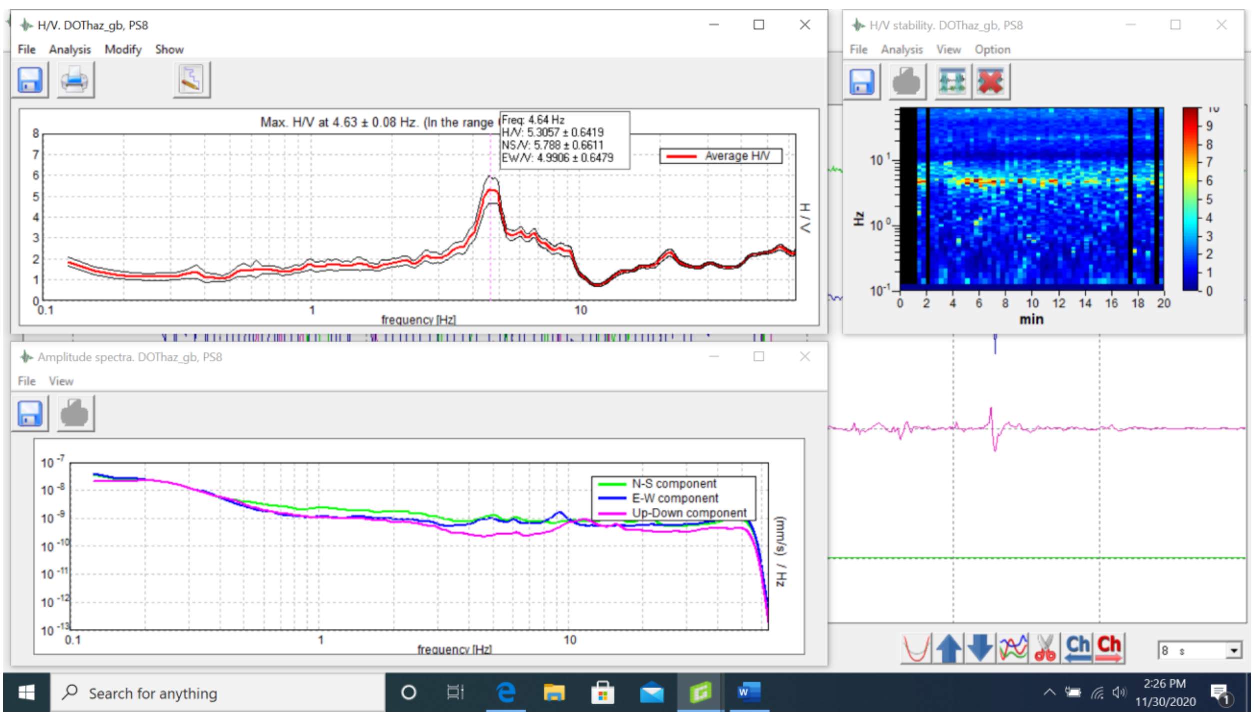
H/V. DOThaz_gb, PS8
File Analysis Modify Show
Max. H/V at 4.63 ± 0.08 Hz. (In the range
Freq: 4.64 Hz
H/V: 5.3057 ± 0.6419
NS/V: 5.788 ± 0.6611
EW/V: 4.9906 ± 0.6479
Average H/V
frequency [Hz]
H/V stability. DOThaz_gb, PS8
File Analysis View Option
Hz
min
Amplitude spectra. DOThaz_gb, PS8
File View
N-S component
E-W component
Up-Down component
(mm/s) / Hz
frequency [Hz]
Search for anything
2:26 PM
11/30/2020

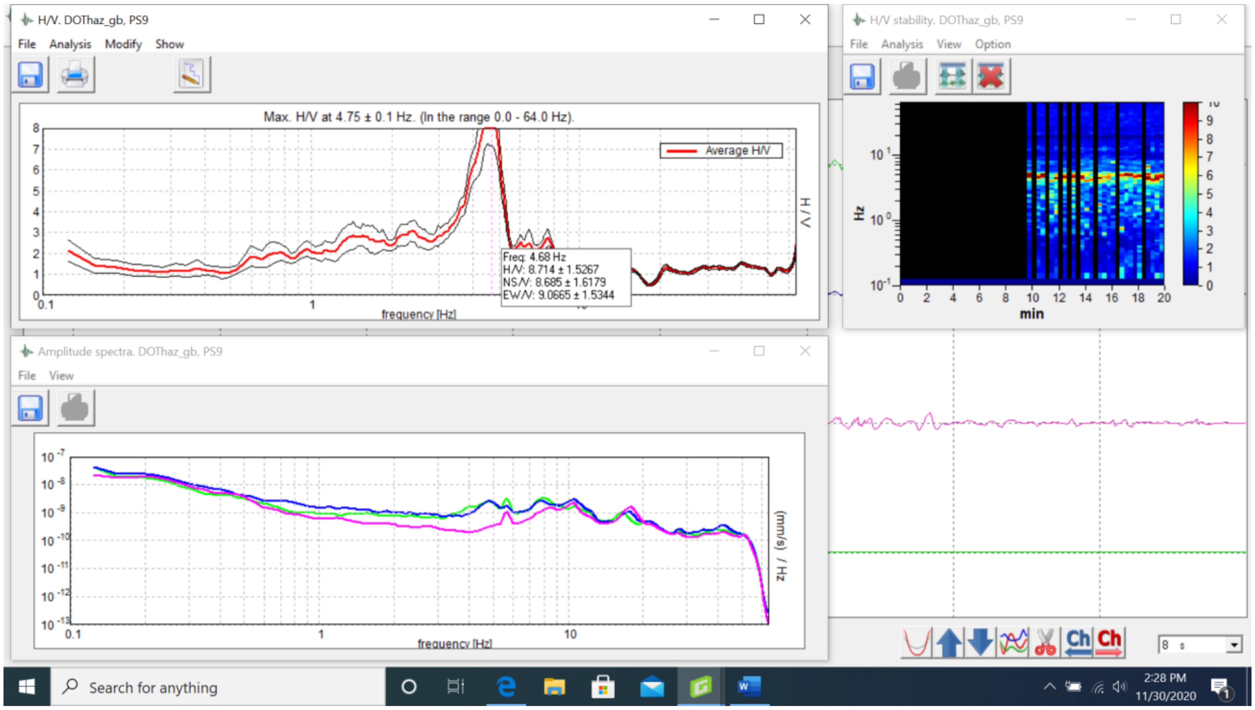
H/V. DOThaz_gb, PS9
File Analysis Modify Show
Max. H/V at 4.75 ± 0.1 Hz. (In the range 0.0 - 64.0 Hz).
Average H/V
Freq: 4.68 Hz
H/V: 8.714 ± 1.5267
NS/V: 8.685 ± 1.6179
EW/V: 9.0665 ± 1.5344
frequency [Hz]
H / V
H/V stability. DOThaz_gb, PS9
File Analysis View Option
Hz
min
Amplitude spectra. DOThaz_gb, PS9
File View
frequency [Hz]
(mm/s) / Hz
Search for anything
2:28 PM
11/30/2020

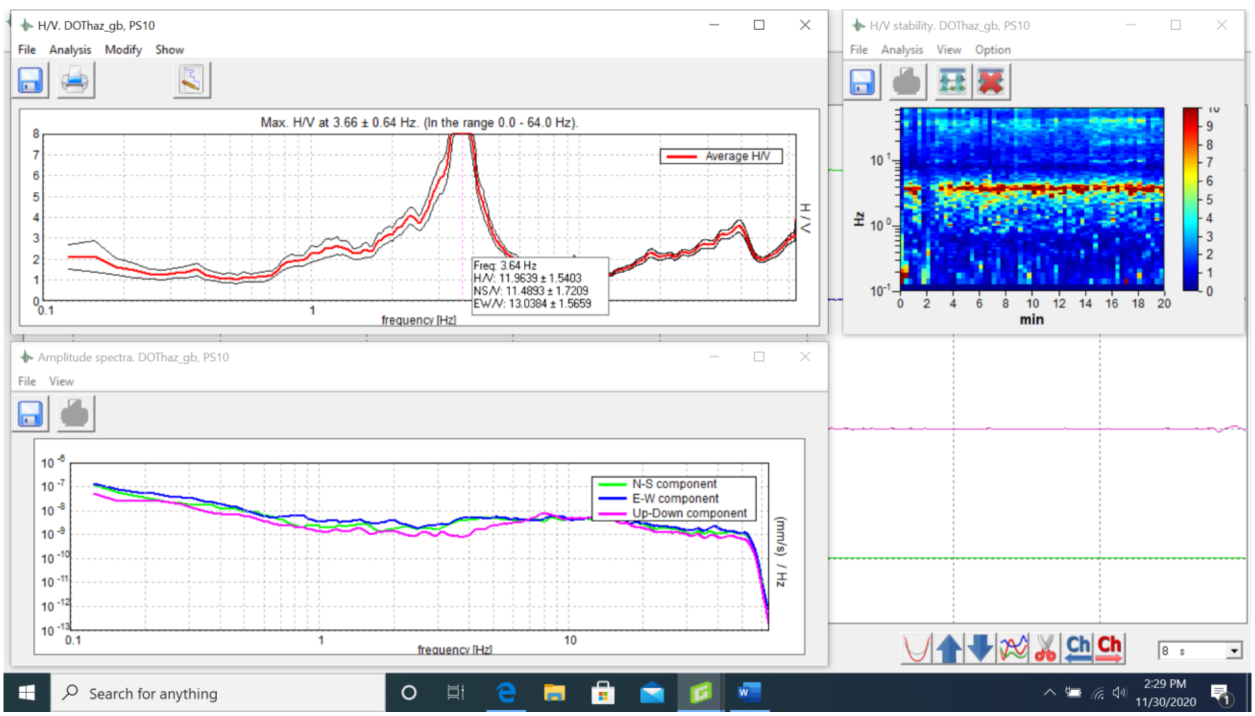
H/V. DOThaz_gb, PS10
File Analysis Modify Show
Max. H/V at 3.66 ± 0.64 Hz. (In the range 0.0 - 64.0 Hz).
Average H/V
Freq: 3.64 Hz
H/V: 11.9639 ± 1.5403
NS/V: 11.4893 ± 1.7209
EW/V: 13.0384 ± 1.5659
frequency [Hz]
H / V
H/V stability. DOThaz_gb, PS10
File Analysis View Option
Hz
min
Amplitude spectra. DOThaz_gb, PS10
File View
N-S component
E-W component
Up-Down component
frequency [Hz]
(mm/s) / Hz
Search for anything
2:29 PM
11/30/2020

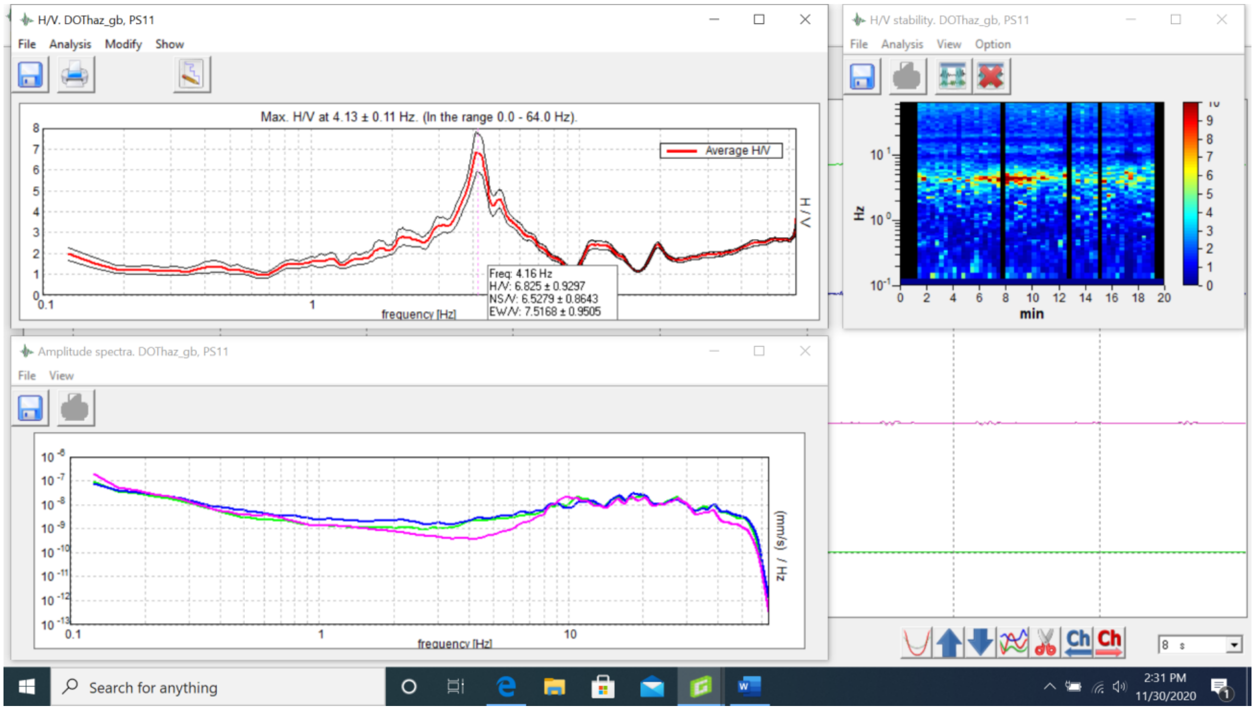
H/V. DOThaz_gb, PS11
File Analysis Modify Show
Max. H/V at 4.13 ± 0.11 Hz. (In the range 0.0 - 64.0 Hz).
Average H/V
Freq: 4.16 Hz
H/V: 6.825 ± 0.9297
NS/V: 6.5279 ± 0.8643
EW/V: 7.5168 ± 0.9505
frequency [Hz]
H / V
H/V stability. DOThaz_gb, PS11
File Analysis View Option
Hz
min
Amplitude spectra. DOThaz_gb, PS11
File View
frequency [Hz]
(mm/s) / Hz
Search for anything
2:31 PM
11/30/2020

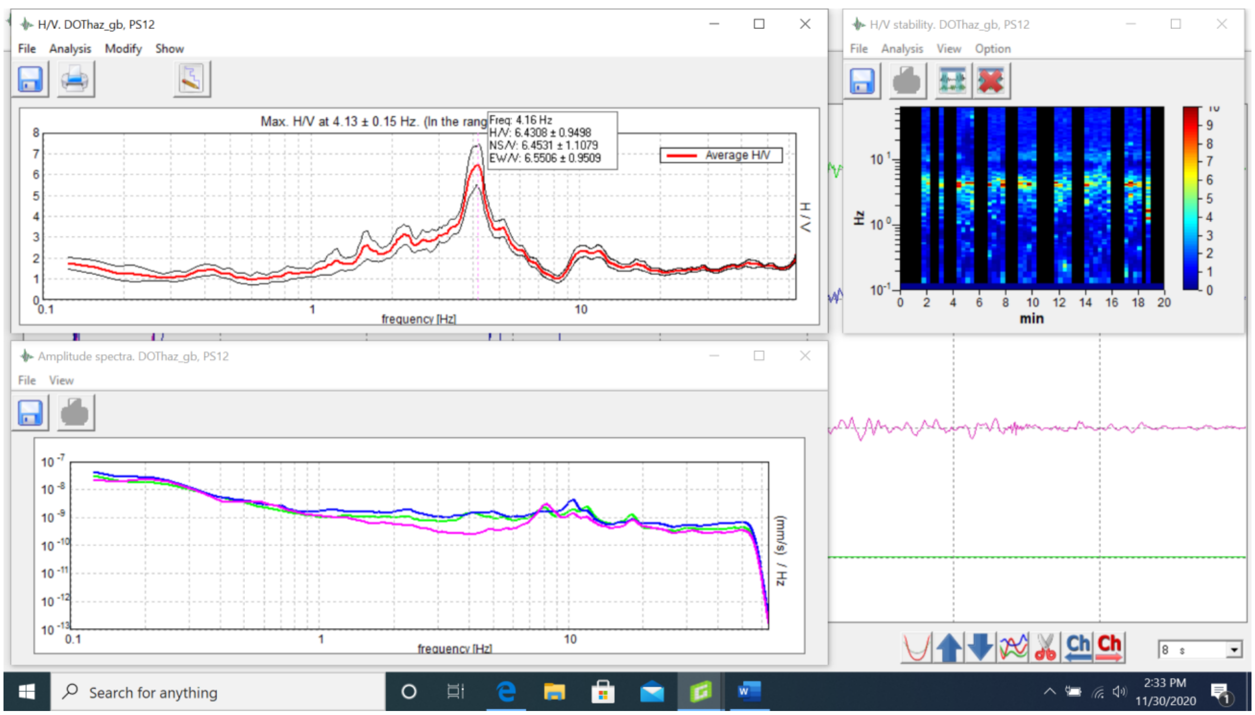
H/V. DOThaz_gb, PS12
File Analysis Modify Show
Max. H/V at 4.13 ± 0.15 Hz. (In the rang
Freq: 4.16 Hz
H/V: 6.4308 ± 0.9498
NS/V: 6.4531 ± 1.1079
EW/V: 6.5506 ± 0.9509
Average H/V
frequency [Hz]
H / V
H/V stability. DOThaz_gb, PS12
File Analysis View Option
Hz
min
Amplitude spectra. DOThaz_gb, PS12
File View
frequency [Hz]
(mm/s) / Hz
Search for anything
2:33 PM
11/30/2020

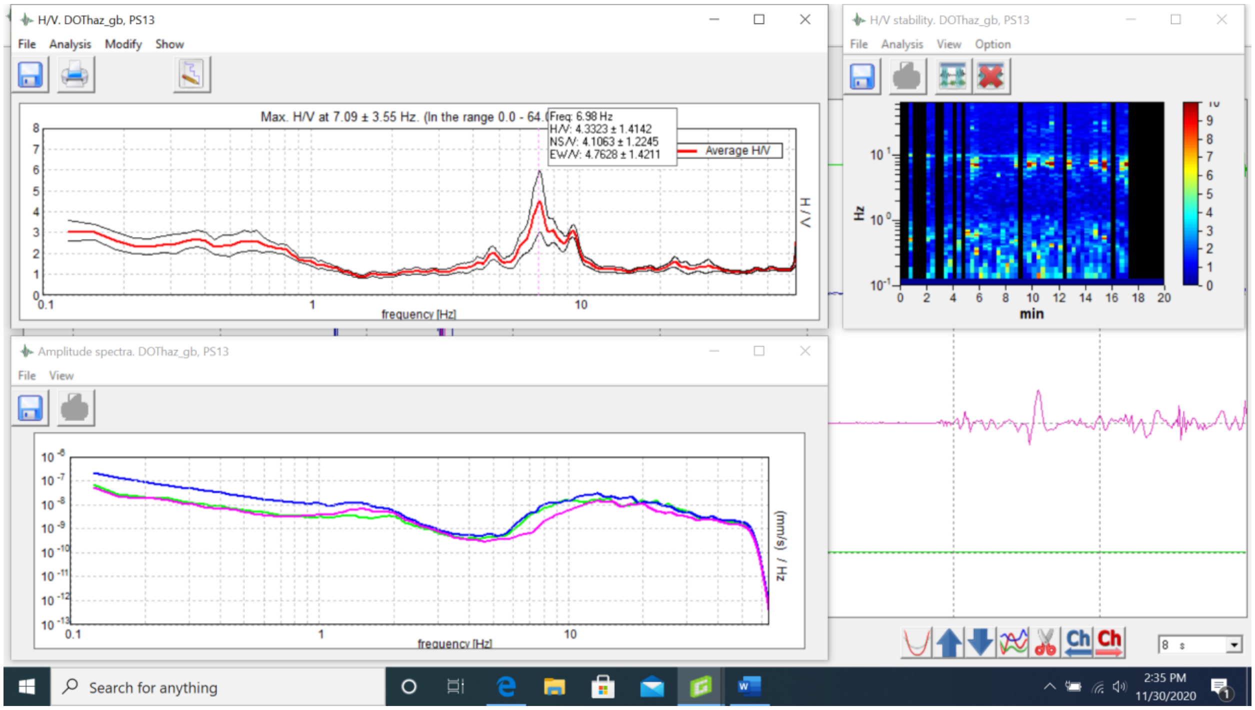
H/V. DOThaz_gb, PS13
File Analysis Modify Show
Max. H/V at 7.09 ± 3.55 Hz. (In the range 0.0 - 64.
Freq: 6.98 Hz
H/V: 4.3323 ± 1.4142
NS/V: 4.1063 ± 1.2245
EW/V: 4.7628 ± 1.4211
Average H/V
frequency [Hz]
H / V
H/V stability. DOThaz_gb, PS13
File Analysis View Option
Hz
min
Amplitude spectra. DOThaz_gb, PS13
File View
frequency [Hz]
(mm/s) / Hz
Search for anything
2:35 PM
11/30/2020

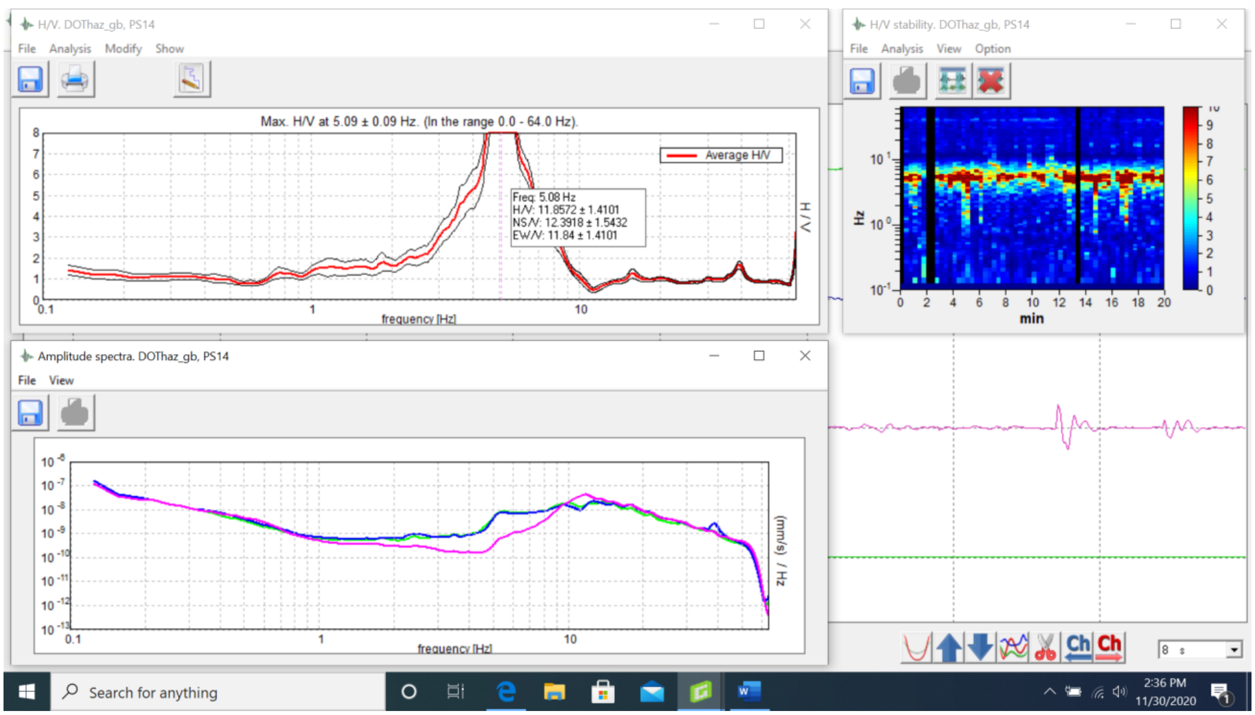
H/V. DOThaz_gb, PS14
File Analysis Modify Show
Max. H/V at 5.09 ± 0.09 Hz. (In the range 0.0 - 64.0 Hz).
Average H/V
Freq: 5.08 Hz
H/V: 11.8572 ± 1.4101
NS/V: 12.3918 ± 1.5432
EW/V: 11.84 ± 1.4101
frequency [Hz]
H / V
H/V stability. DOThaz_gb, PS14
File Analysis View Option
Hz
min
Amplitude spectra. DOThaz_gb, PS14
File View
frequency [Hz]
(mm/s) / Hz
Search for anything
2:36 PM
11/30/2020

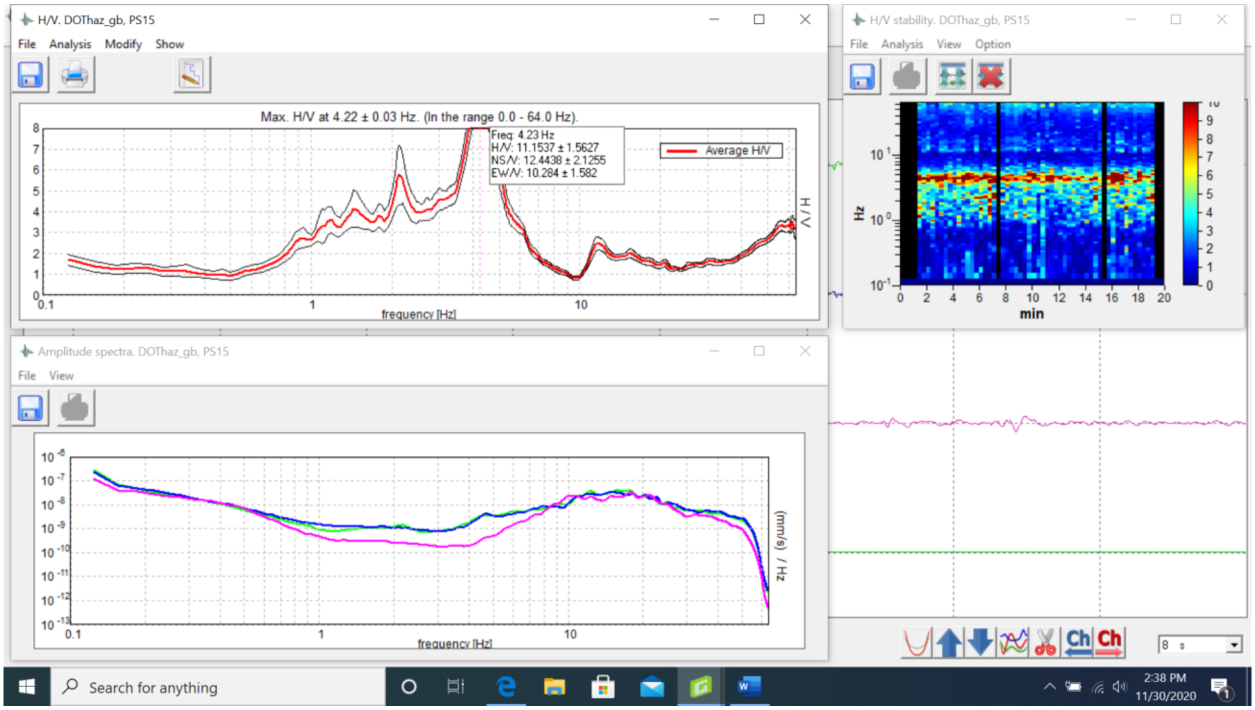
H/V. DOThaz_gb, PS15
Max. H/V at 4.22 ± 0.03 Hz. (In the range 0.0 - 64.0 Hz).
Freq: 4.23 Hz
H/V: 11.1537 ± 1.5627
NS/V: 12.4438 ± 2.1255
EW/V: 10.284 ± 1.582
Average H/V
frequency [Hz]
H / V
H/V stability. DOThaz_gb, PS15
Hz
min
Amplitude spectra. DOThaz_gb, PS15
frequency [Hz]
(mm/s) / Hz
Search for anything
2:38 PM
11/30/2020

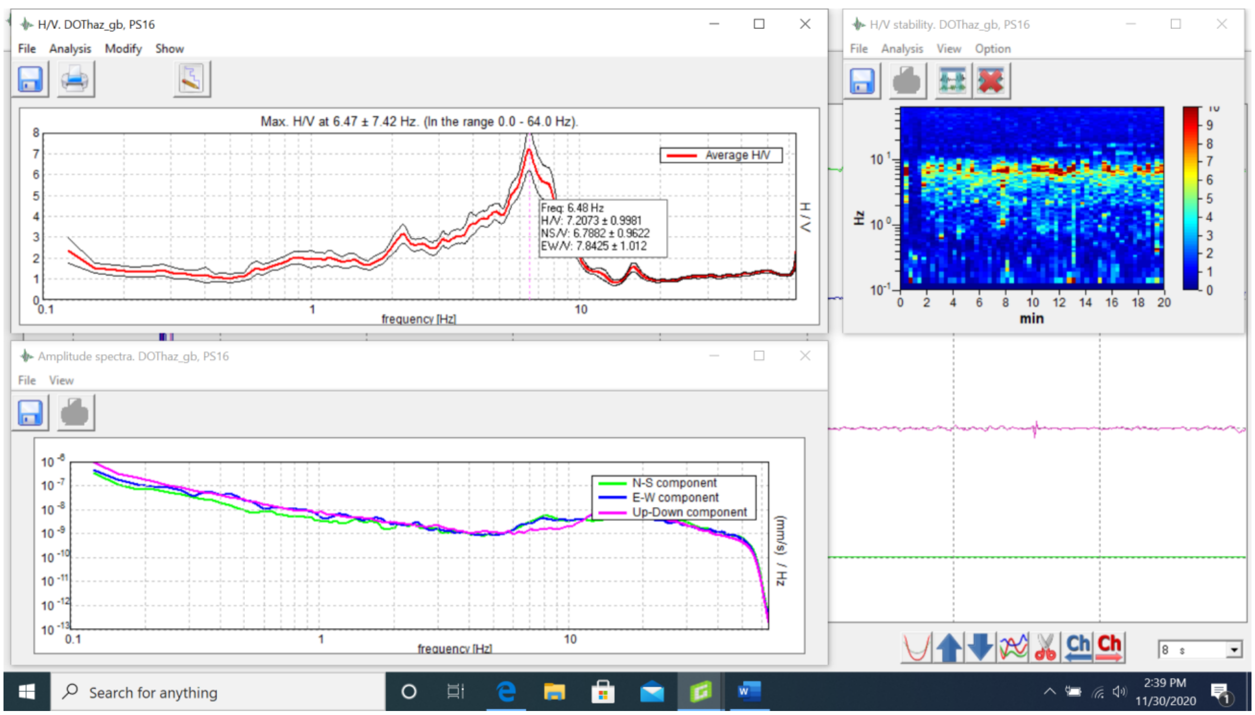
H/V. DOThaz_gb, PS16
Max. H/V at 6.47 ± 7.42 Hz. (In the range 0.0 - 64.0 Hz).
Freq: 6.48 Hz
H/V: 7.2073 ± 0.9981
NS/V: 6.7882 ± 0.9622
EW/V: 7.8425 ± 1.012
Average H/V
frequency [Hz]
H / V
H/V stability. DOThaz_gb, PS16
Hz
min
Amplitude spectra. DOThaz_gb, PS16
N-S component
E-W component
Up-Down component
frequency [Hz]
(mm/s) / Hz
Search for anything
2:39 PM
11/30/2020

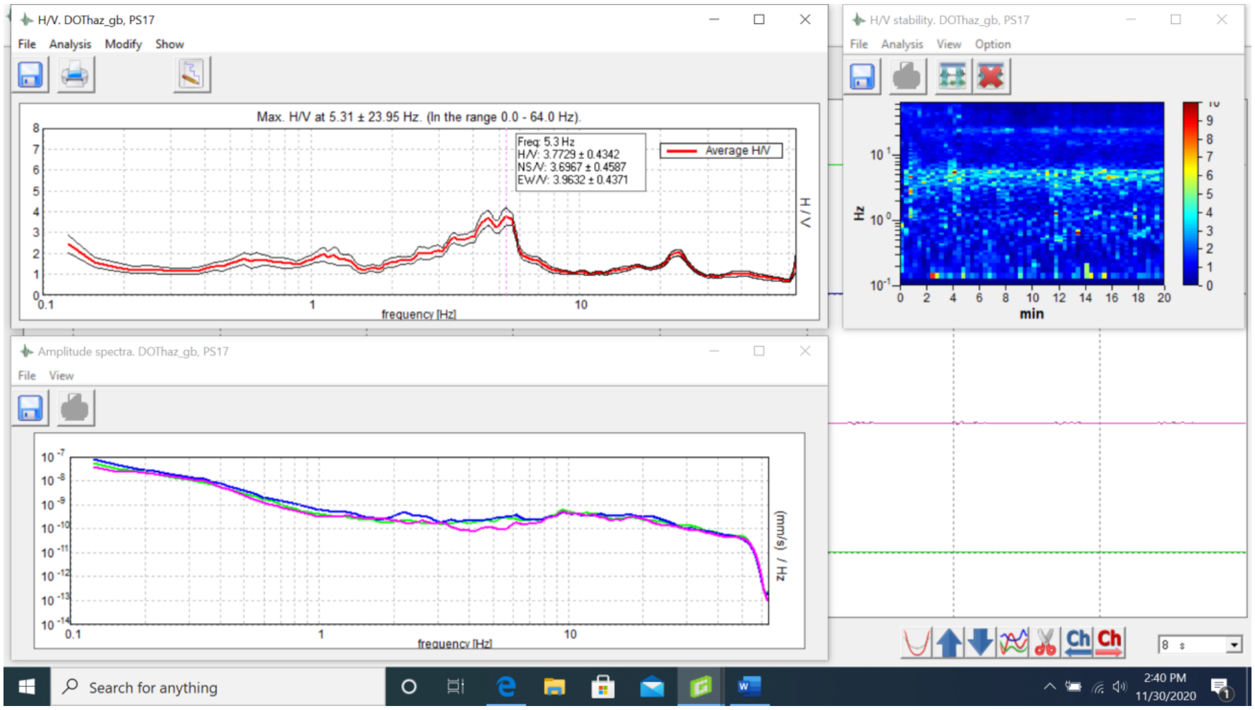
H/V. DOThaz_gb, PS17
Max. H/V at 5.31 ± 23.95 Hz. (In the range 0.0 - 64.0 Hz).
Freq: 5.3 Hz
H/V: 3.7729 ± 0.4342
NS/V: 3.6967 ± 0.4587
EW/V: 3.9632 ± 0.4371
Average H/V
frequency [Hz]
H / V
H/V stability. DOThaz_gb, PS17
Hz
min
Amplitude spectra. DOThaz_gb, PS17
(mm/s) / Hz
Search for anything
2:40 PM
11/30/2020

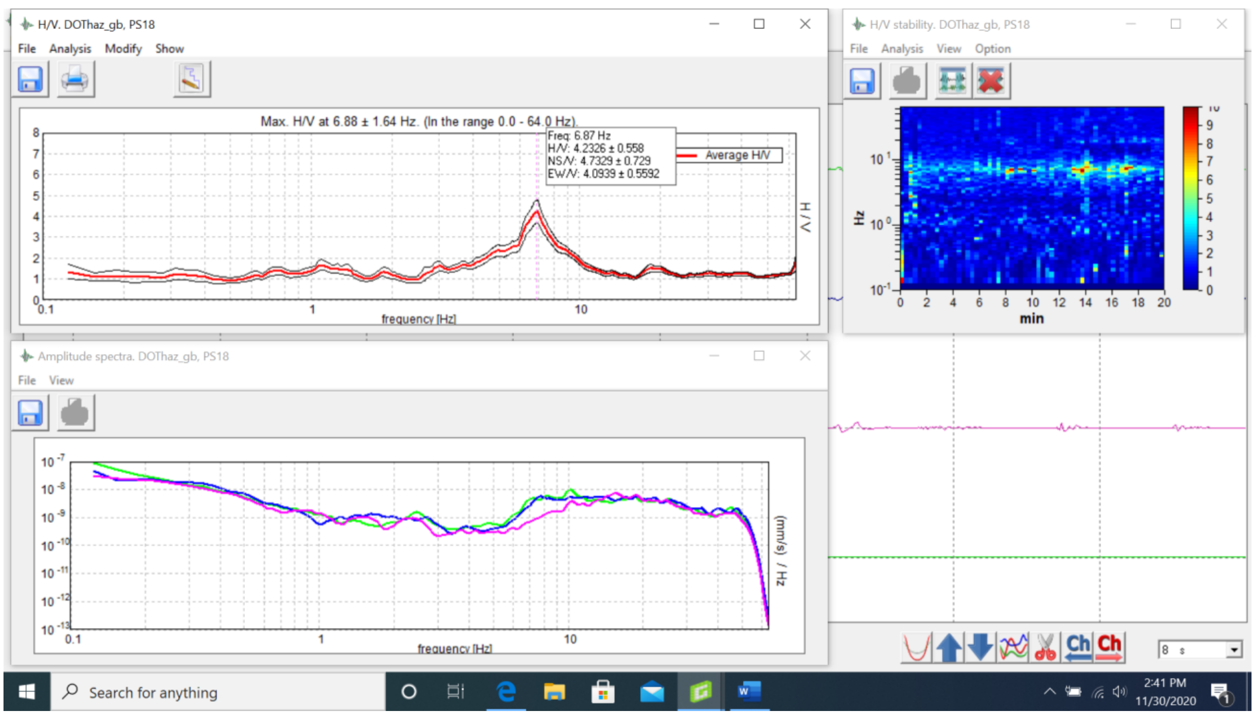
H/V. DOThaz_gb, PS18
Max. H/V at 6.88 ± 1.64 Hz. (In the range 0.0 - 64.0 Hz).
Freq: 6.87 Hz
H/V: 4.2326 ± 0.558
NS/V: 4.7329 ± 0.729
EW/V: 4.0939 ± 0.5592
Average H/V
frequency [Hz]
H / V
H/V stability. DOThaz_gb, PS18
Hz
min
Amplitude spectra. DOThaz_gb, PS18
(mm/s) / Hz
Search for anything
2:41 PM
11/30/2020

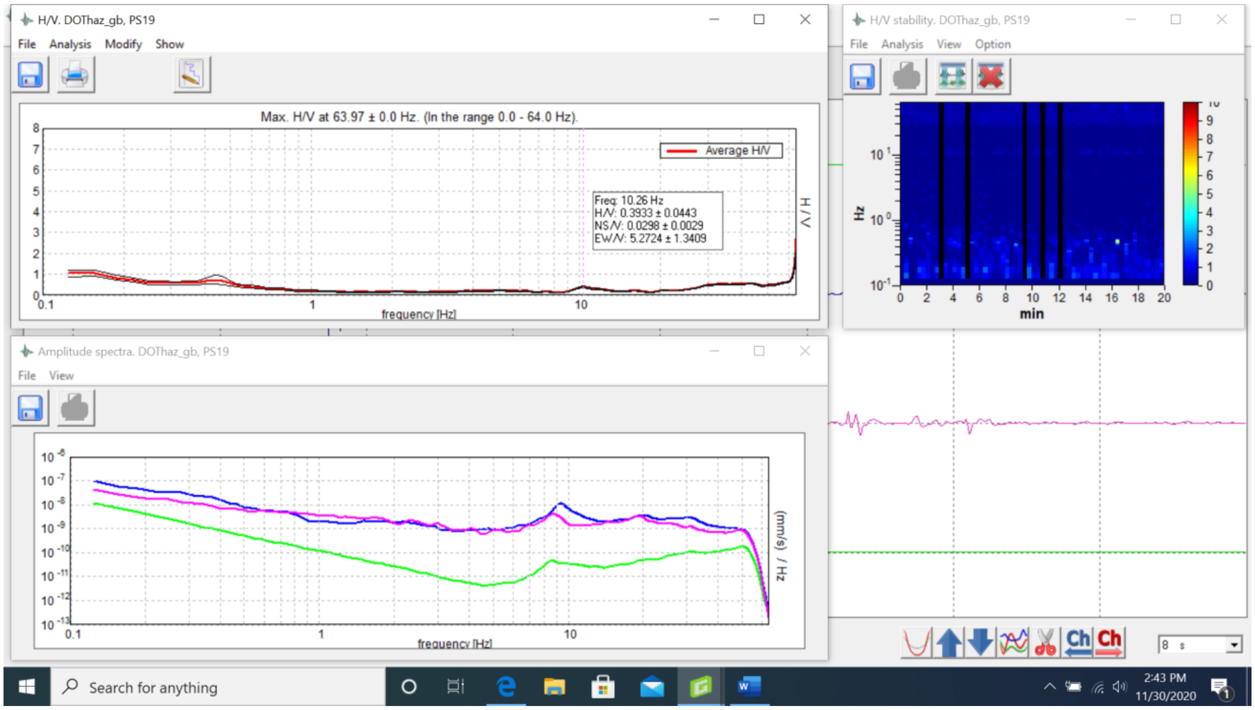
H/V. DOThaz_gb, PS19
File Analysis Modify Show
Max. H/V at 63.97 ± 0.0 Hz. (In the range 0.0 - 64.0 Hz).
Average H/V
Freq: 10.26 Hz
H/V: 0.3933 ± 0.0443
NS/V: 0.0298 ± 0.0029
EW/V: 5.2724 ± 1.3409
frequency [Hz]
H/V. stability. DOThaz_gb, PS19
File Analysis View Option
Hz
min
Amplitude spectra. DOThaz_gb, PS19
File View
frequency [Hz]
(mm/s) / Hz
Search for anything
2:43 PM
11/30/2020

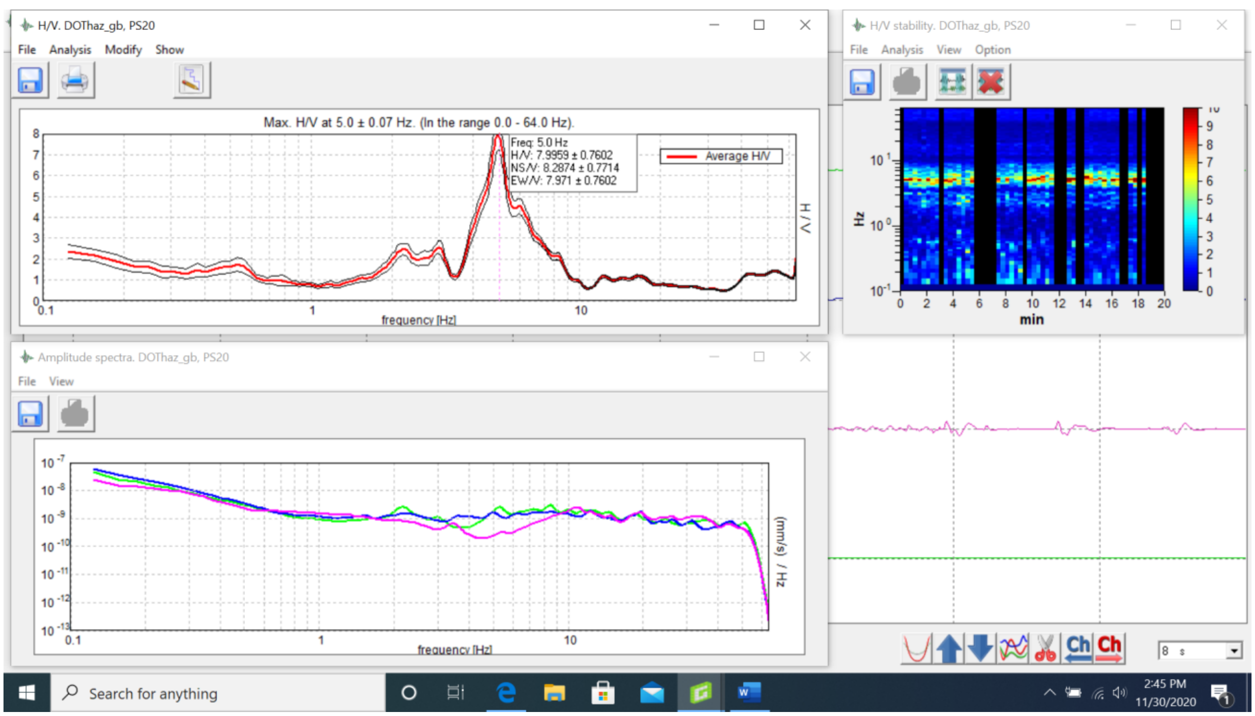
H/V. DOThaz_gb, PS20
File Analysis Modify Show
Max. H/V at 5.0 ± 0.07 Hz. (In the range 0.0 - 64.0 Hz).
Freq: 5.0 Hz
H/V: 7.9959 ± 0.7602
NS/V: 8.2874 ± 0.7714
EW/V: 7.971 ± 0.7602
Average H/V
frequency [Hz]
H/V stability. DOThaz_gb, PS20
File Analysis View Option
Hz
min
Amplitude spectra. DOThaz_gb, PS20
File View
frequency [Hz]
(mm/s) / Hz
Search for anything
2:45 PM
11/30/2020

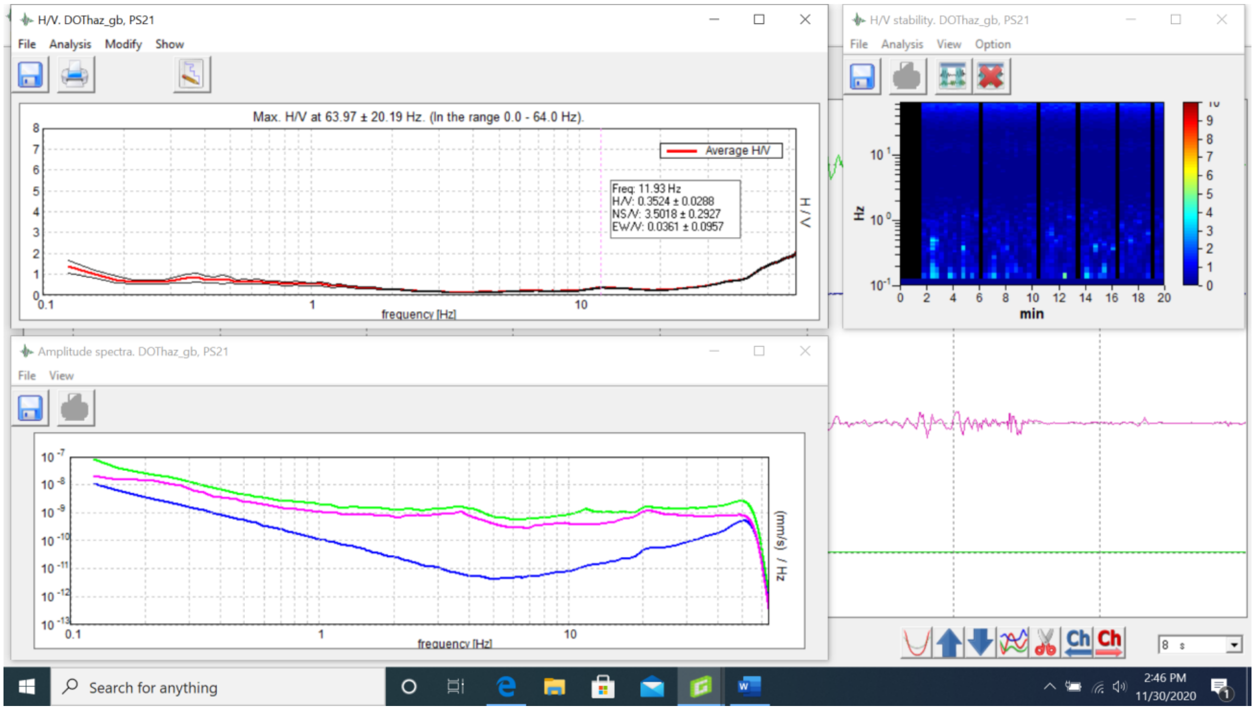
H/V. DOThaz_gb, PS21
File Analysis Modify Show
Max. H/V at 63.97 ± 20.19 Hz. (In the range 0.0 - 64.0 Hz).
Average H/V
Freq: 11.93 Hz
H/V: 0.3524 ± 0.0288
NS/V: 3.5018 ± 0.2927
EW/V: 0.0361 ± 0.0957
H / V
frequency [Hz]
H/V stability. DOThaz_gb, PS21
File Analysis View Option
Hz
min
Amplitude spectra. DOThaz_gb, PS21
File View
(mm/s) / Hz
frequency [Hz]
Search for anything
2:46 PM
11/30/2020

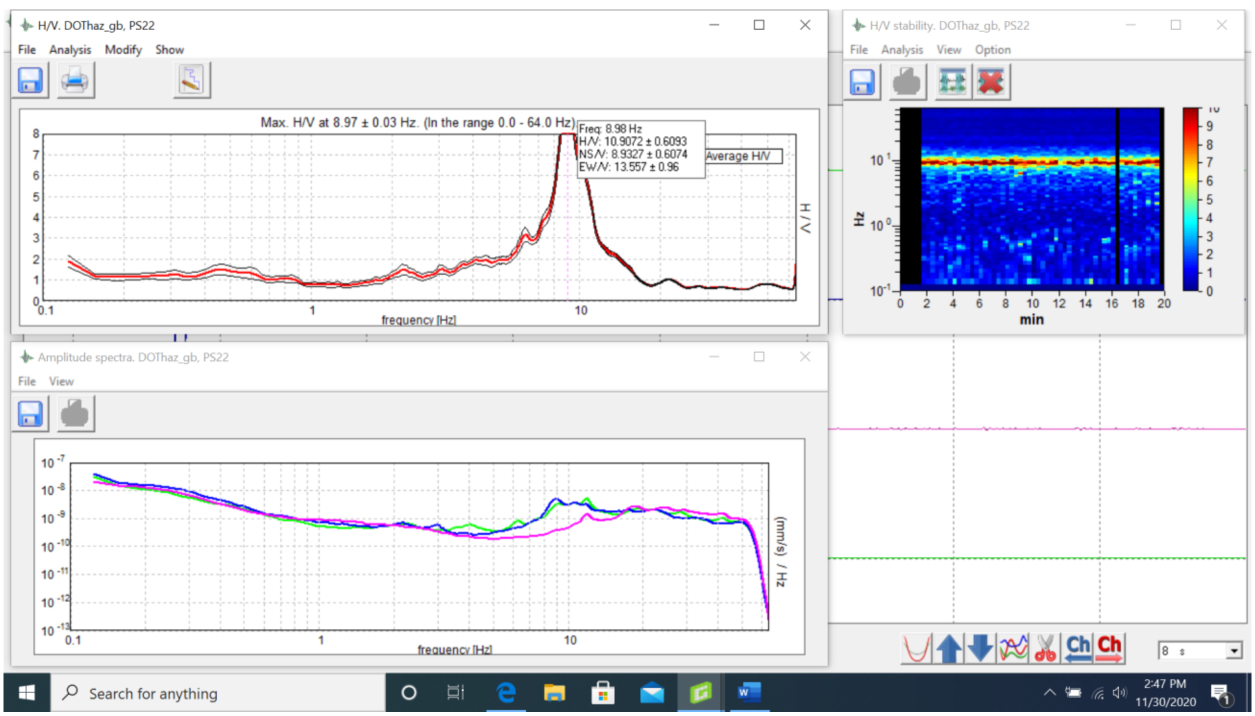
H/V. DOThaz_gb, PS22
File Analysis Modify Show
Max. H/V at 8.97 ± 0.03 Hz. (In the range 0.0 - 64.0 Hz)
Freq: 8.98 Hz
H/V: 10.9072 ± 0.6093
NS/V: 8.9327 ± 0.6074
EW/V: 13.557 ± 0.96
Average H/V
H / V
frequency [Hz]
H/V stability. DOThaz_gb, PS22
File Analysis View Option
Hz
min
Amplitude spectra. DOThaz_gb, PS22
File View
(mm/s) / Hz
frequency [Hz]
Search for anything
2:47 PM
11/30/2020

Worth County: PS23-PS53

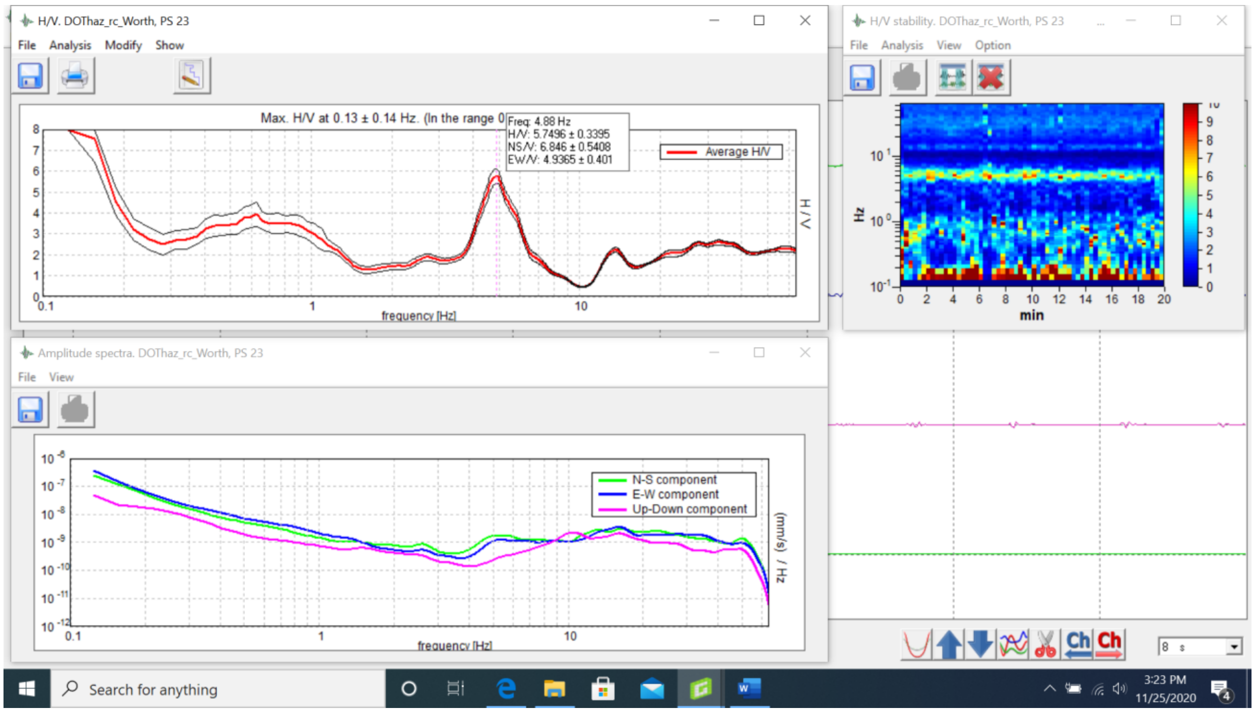


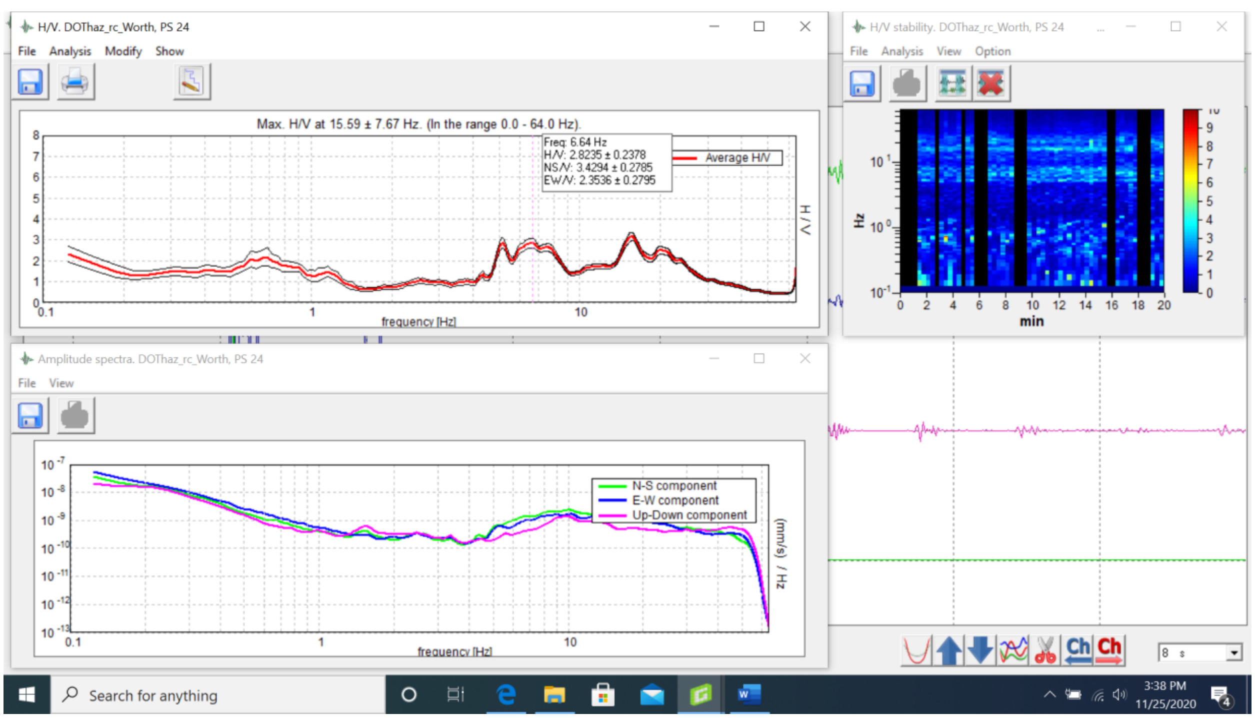

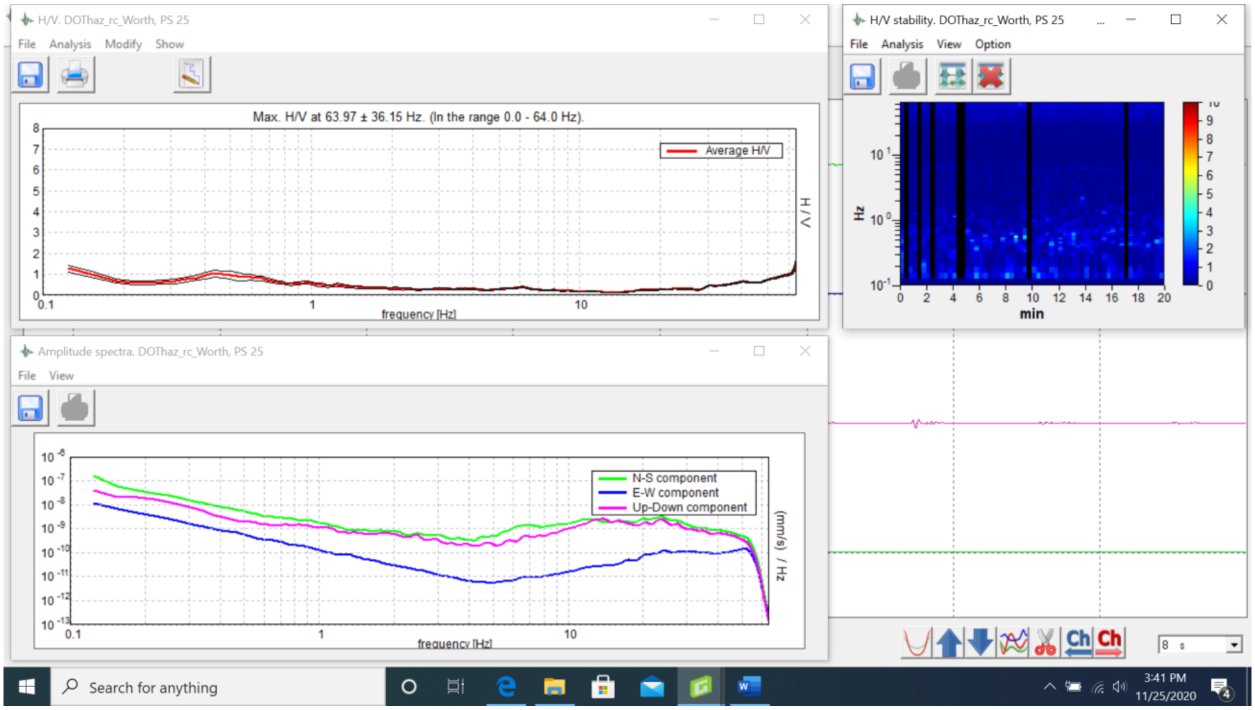
H/V. DOThaz_rc_Worth, PS 25
File Analysis Modify Show
Max. H/V at 63.97 ± 36.15 Hz. (In the range 0.0 - 64.0 Hz).
Average H/V
frequency [Hz]
H / V
H/V stability. DOThaz_rc_Worth, PS 25
File Analysis View Option
Hz
min
Amplitude spectra. DOThaz_rc_Worth, PS 25
File View
N-S component
E-W component
Up-Down component
frequency [Hz]
(mm/s) / Hz
Search for anything
3:41 PM
11/25/2020

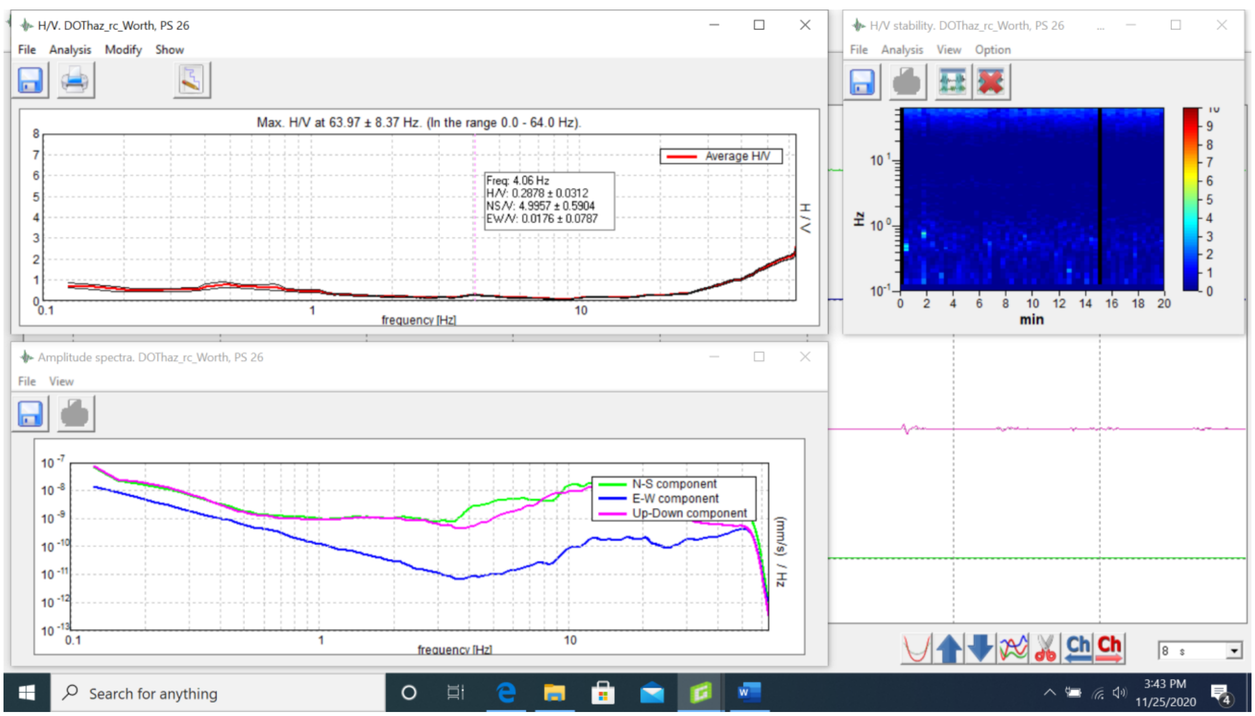
H/V. DOThaz_rc_Worth, PS 26
File Analysis Modify Show
Max. H/V at 63.97 ± 8.37 Hz. (In the range 0.0 - 64.0 Hz).
Average H/V
Freq: 4.06 Hz
H/V: 0.2878 ± 0.0312
NS/V: 4.9957 ± 0.5904
EW/V: 0.0176 ± 0.0787
frequency [Hz]
H / V
H/V stability. DOThaz_rc_Worth, PS 26
File Analysis View Option
Hz
min
Amplitude spectra. DOThaz_rc_Worth, PS 26
File View
N-S component
E-W component
Up-Down component
frequency [Hz]
(mm/s) / Hz
Search for anything
3:43 PM
11/25/2020

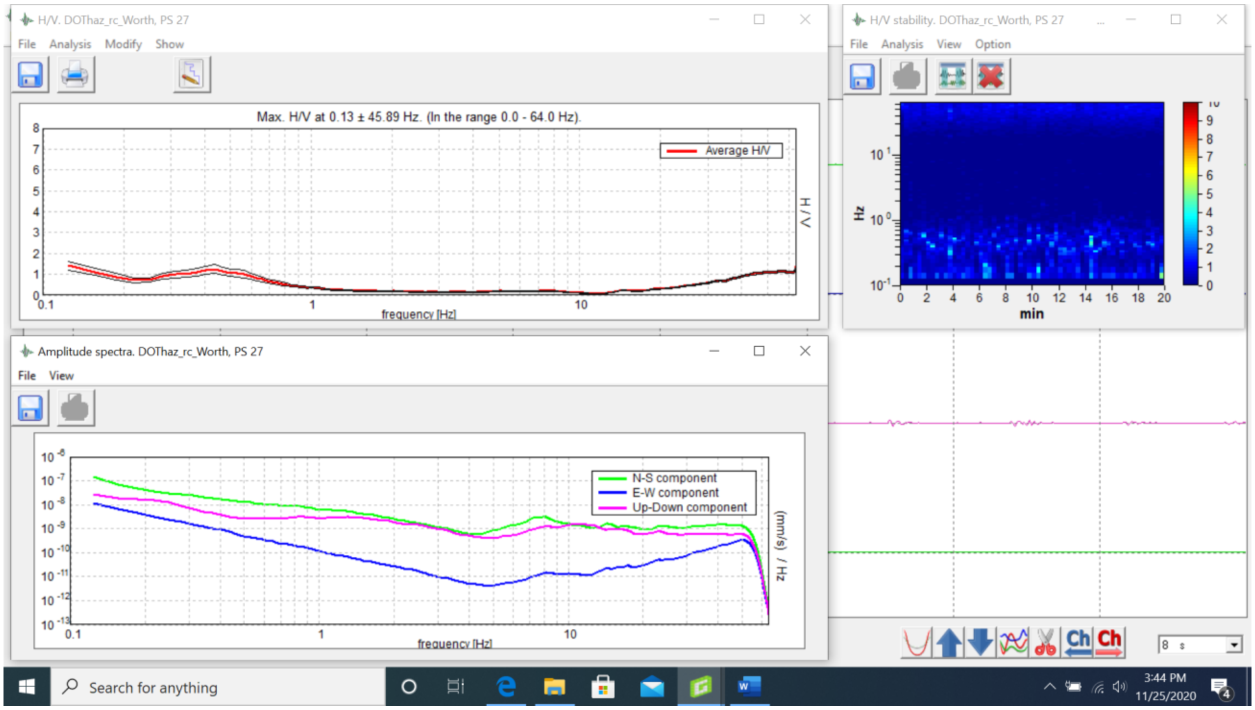
H/V. DOThaz_rc_Worth, PS 27
Max. H/V at 0.13 ± 45.89 Hz. (In the range 0.0 - 64.0 Hz).
Average H/V
frequency [Hz]
H/V stability. DOThaz_rc_Worth, PS 27
Amplitude spectra. DOThaz_rc_Worth, PS 27
N-S component
E-W component
Up-Down component
3:44 PM
11/25/2020

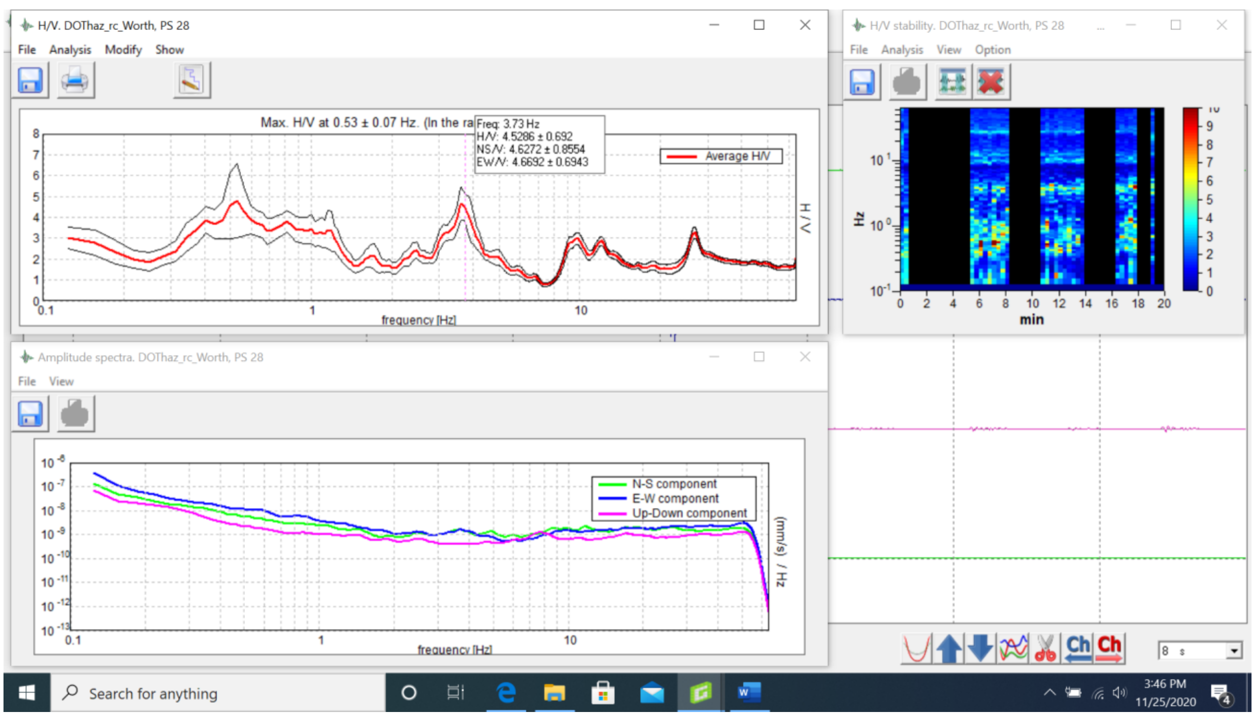
H/V. DOThaz_rc_Worth, PS 28
Max. H/V at 0.53 ± 0.07 Hz.
Freq: 3.73 Hz
H/V: 4.5286 ± 0.692
NS/V: 4.6272 ± 0.8554
EW/V: 4.6692 ± 0.6943
Average H/V
frequency [Hz]
H/V stability. DOThaz_rc_Worth, PS 28
Amplitude spectra. DOThaz_rc_Worth, PS 28
N-S component
E-W component
Up-Down component
3:46 PM
11/25/2020

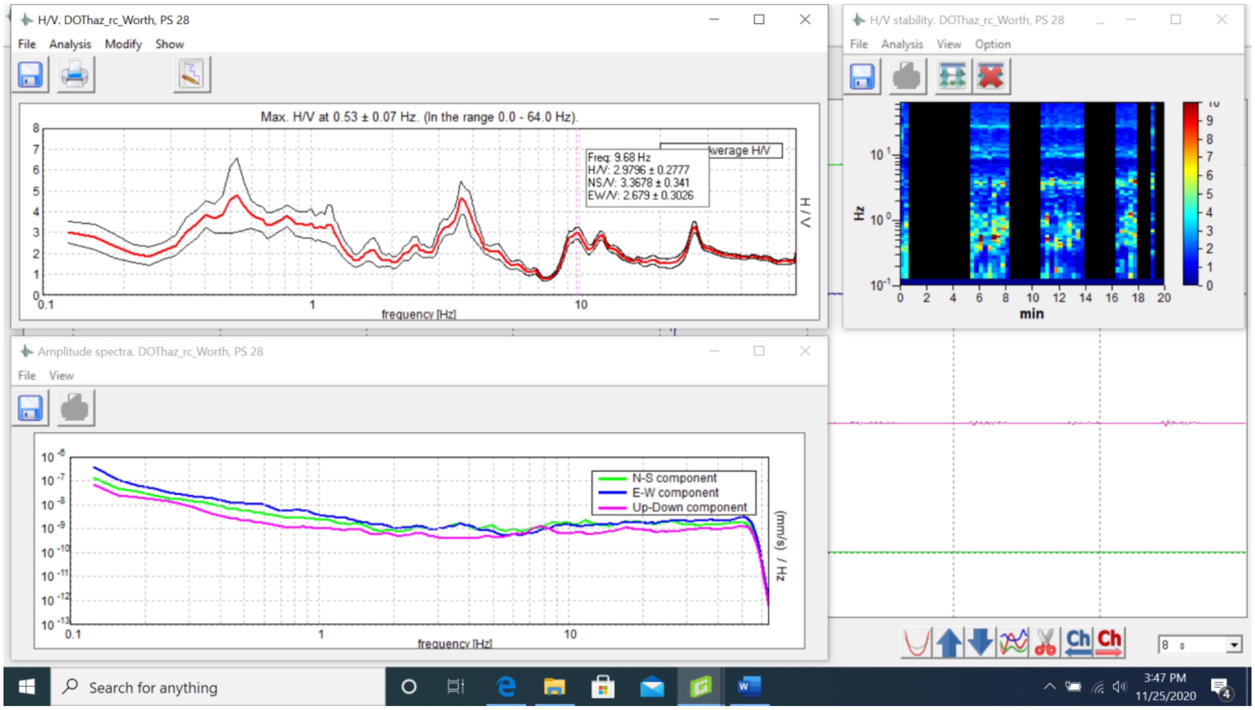
H/V. DOThaz_rc_Worth, PS 28
Max. H/V at 0.53 ± 0.07 Hz. (In the range 0.0 - 64.0 Hz).
Average H/V
Freq: 9.68 Hz
H/V: 2.9796 ± 0.2777
NS/V: 3.3678 ± 0.341
EW/V: 2.679 ± 0.3026
frequency [Hz]
H/V stability. DOThaz_rc_Worth, PS 28
min
Hz
Amplitude spectra. DOThaz_rc_Worth, PS 28
N-S component
E-W component
Up-Down component
(mm/s) / Hz
frequency [Hz]
Search for anything
3:47 PM
11/25/2020

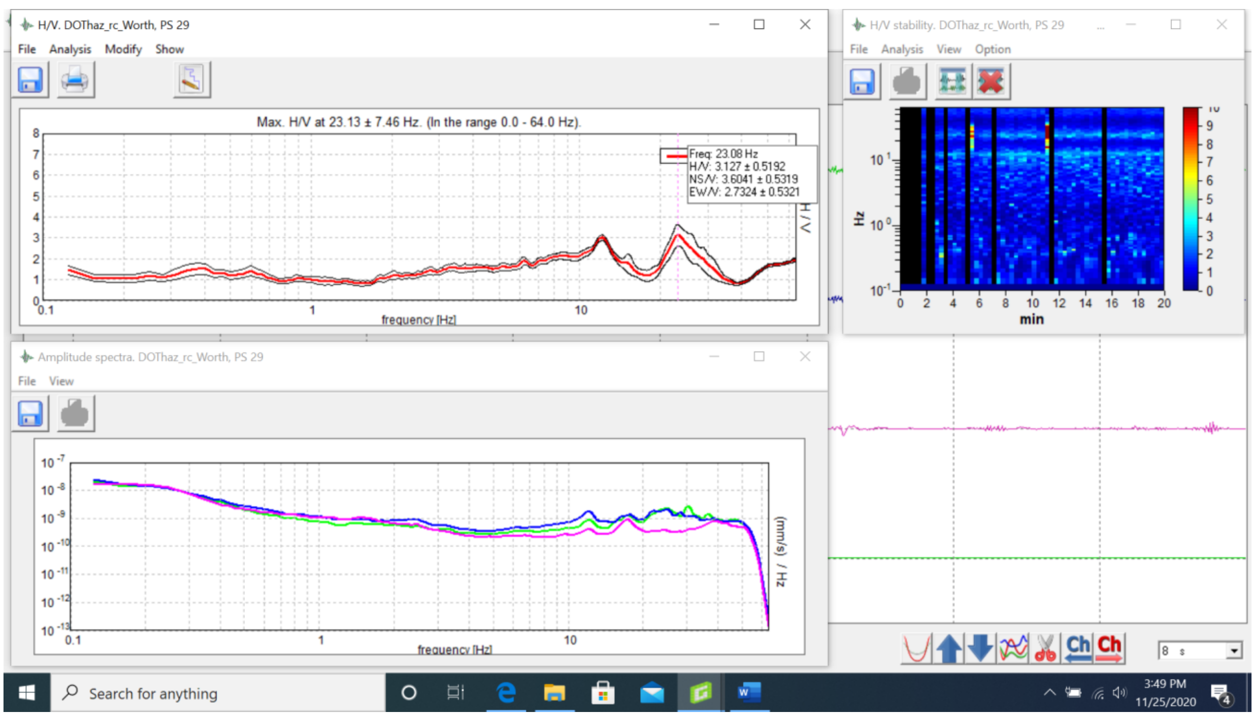
H/V. DOThaz_rc_Worth, PS 29
Max. H/V at 23.13 ± 7.46 Hz. (In the range 0.0 - 64.0 Hz).
Freq: 23.08 Hz
H/V: 3.127 ± 0.5192
NS/V: 3.6041 ± 0.5319
EW/V: 2.7324 ± 0.5321
frequency [Hz]
H/V stability. DOThaz_rc_Worth, PS 29
min
Hz
Amplitude spectra. DOThaz_rc_Worth, PS 29
(mm/s) / Hz
frequency [Hz]
Search for anything
3:49 PM
11/25/2020

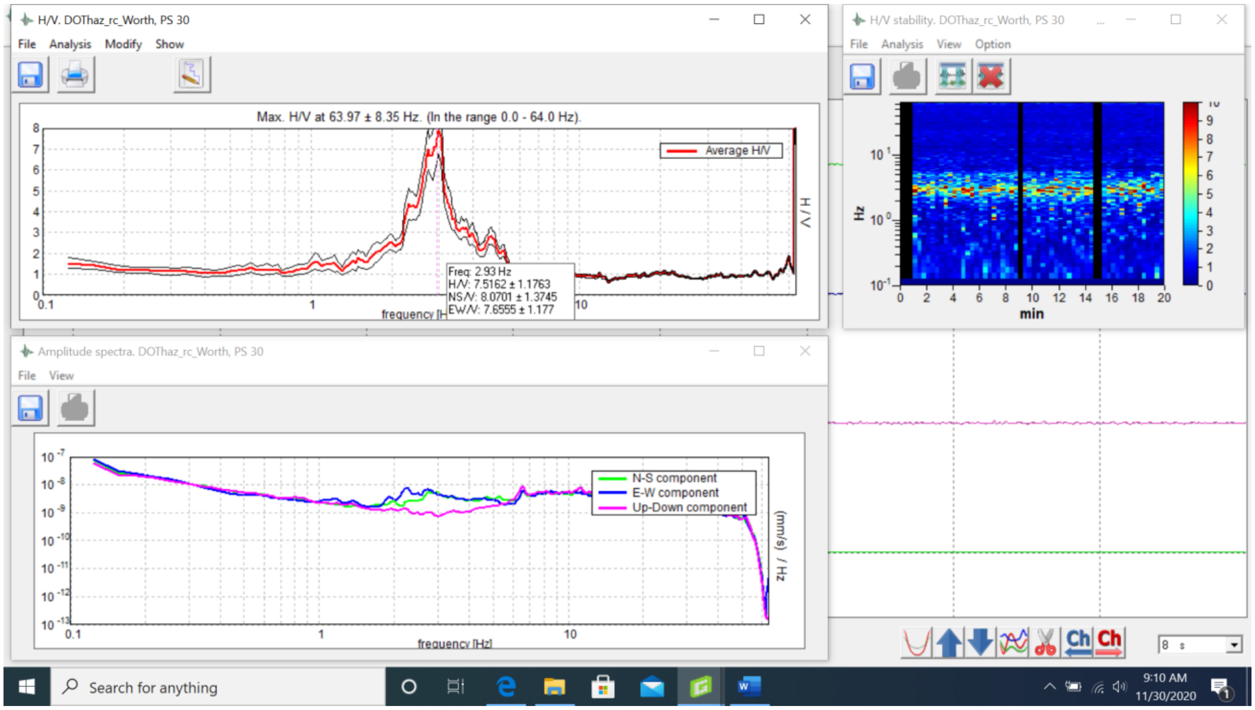
H/V. DOThaz_rc_Worth, PS 30
Max. H/V at 63.97 ± 8.35 Hz. (In the range 0.0 - 64.0 Hz).
Average H/V
Freq: 2.93 Hz
H/V: 7.5162 ± 1.1763
NS/V: 8.0701 ± 1.3745
EW/V: 7.6555 ± 1.177
H/V stability. DOThaz_rc_Worth, PS 30
Hz
min
Amplitude spectra. DOThaz_rc_Worth, PS 30
N-S component
E-W component
Up-Down component
frequency [Hz]
(mm/s) / Hz
Search for anything
9:10 AM
11/30/2020

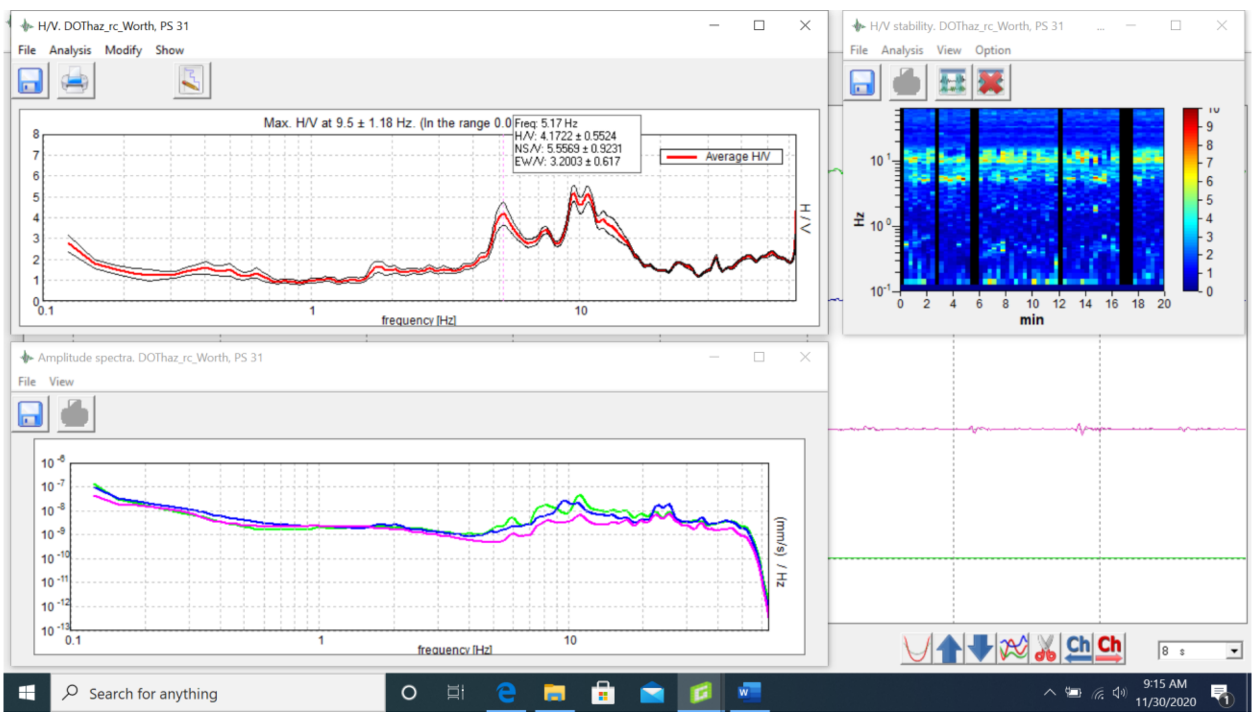
H/V. DOThaz_rc_Worth, PS 31
Max. H/V at 9.5 ± 1.18 Hz. (In the range 0.0
Freq: 5.17 Hz
H/V: 4.1722 ± 0.5524
NS/V: 5.5569 ± 0.9231
EW/V: 3.2003 ± 0.617
Average H/V
frequency [Hz]
H/V stability. DOThaz_rc_Worth, PS 31
Hz
min
Amplitude spectra. DOThaz_rc_Worth, PS 31
(mm/s) / Hz
Search for anything
9:15 AM
11/30/2020

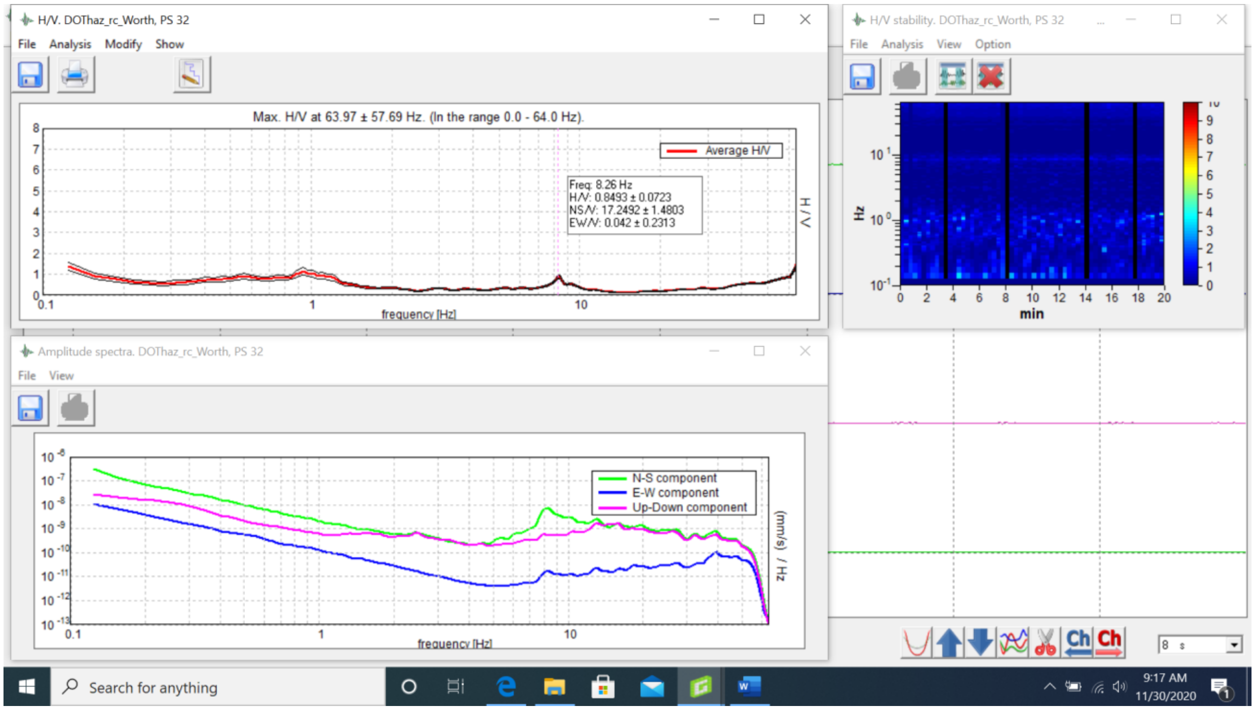
H/V. DOThaz_rc_Worth, PS 32
File Analysis Modify Show
Max. H/V at 63.97 ± 57.69 Hz. (In the range 0.0 - 64.0 Hz).
Average H/V
Freq: 8.26 Hz
H/V: 0.8493 ± 0.0723
NS/V: 17.2492 ± 1.4803
EW/V: 0.042 ± 0.2313
frequency [Hz]
H / V
H/V stability. DOThaz_rc_Worth, PS 32
File Analysis View Option
Hz
min
Amplitude spectra. DOThaz_rc_Worth, PS 32
File View
N-S component
E-W component
Up-Down component
frequency [Hz]
(mm/s) / Hz
Search for anything
9:17 AM
11/30/2020

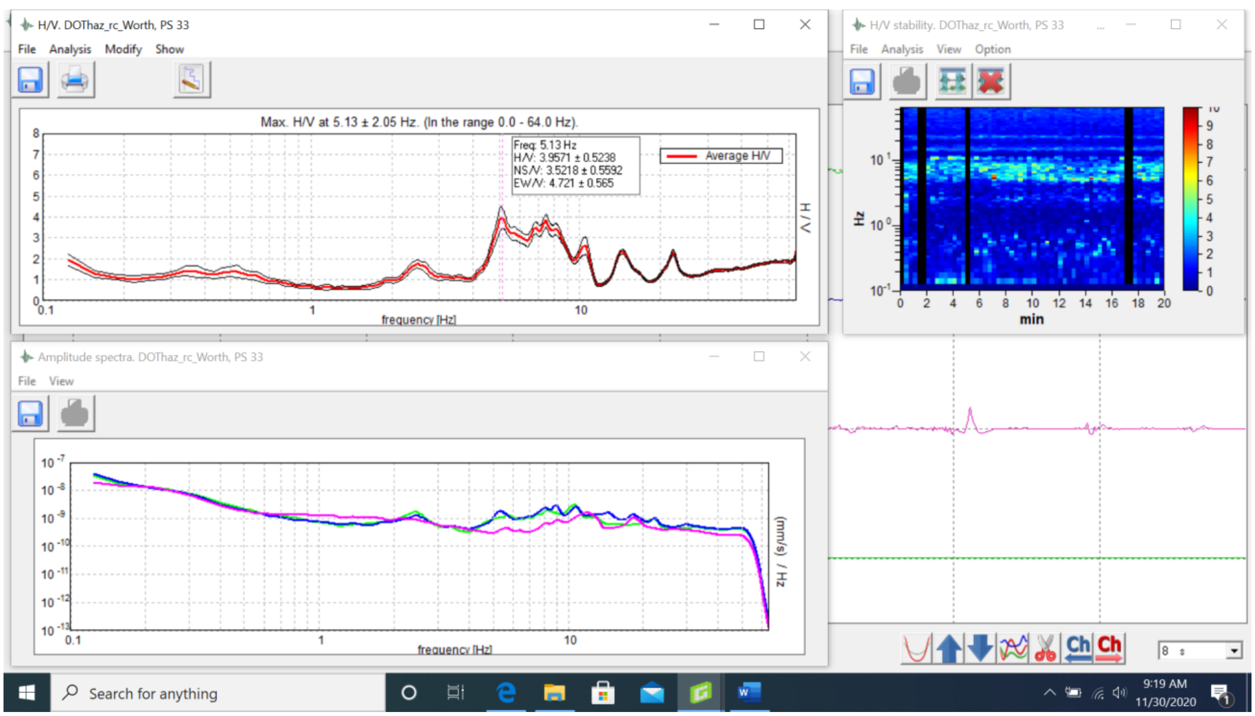
H/V. DOThaz_rc_Worth, PS 33
File Analysis Modify Show
Max. H/V at 5.13 ± 2.05 Hz. (In the range 0.0 - 64.0 Hz).
Freq: 5.13 Hz
H/V: 3.9571 ± 0.5238
NS/V: 3.5218 ± 0.5592
EW/V: 4.721 ± 0.565
Average H/V
frequency [Hz]
H / V
H/V stability. DOThaz_rc_Worth, PS 33
File Analysis View Option
Hz
min
Amplitude spectra. DOThaz_rc_Worth, PS 33
File View
frequency [Hz]
(mm/s) / Hz
Search for anything
9:19 AM
11/30/2020

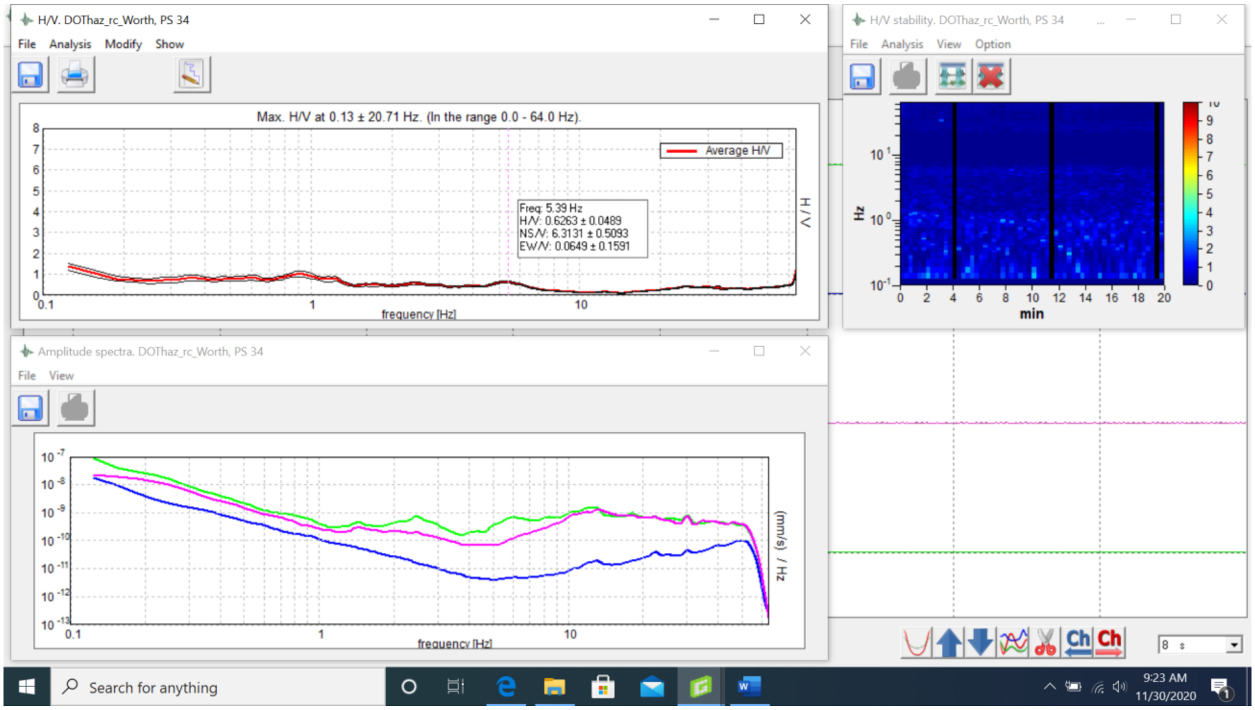
H/V. DOThaz_rc_Worth, PS 34
File Analysis Modify Show
Max. H/V at 0.13 ± 20.71 Hz. (In the range 0.0 - 64.0 Hz).
Average H/V
Freq: 5.39 Hz
H/V: 0.6263 ± 0.0489
NS/V: 6.3131 ± 0.5093
EW/V: 0.0649 ± 0.1591
H / V
frequency [Hz]
H/V stability. DOThaz_rc_Worth, PS 34
File Analysis View Option
Hz
min
Amplitude spectra. DOThaz_rc_Worth, PS 34
File View
(mm/s) / Hz
frequency [Hz]
Search for anything
9:23 AM
11/30/2020

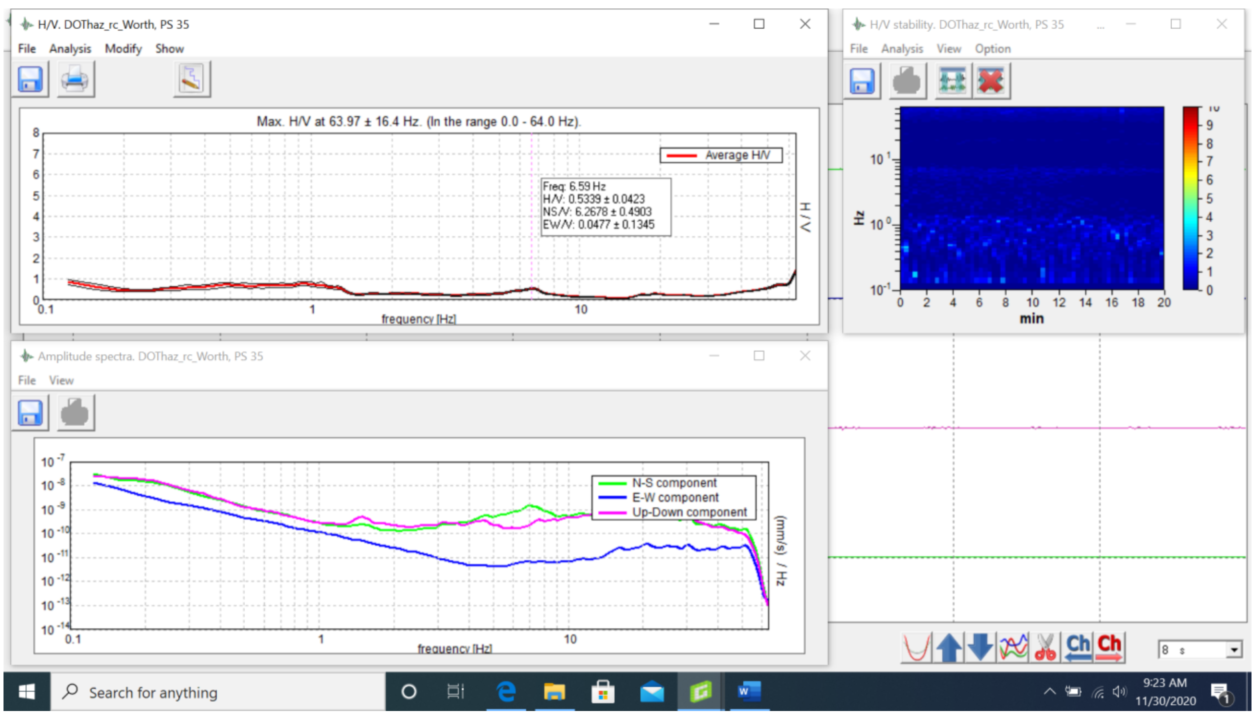
H/V. DOThaz_rc_Worth, PS 35
File Analysis Modify Show
Max. H/V at 63.97 ± 16.4 Hz. (In the range 0.0 - 64.0 Hz).
Average H/V
Freq: 6.59 Hz
H/V: 0.5339 ± 0.0423
NS/V: 6.2678 ± 0.4903
EW/V: 0.0477 ± 0.1345
H / V
frequency [Hz]
H/V stability. DOThaz_rc_Worth, PS 35
File Analysis View Option
Hz
min
Amplitude spectra. DOThaz_rc_Worth, PS 35
File View
N-S component
E-W component
Up-Down component
(mm/s) / Hz
frequency [Hz]
Search for anything
9:23 AM
11/30/2020

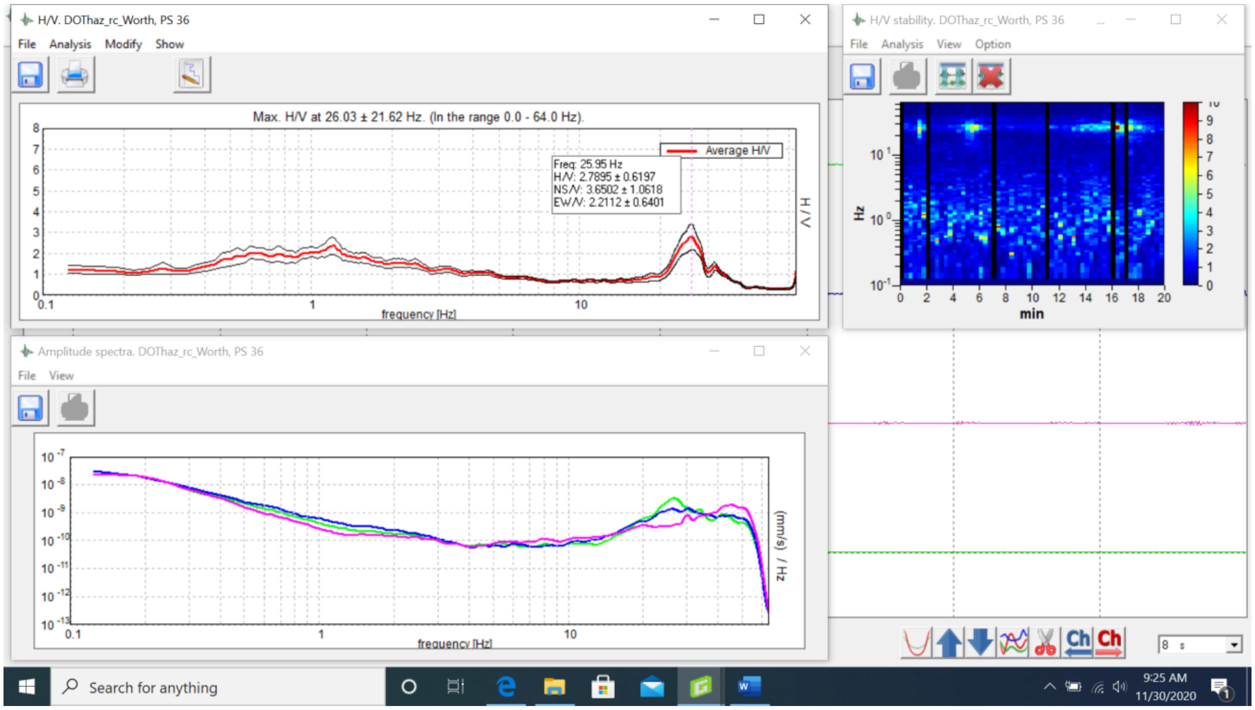
H/V. DOThaz_rc_Worth, PS 36
File Analysis Modify Show
Max. H/V at 26.03 ± 21.62 Hz. (In the range 0.0 - 64.0 Hz).
Average H/V
Freq: 25.95 Hz
H/V: 2.7895 ± 0.6197
NS/V: 3.6502 ± 1.0618
EW/V: 2.2112 ± 0.6401
H / V
frequency [Hz]
H/V stability. DOThaz_rc_Worth, PS 36
File Analysis View Option
Hz
min
Amplitude spectra. DOThaz_rc_Worth, PS 36
File View
(mm/s) / Hz
frequency [Hz]
Search for anything
9:25 AM
11/30/2020

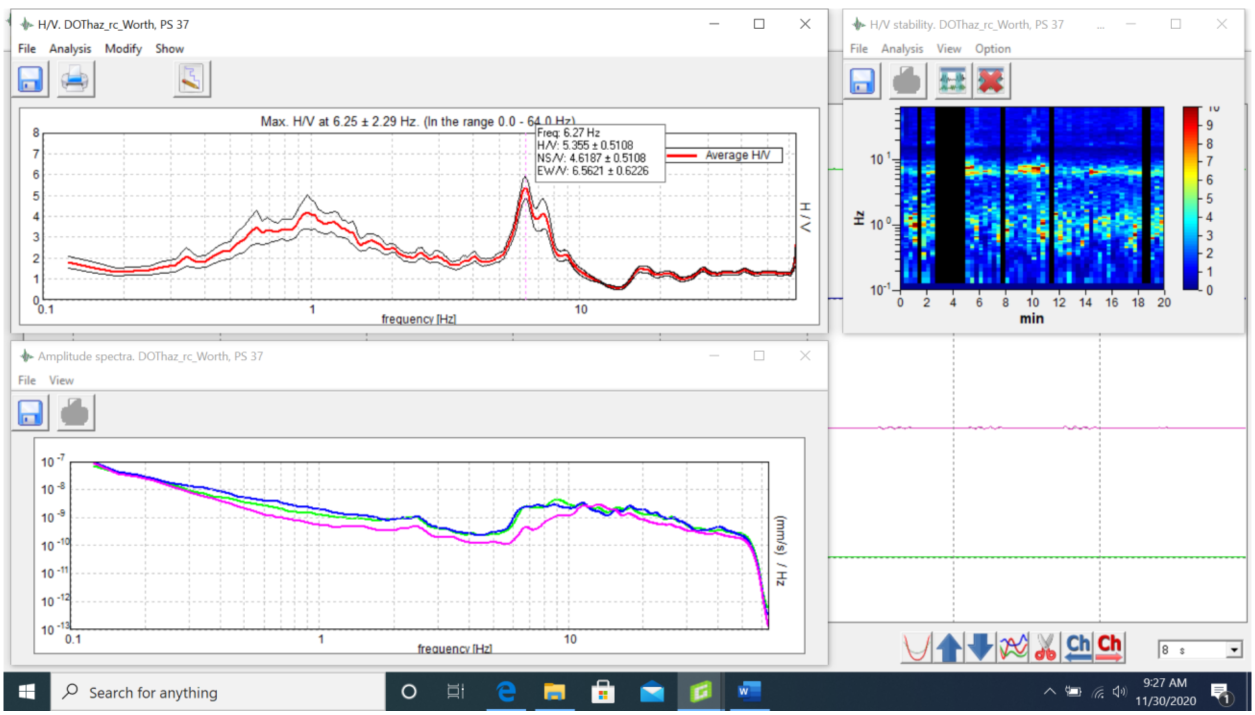
H/V. DOThaz_rc_Worth, PS 37
File Analysis Modify Show
Max. H/V at 6.25 ± 2.29 Hz. (In the range 0.0 - 64.0 Hz).
Freq: 6.27 Hz
H/V: 5.355 ± 0.5108
NS/V: 4.6187 ± 0.5108
EW/V: 6.5621 ± 0.6226
Average H/V
H / V
frequency [Hz]
H/V stability. DOThaz_rc_Worth, PS 37
File Analysis View Option
Hz
min
Amplitude spectra. DOThaz_rc_Worth, PS 37
File View
(mm/s) / Hz
frequency [Hz]
Search for anything
9:27 AM
11/30/2020

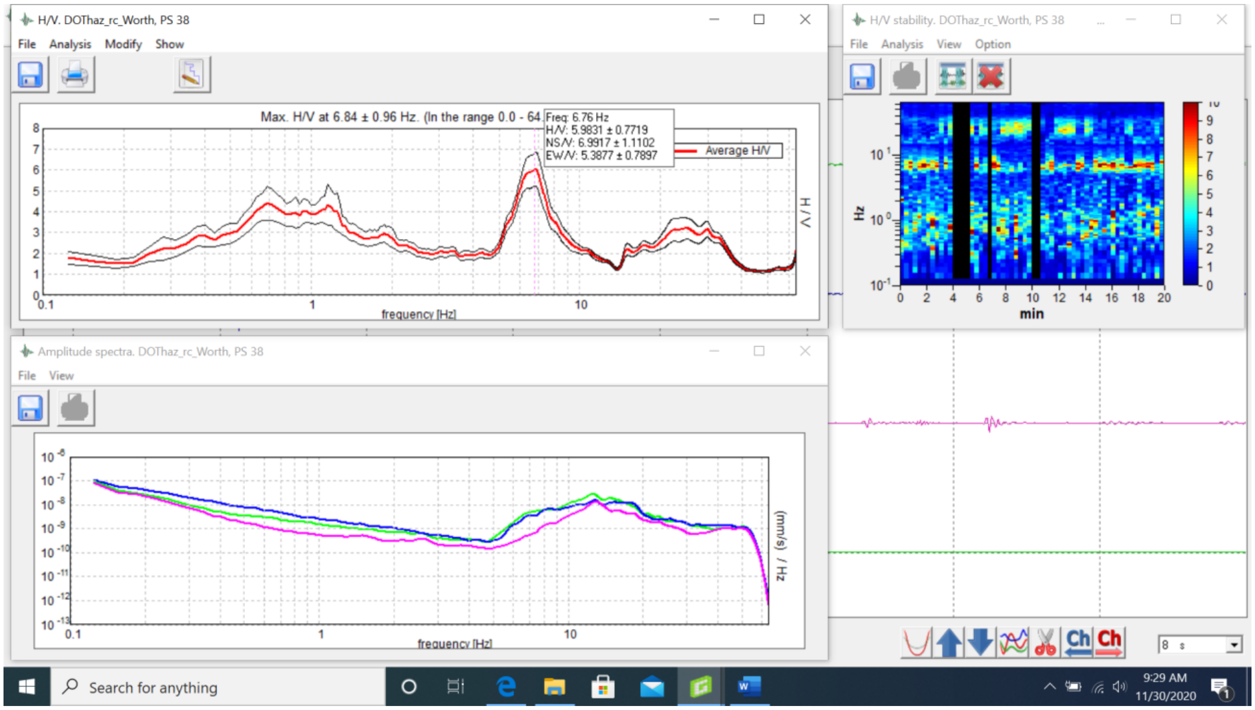
H/V. DOThaz_rc_Worth, PS 38
File Analysis Modify Show
Max. H/V at 6.84 ± 0.96 Hz. (In the range 0.0 - 64
Freq: 6.76 Hz
H/V: 5.9831 ± 0.7719
NS/V: 6.9917 ± 1.1102
EW/V: 5.3877 ± 0.7897
Average H/V
frequency [Hz]
H / V
H/V stability. DOThaz_rc_Worth, PS 38
File Analysis View Option
Hz
min
Amplitude spectra. DOThaz_rc_Worth, PS 38
File View
frequency [Hz]
(mm/s) / Hz
Search for anything
9:29 AM
11/30/2020

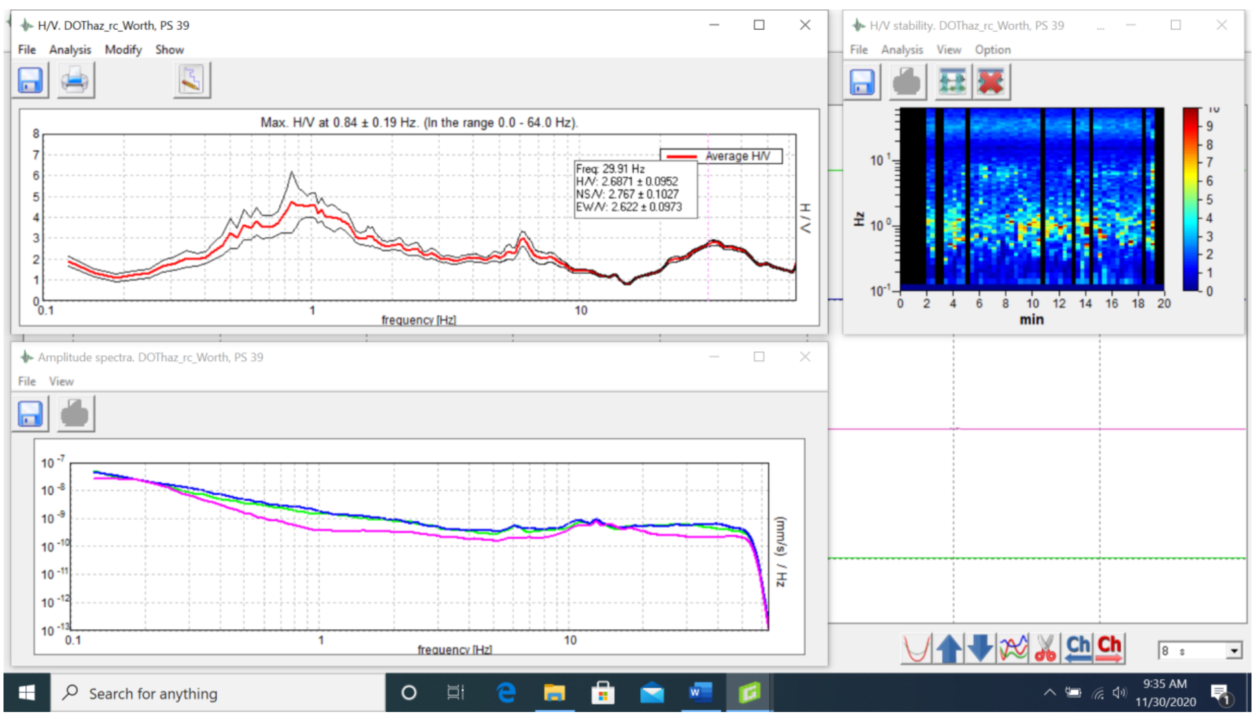
H/V. DOThaz_rc_Worth, PS 39
File Analysis Modify Show
Max. H/V at 0.84 ± 0.19 Hz. (In the range 0.0 - 64.0 Hz).
Average H/V
Freq: 29.91 Hz
H/V: 2.6871 ± 0.0952
NS/V: 2.767 ± 0.1027
EW/V: 2.622 ± 0.0973
frequency [Hz]
H / V
H/V stability. DOThaz_rc_Worth, PS 39
File Analysis View Option
Hz
min
Amplitude spectra. DOThaz_rc_Worth, PS 39
File View
frequency [Hz]
(mm/s) / Hz
Search for anything
9:35 AM
11/30/2020

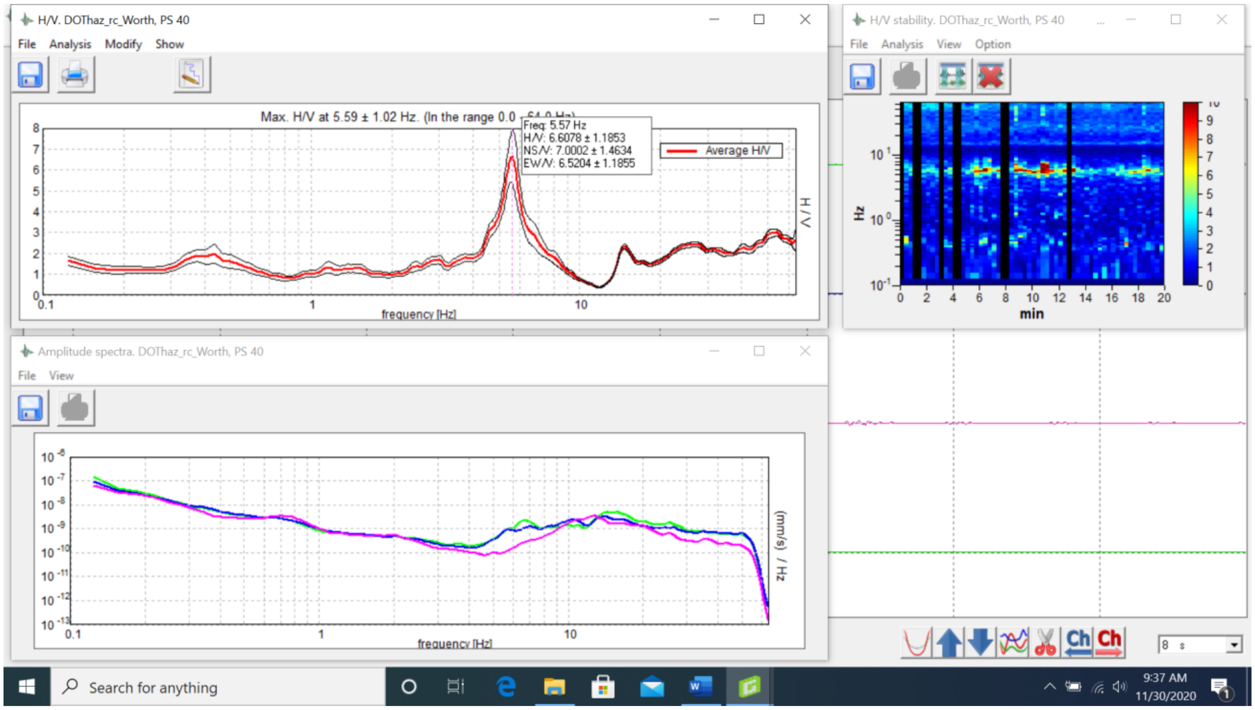
H/V. DOThaz_rc_Worth, PS 40
File Analysis Modify Show
Max. H/V at 5.59 ± 1.02 Hz. (In the range 0.0 - 64.0 Hz).
Freq: 5.57 Hz
H/V: 6.6078 ± 1.1853
NS/V: 7.0002 ± 1.4634
EW/V: 6.5204 ± 1.1855
Average H/V
frequency [Hz]
H / V
H/V stability. DOThaz_rc_Worth, PS 40
File Analysis View Option
Hz
min
Amplitude spectra. DOThaz_rc_Worth, PS 40
File View
frequency [Hz]
(mm/s) / Hz
Search for anything
9:37 AM
11/30/2020

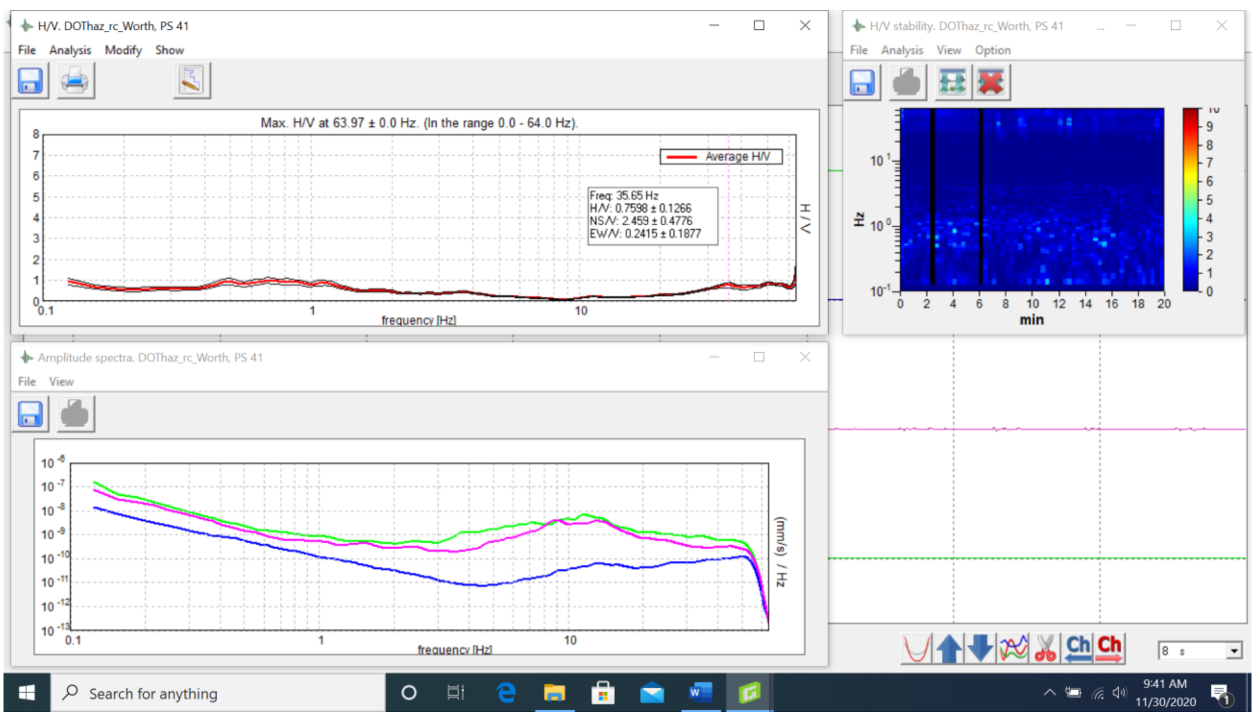
H/V. DOThaz_rc_Worth, PS 41
File Analysis Modify Show
Max. H/V at 63.97 ± 0.0 Hz. (In the range 0.0 - 64.0 Hz).
Average H/V
Freq: 35.65 Hz
H/V: 0.7598 ± 0.1266
NS/V: 2.459 ± 0.4776
EW/V: 0.2415 ± 0.1877
frequency [Hz]
H / V
H/V stability. DOThaz_rc_Worth, PS 41
File Analysis View Option
Hz
min
Amplitude spectra. DOThaz_rc_Worth, PS 41
File View
frequency [Hz]
(mm/s) / Hz
Search for anything
9:41 AM
11/30/2020

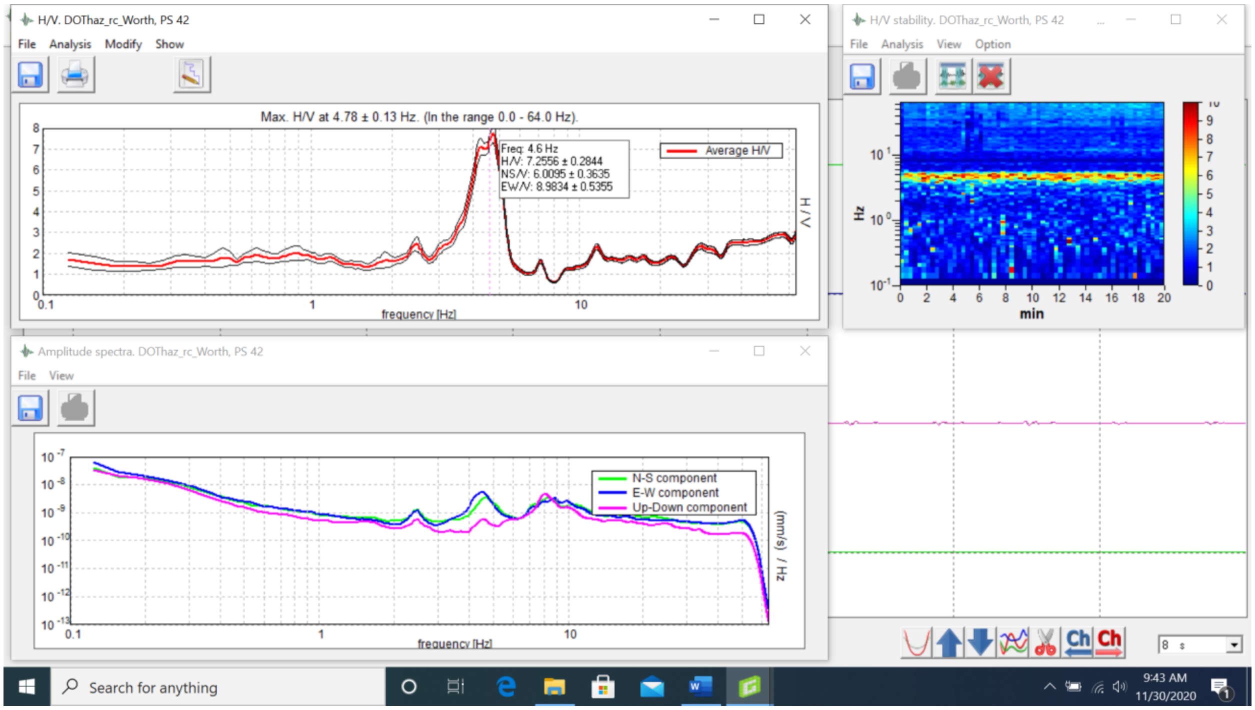
H/V. DOThaz_rc_Worth, PS 42
File Analysis Modify Show
Max. H/V at 4.78 ± 0.13 Hz. (In the range 0.0 - 64.0 Hz).
Freq: 4.6 Hz
H/V: 7.2556 ± 0.2844
NS/V: 6.0095 ± 0.3635
EW/V: 8.9834 ± 0.5355
Average H/V
frequency [Hz]
H / V
H/V stability. DOThaz_rc_Worth, PS 42
File Analysis View Option
Hz
min
Amplitude spectra. DOThaz_rc_Worth, PS 42
File View
N-S component
E-W component
Up-Down component
frequency [Hz]
(mm/s) / Hz
Search for anything
9:43 AM
11/30/2020

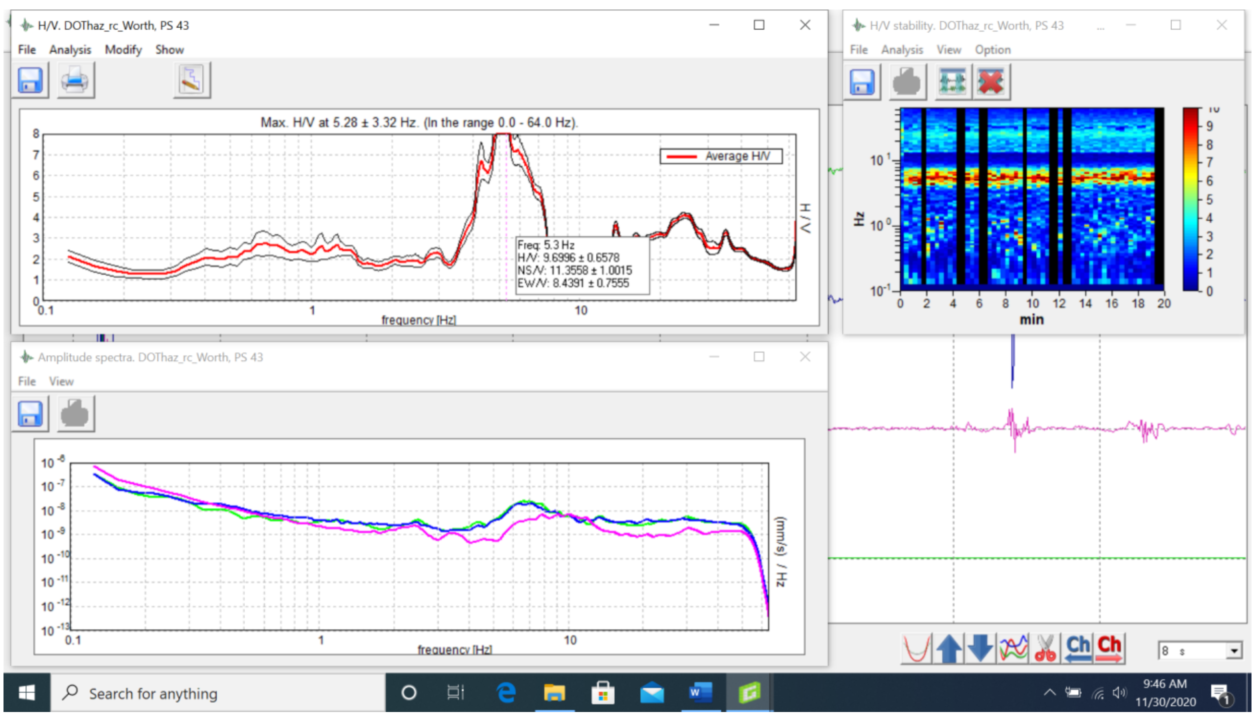
H/V. DOThaz_rc_Worth, PS 43
File Analysis Modify Show
Max. H/V at 5.28 ± 3.32 Hz. (In the range 0.0 - 64.0 Hz).
Freq: 5.3 Hz
H/V: 9.6996 ± 0.6578
NS/V: 11.3558 ± 1.0015
EW/V: 8.4391 ± 0.7555
Average H/V
frequency [Hz]
H / V
H/V stability. DOThaz_rc_Worth, PS 43
File Analysis View Option
Hz
min
Amplitude spectra. DOThaz_rc_Worth, PS 43
File View
frequency [Hz]
(mm/s) / Hz
Search for anything
9:46 AM
11/30/2020

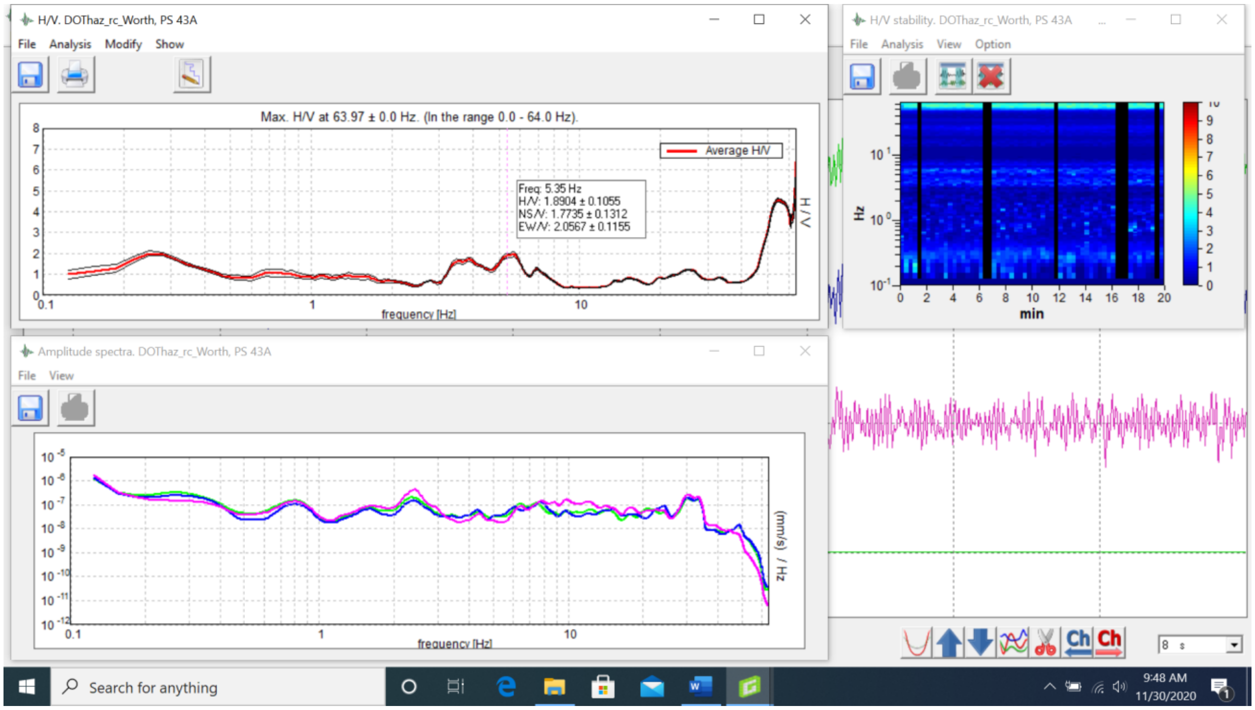
H/V. DOThaz_rc_Worth, PS 43A
File Analysis Modify Show
Max. H/V at 63.97 ± 0.0 Hz. (In the range 0.0 - 64.0 Hz).
Average H/V
Freq: 5.35 Hz
H/V: 1.8904 ± 0.1055
NS/V: 1.7735 ± 0.1312
EW/V: 2.0567 ± 0.1155
H / V
frequency [Hz]
H/V stability. DOThaz_rc_Worth, PS 43A
File Analysis View Option
Hz
min
Amplitude spectra. DOThaz_rc_Worth, PS 43A
File View
(mm/s) / Hz
frequency [Hz]
Search for anything
9:48 AM
11/30/2020

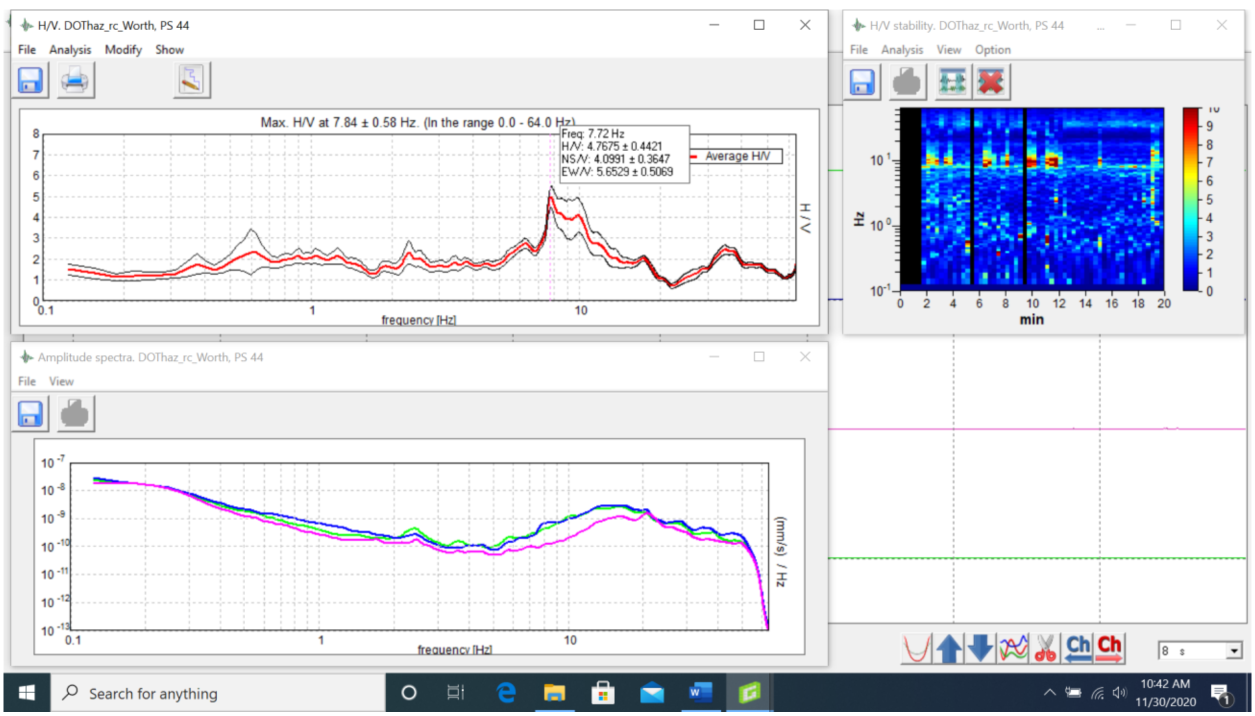
H/V. DOThaz_rc_Worth, PS 44
File Analysis Modify Show
Max. H/V at 7.84 ± 0.58 Hz. (In the range 0.0 - 64.0 Hz).
Freq: 7.72 Hz
H/V: 4.7675 ± 0.4421
NS/V: 4.0991 ± 0.3647
EW/V: 5.6529 ± 0.5069
Average H/V
H / V
frequency [Hz]
H/V stability. DOThaz_rc_Worth, PS 44
File Analysis View Option
Hz
min
Amplitude spectra. DOThaz_rc_Worth, PS 44
File View
(mm/s) / Hz
frequency [Hz]
Search for anything
10:42 AM
11/30/2020

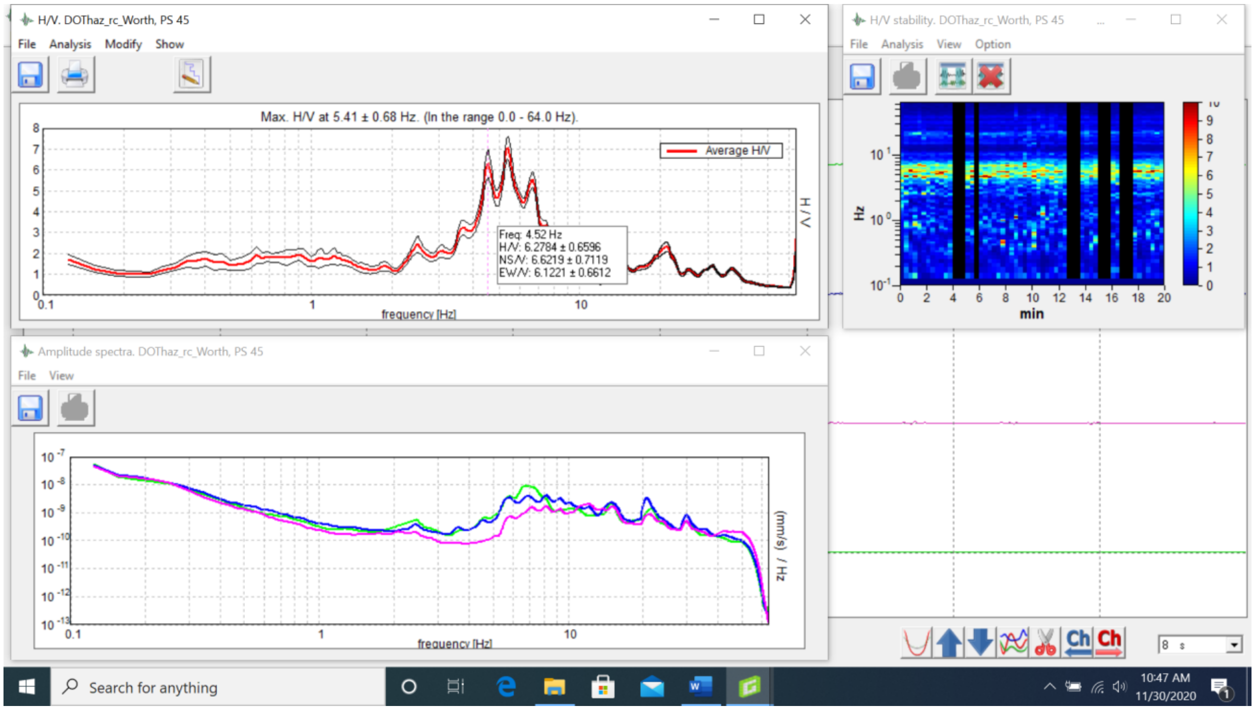
H/V. DOThaz_rc_Worth, PS 45
Max. H/V at 5.41 ± 0.68 Hz. (In the range 0.0 - 64.0 Hz).
Average H/V
Freq: 4.52 Hz
H/V: 6.2784 ± 0.6596
NS/V: 6.6219 ± 0.7119
EW/V: 6.1221 ± 0.6612
frequency [Hz]
H/V stability. DOThaz_rc_Worth, PS 45
min
Amplitude spectra. DOThaz_rc_Worth, PS 45
frequency [Hz]
(mm/s) / Hz
10:47 AM
11/30/2020

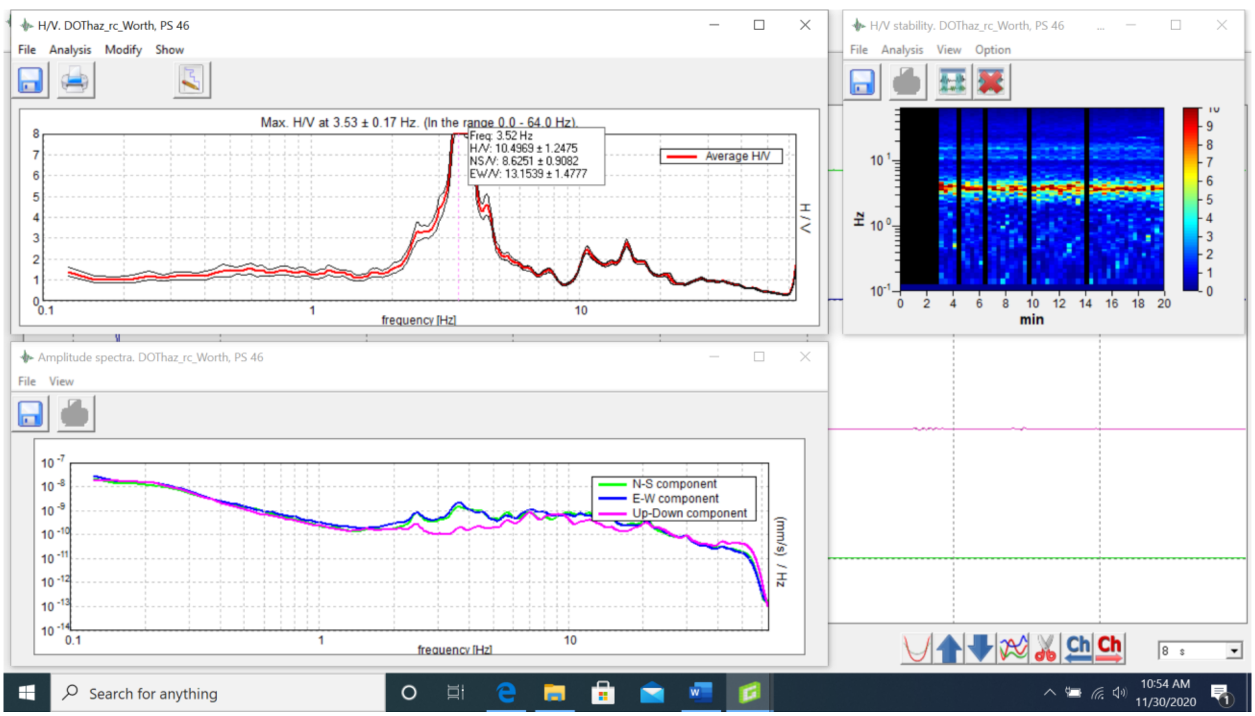
H/V. DOThaz_rc_Worth, PS 46
Max. H/V at 3.53 ± 0.17 Hz. (In the range 0.0 - 64.0 Hz).
Freq: 3.52 Hz
H/V: 10.4969 ± 1.2475
NS/V: 8.6251 ± 0.9082
EW/V: 13.1539 ± 1.4777
Average H/V
frequency [Hz]
H/V stability. DOThaz_rc_Worth, PS 46
min
Amplitude spectra. DOThaz_rc_Worth, PS 46
N-S component
E-W component
Up-Down component
frequency [Hz]
(mm/s) / Hz
10:54 AM
11/30/2020

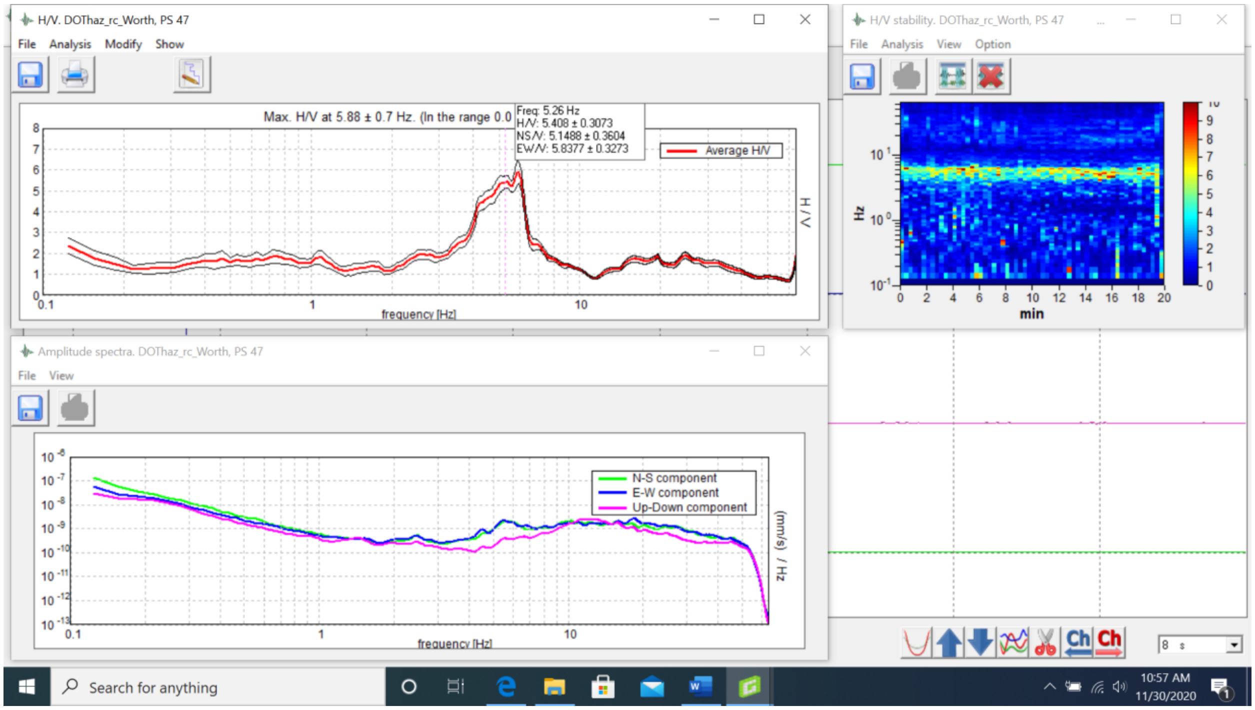
H/V. DOThaz_rc_Worth, PS 47
File Analysis Modify Show
Max. H/V at 5.88 ± 0.7 Hz. (In the range 0.0
Freq: 5.26 Hz
H/V: 5.408 ± 0.3073
NS/V: 5.1488 ± 0.3604
EW/V: 5.8377 ± 0.3273
Average H/V
H / V
frequency [Hz]
H/V stability. DOThaz_rc_Worth, PS 47
File Analysis View Option
Hz
min
Amplitude spectra. DOThaz_rc_Worth, PS 47
File View
N-S component
E-W component
Up-Down component
(mm/s) / Hz
frequency [Hz]
Search for anything
10:57 AM
11/30/2020

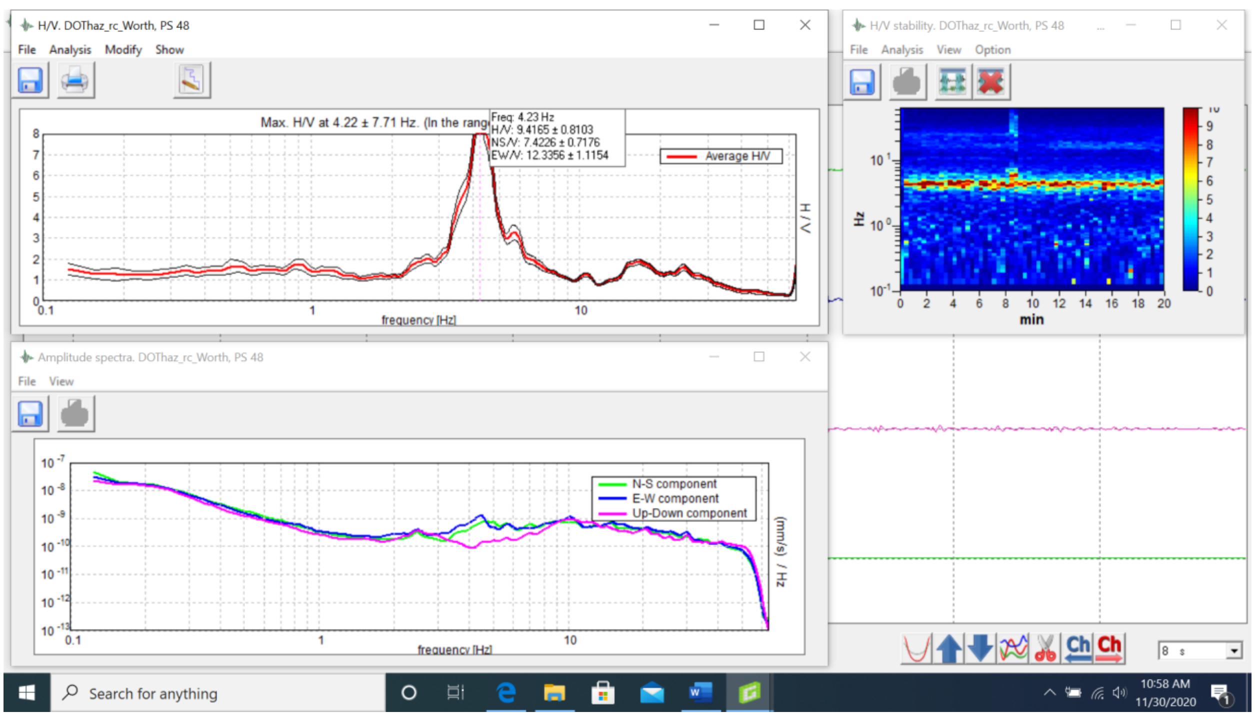
H/V. DOThaz_rc_Worth, PS 48
File Analysis Modify Show
Max. H/V at 4.22 ± 7.71 Hz. (In the rang
Freq: 4.23 Hz
H/V: 9.4165 ± 0.8103
NS/V: 7.4226 ± 0.7176
EW/V: 12.3356 ± 1.1154
Average H/V
H / V
frequency [Hz]
H/V stability. DOThaz_rc_Worth, PS 48
File Analysis View Option
Hz
min
Amplitude spectra. DOThaz_rc_Worth, PS 48
File View
N-S component
E-W component
Up-Down component
(mm/s) / Hz
frequency [Hz]
Search for anything
10:58 AM
11/30/2020

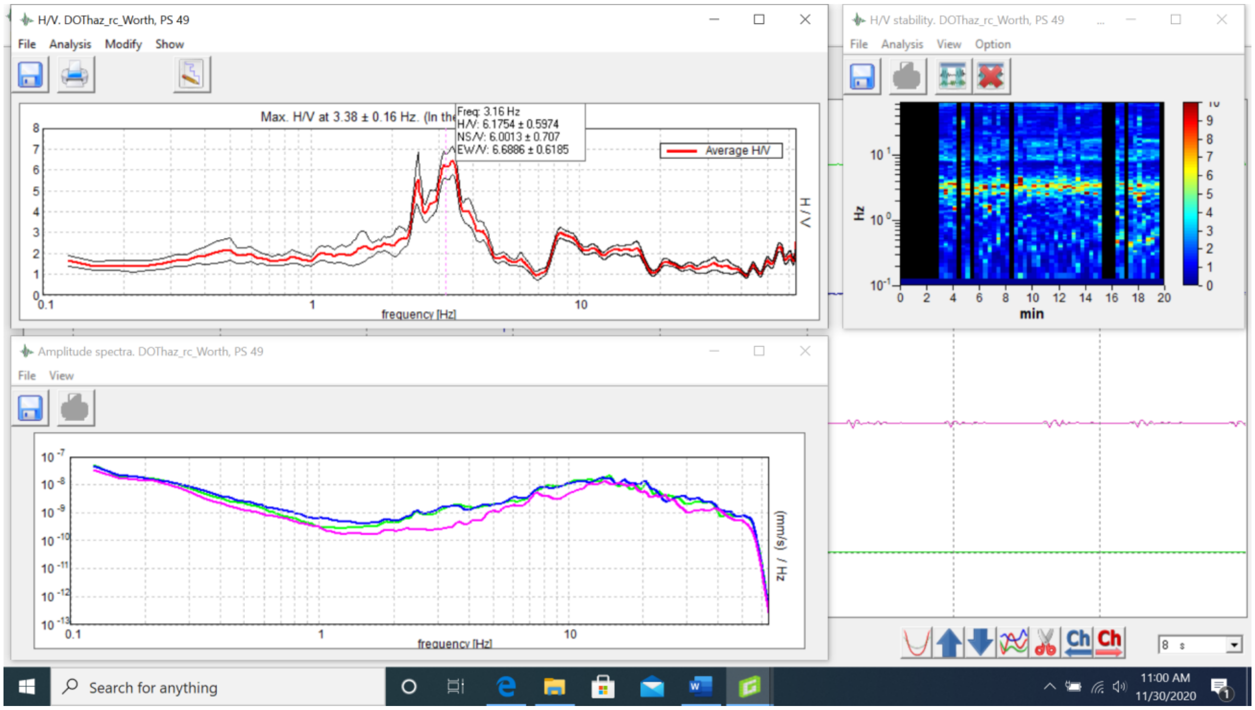
H/V. DOThaz_rc_Worth, PS 49
File Analysis Modify Show
Max. H/V at 3.38 ± 0.16 Hz.
Freq: 3.16 Hz
H/V: 6.1754 ± 0.5974
NS/V: 6.0013 ± 0.707
EW/V: 6.6886 ± 0.6185
Average H/V
frequency [Hz]
H / V
H/V stability. DOThaz_rc_Worth, PS 49
File Analysis View Option
Hz
min
Amplitude spectra. DOThaz_rc_Worth, PS 49
File View
frequency [Hz]
(mm/s) / Hz
Search for anything
11:00 AM
11/30/2020

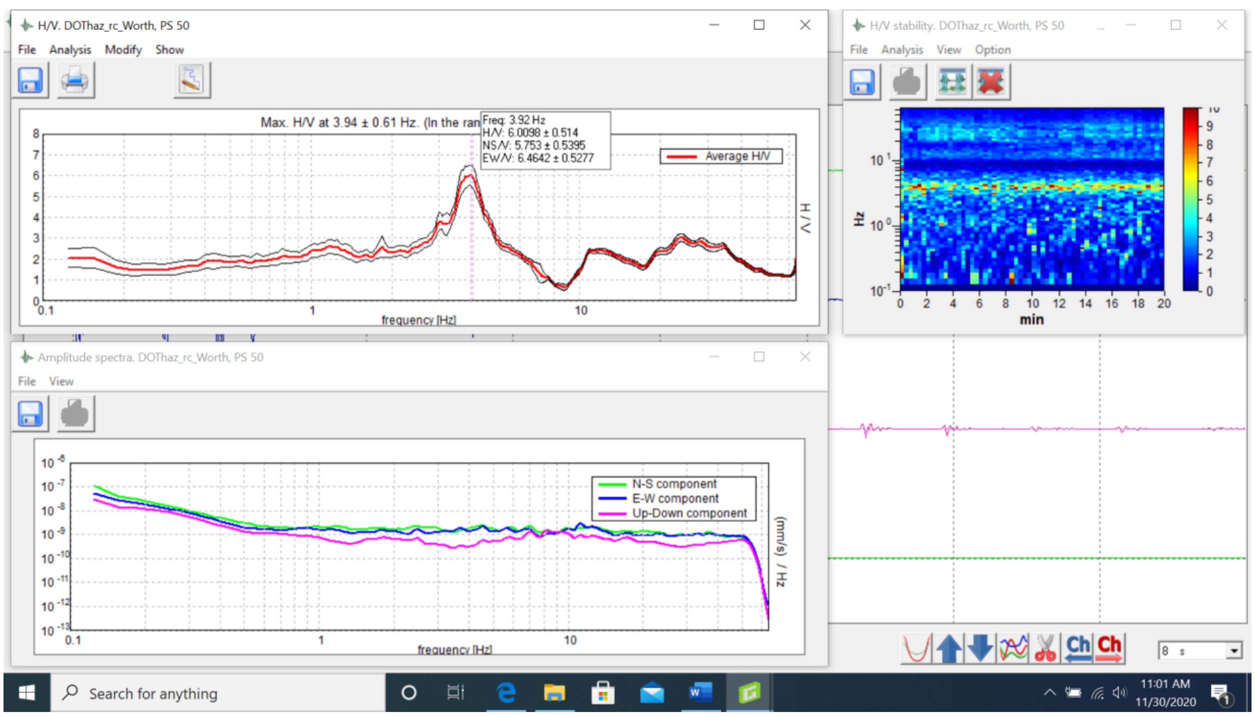
H/V. DOThaz_rc_Worth, PS 50
File Analysis Modify Show
Max. H/V at 3.94 ± 0.61 Hz. (In the ran
Freq: 3.92 Hz
H/V: 6.0098 ± 0.514
NS/V: 5.753 ± 0.5395
EW/V: 6.4642 ± 0.5277
Average H/V
frequency [Hz]
H / V
H/V stability. DOThaz_rc_Worth, PS 50
File Analysis View Option
Hz
min
Amplitude spectra. DOThaz_rc_Worth, PS 50
File View
N-S component
E-W component
Up-Down component
frequency [Hz]
(mm/s) / Hz
Search for anything
11:01 AM
11/30/2020

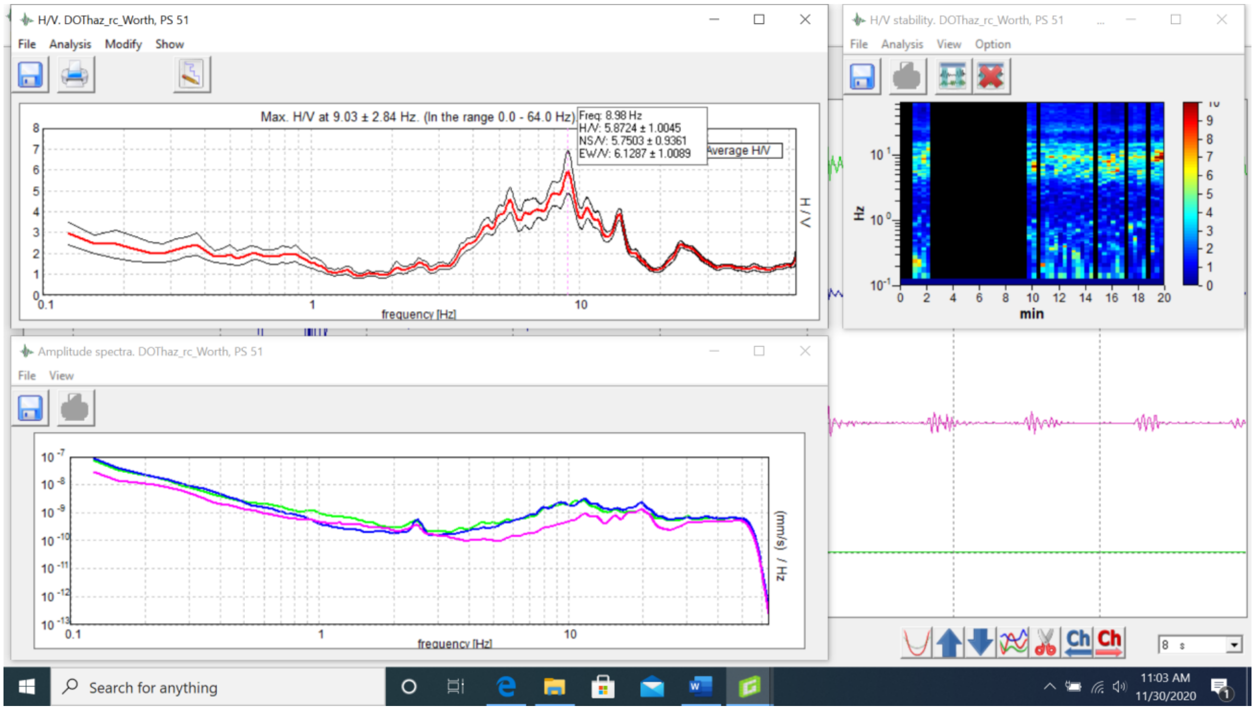
H/V. DOThaz_rc_Worth, PS 51
File Analysis Modify Show
Max. H/V at 9.03 ± 2.84 Hz. (In the range 0.0 - 64.0 Hz)
Freq: 8.98 Hz
H/V: 5.8724 ± 1.0045
NS/V: 5.7503 ± 0.9361
EW/V: 6.1287 ± 1.0089
Average H/V
frequency [Hz]
H / V
H/V stability. DOThaz_rc_Worth, PS 51
File Analysis View Option
Hz
min
Amplitude spectra. DOThaz_rc_Worth, PS 51
File View
frequency [Hz]
(mm/s) / Hz
Search for anything
11:03 AM
11/30/2020

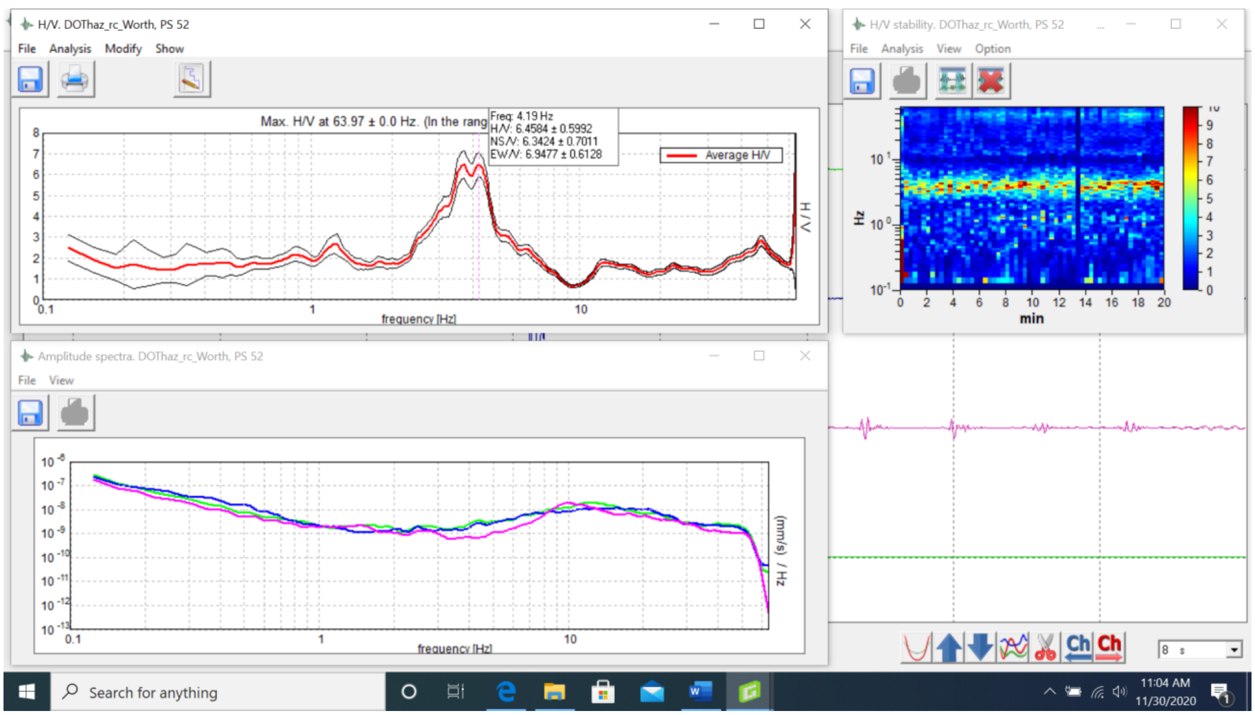
H/V. DOThaz_rc_Worth, PS 52
File Analysis Modify Show
Max. H/V at 63.97 ± 0.0 Hz. (In the rang
Freq: 4.19 Hz
H/V: 6.4584 ± 0.5992
NS/V: 6.3424 ± 0.7011
EW/V: 6.9477 ± 0.6128
Average H/V
frequency [Hz]
H / V
H/V stability. DOThaz_rc_Worth, PS 52
File Analysis View Option
Hz
min
Amplitude spectra. DOThaz_rc_Worth, PS 52
File View
frequency [Hz]
(mm/s) / Hz
Search for anything
11:04 AM
11/30/2020

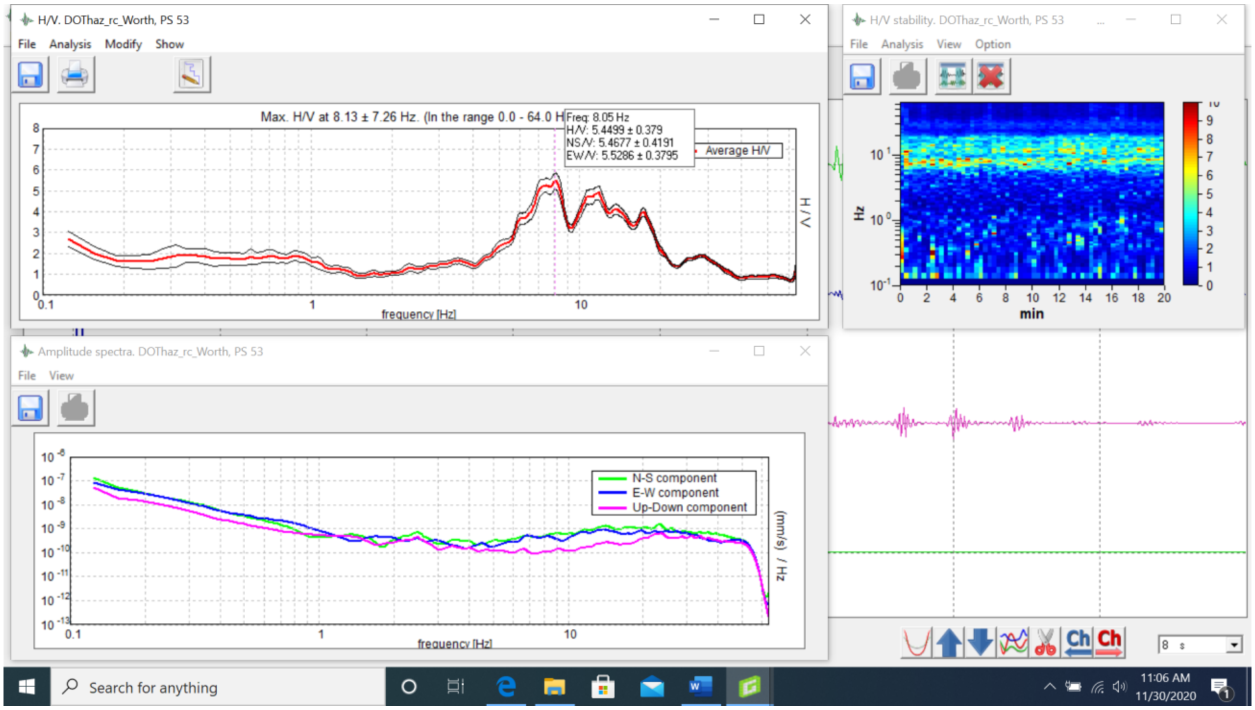
H/V. DOThaz_rc_Worth, PS 53
File Analysis Modify Show
Max. H/V at 8.13 ± 7.26 Hz. (In the range 0.0 - 64.0 H
Freq: 8.05 Hz
H/V: 5.4499 ± 0.379
NS/V: 5.4677 ± 0.4191
EW/V: 5.5286 ± 0.3795
Average H/V
frequency [Hz]
H / V
H/V stability. DOThaz_rc_Worth, PS 53
File Analysis View Option
Hz
min
Amplitude spectra. DOThaz_rc_Worth, PS 53
File View
N-S component
E-W component
Up-Down component
frequency [Hz]
(mm/s) / Hz
Search for anything
11:06 AM
11/30/2020

# APPENDIX B

## Electrical Resistivity Results

# Rachut site- lines A and B

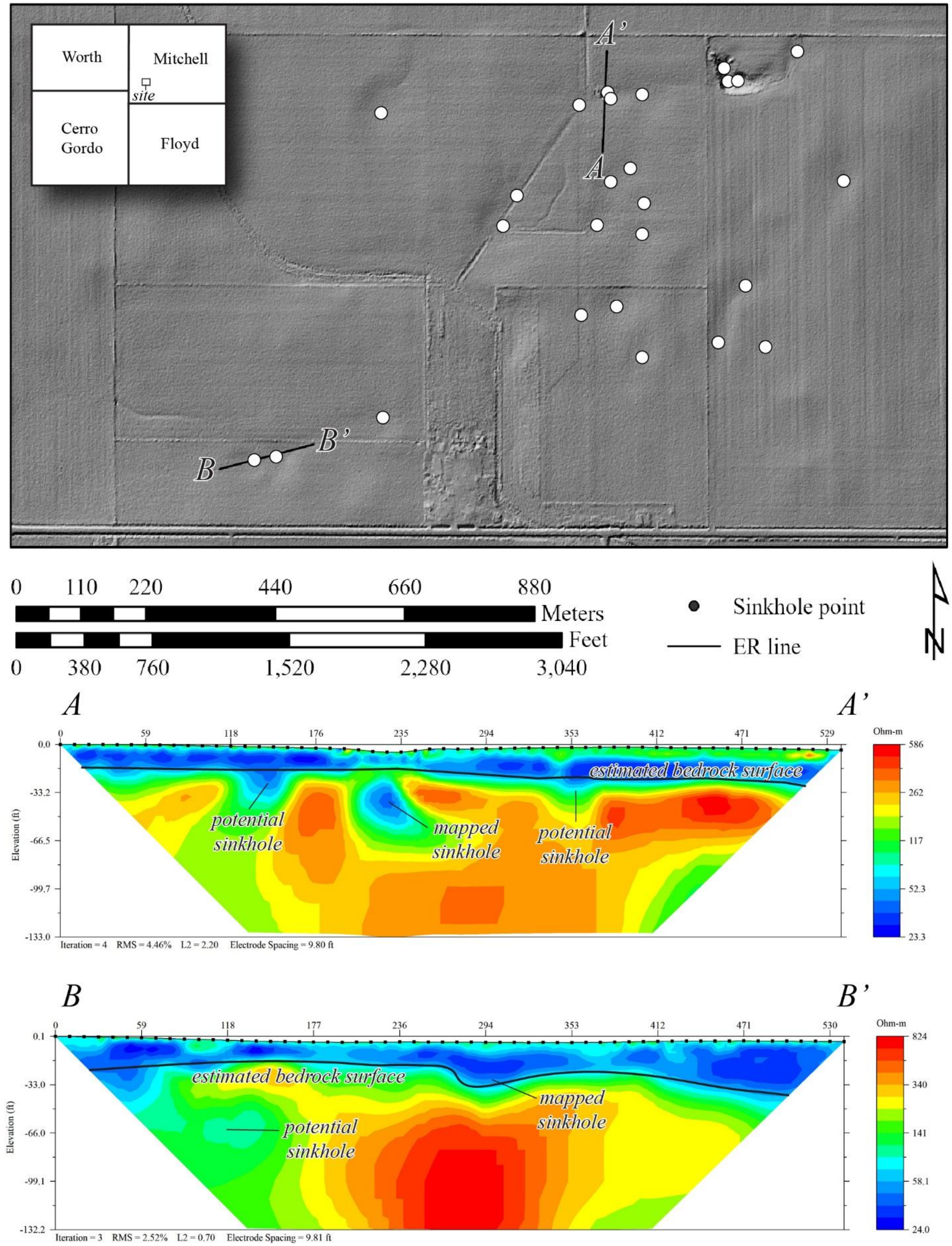

# Rachut site- line A

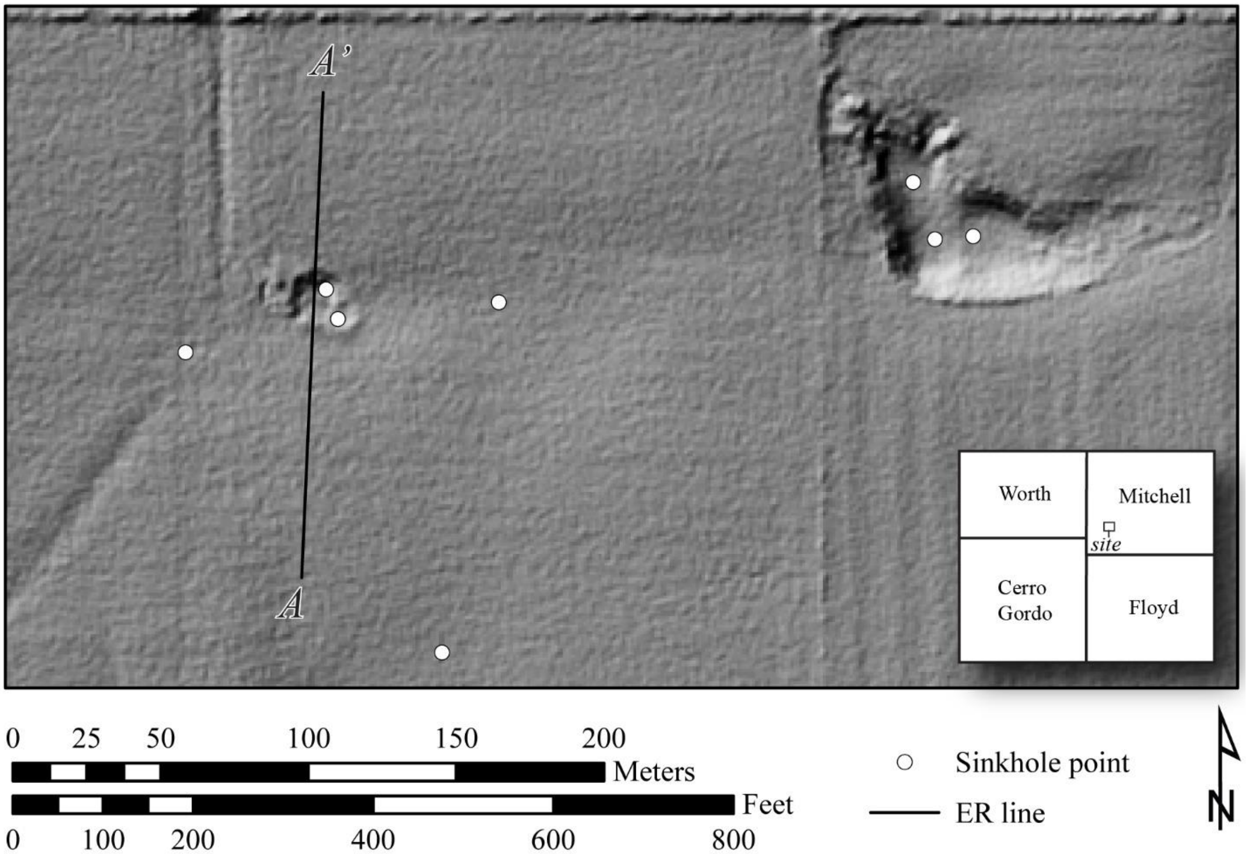


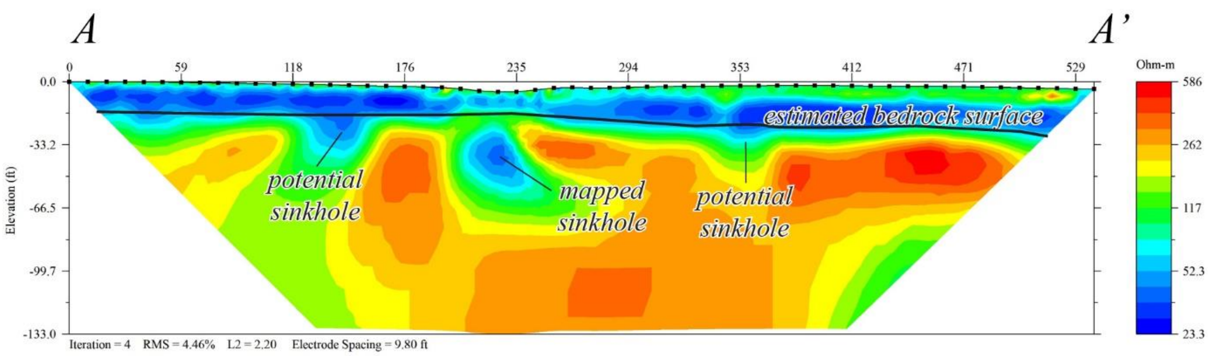

**Rachut site- line B**

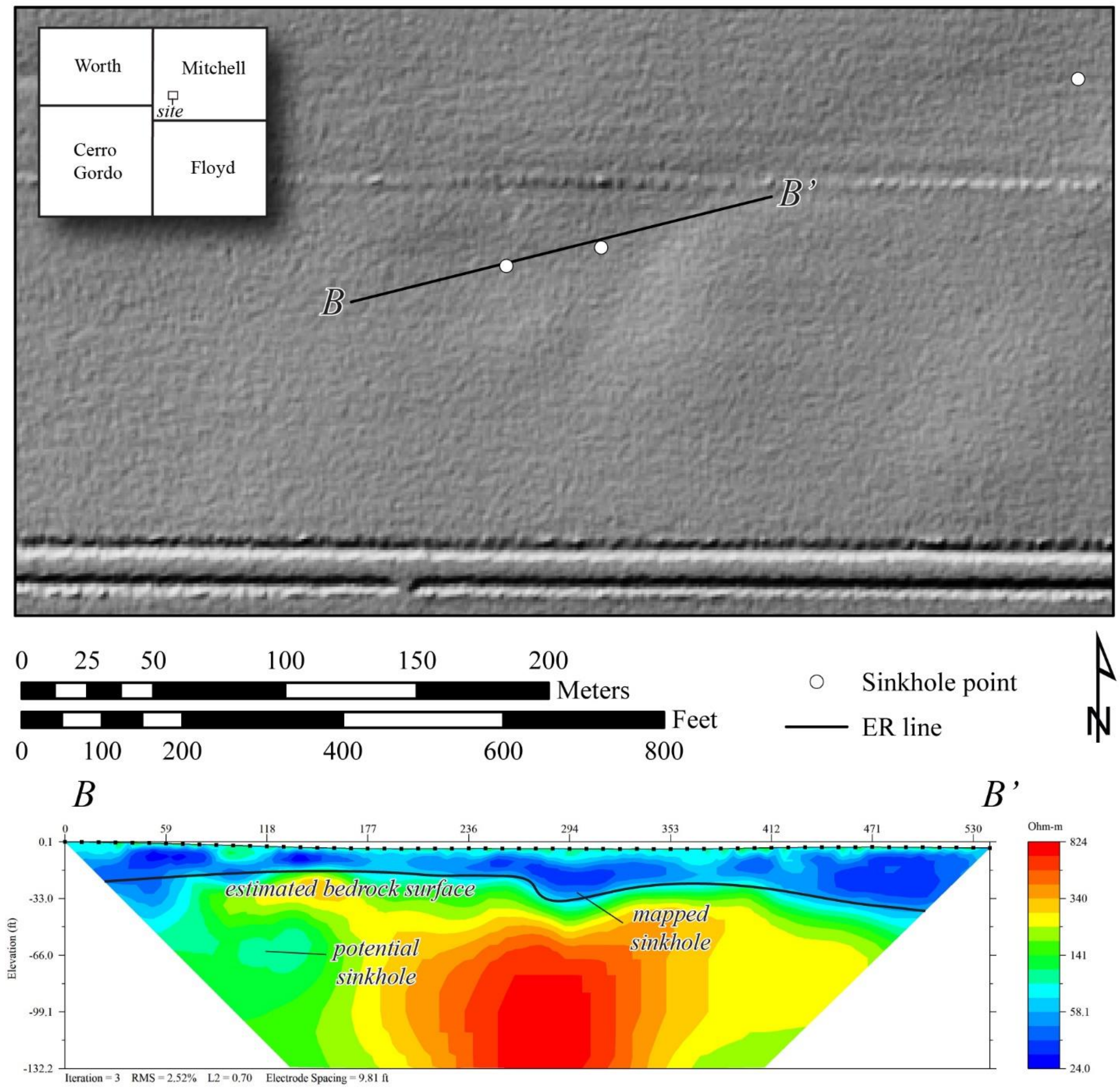

## Mitchell County Conservation Board site- lines A, B, and C

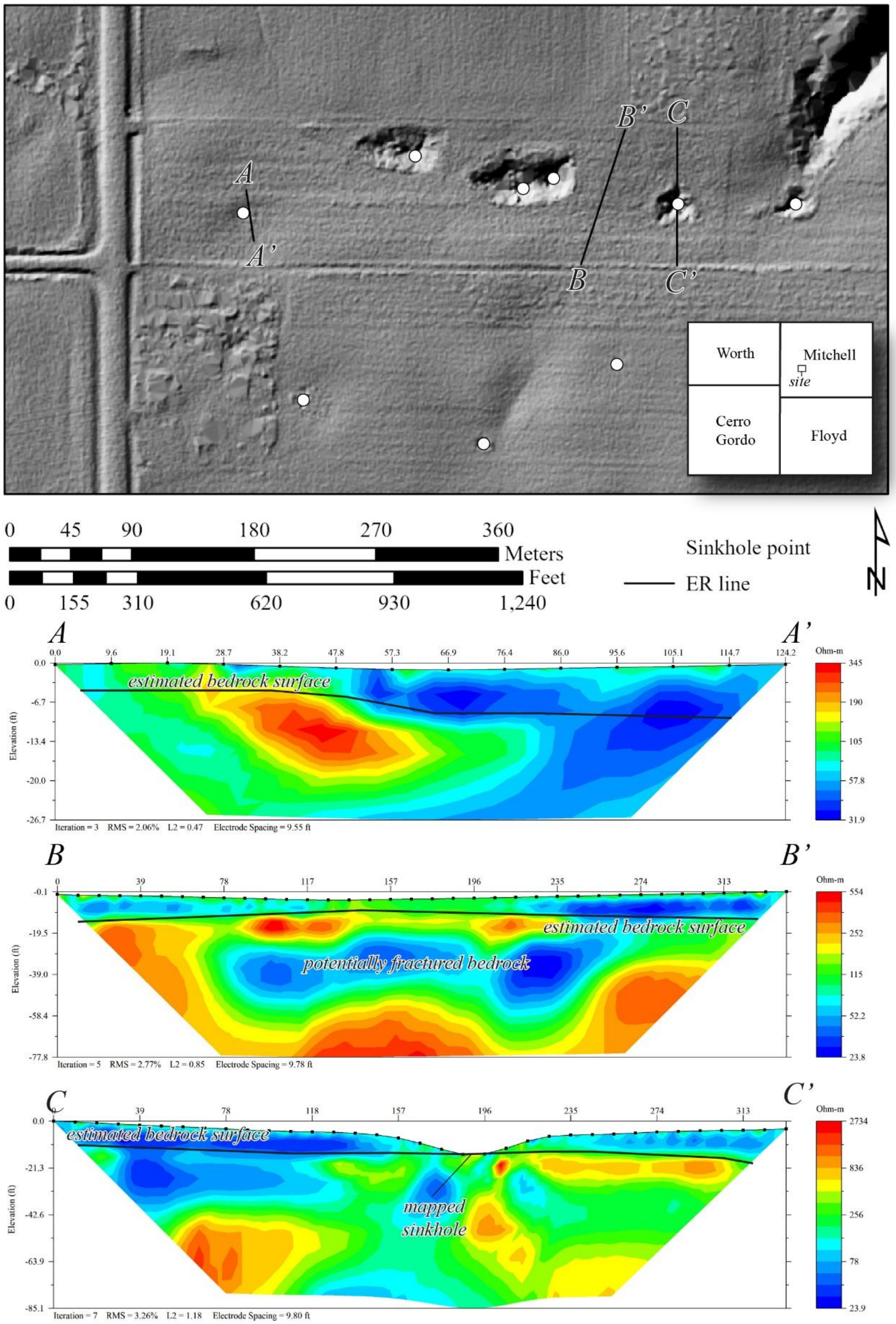

## Mitchell County Conservation Board site- line A

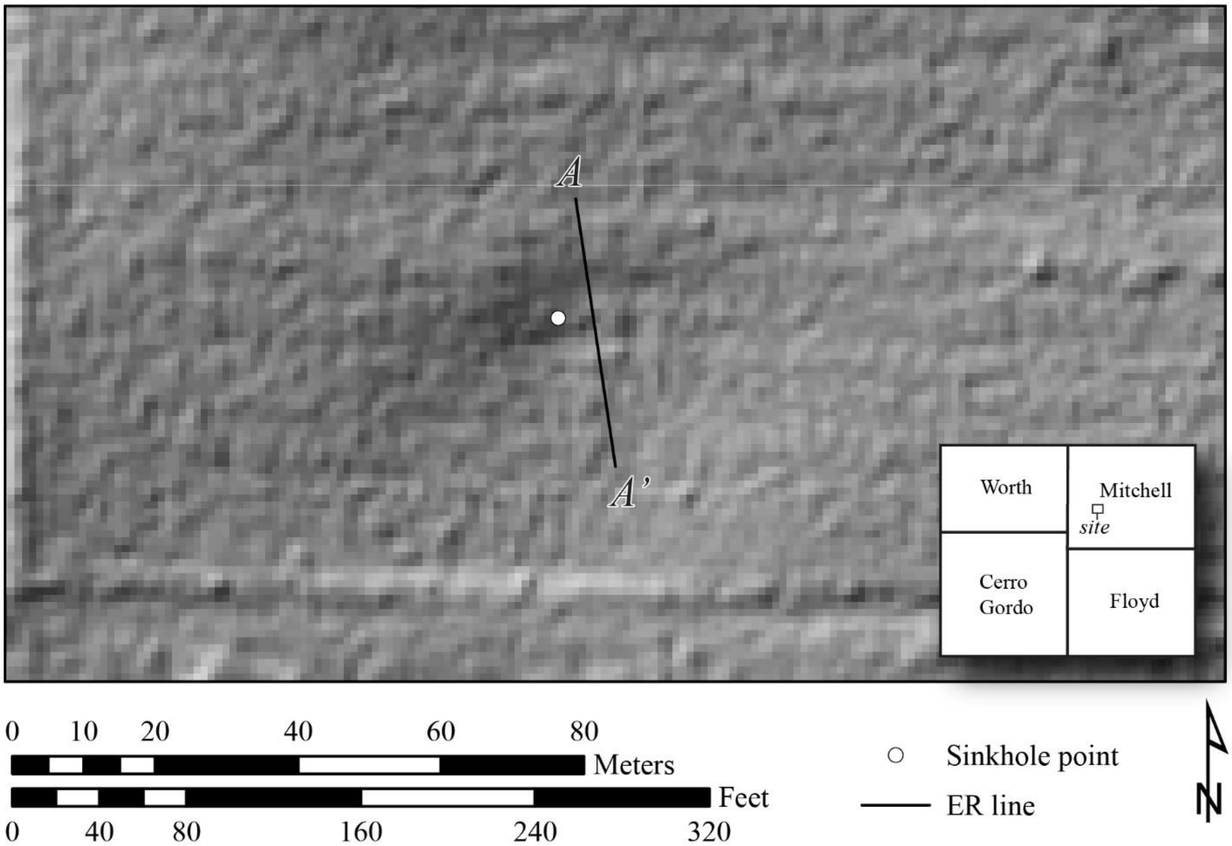


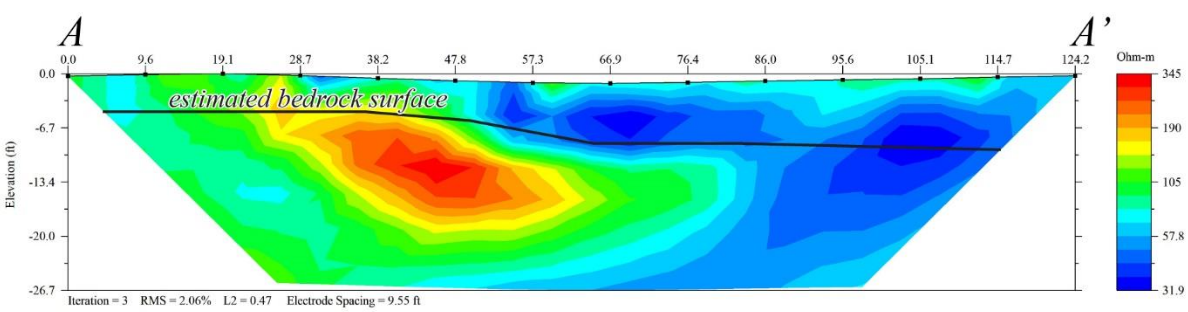

# Mitchell County Conservation Board site- lines B and C

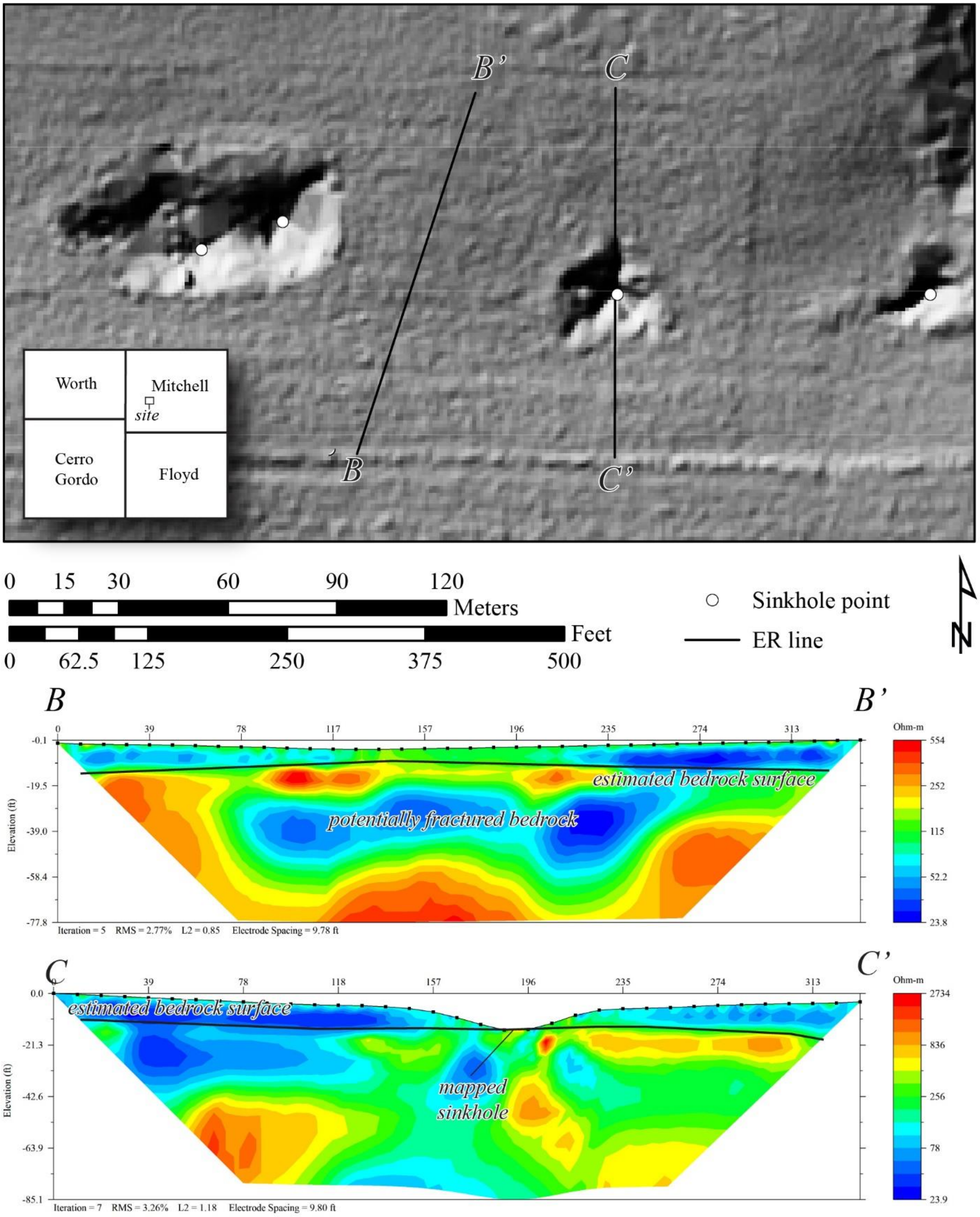

**Falk site- lines A, B, and C**

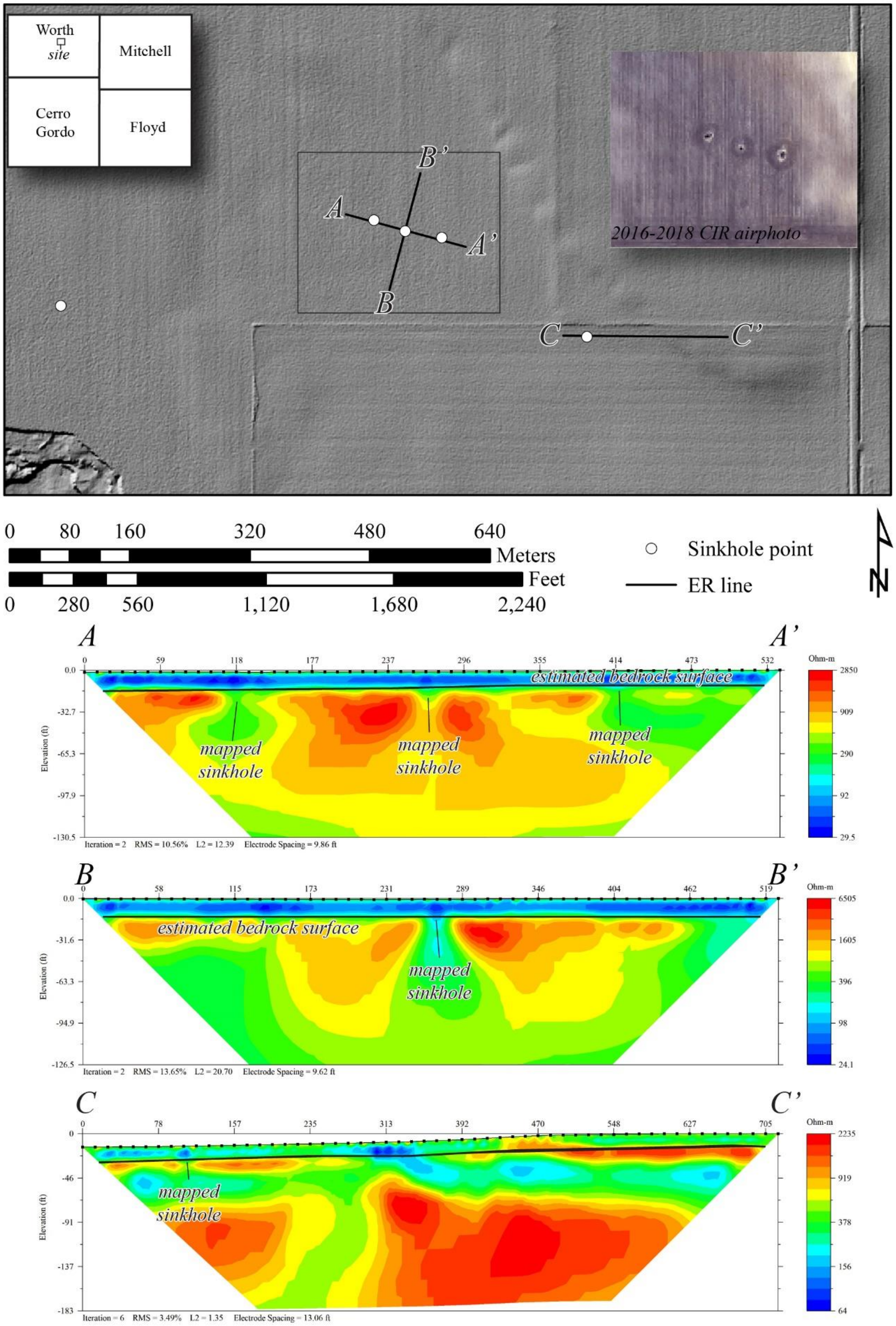

# Falk site- lines A and B

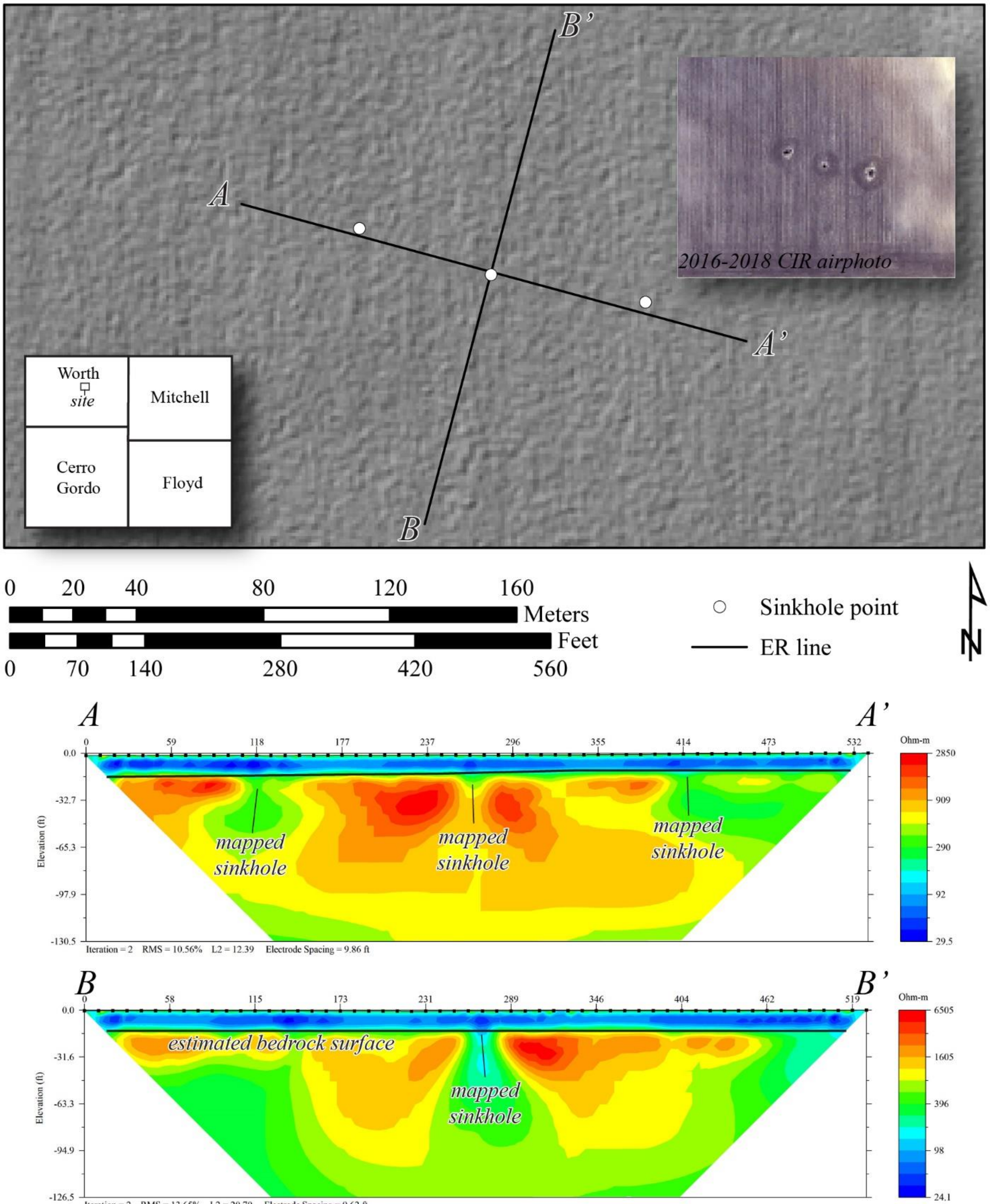

**Falk site- line C**